

UCSF

UC San Francisco Electronic Theses and Dissertations

Title

The chromatin remodeller ACF acts as a dimer and exploits the histone H4 tail and flanking DNA substrate cues to move nucleosomes

Permalink

<https://escholarship.org/uc/item/4b96s646>

Author

Racki, Lisa R

Publication Date

2011

Peer reviewed|Thesis/dissertation

The chromatin remodeller ACF acts as a dimer and exploits the histone H4 tail and flanking DNA substrate cues to move nucleosomes.

by

Lisa R. Racki

DISSERTATION

Submitted in partial satisfaction of the requirements for the degree of

DOCTOR OF PHILOSOPHY

in

Biochemistry

in the

GRADUATE DIVISION

of the

UNIVERSITY OF CALIFORNIA, SAN FRANCISCO

DEDICATION

For my parents Reena and Jeffrey Racki

Your passion, creativity, and integrity inspire me.

ACKNOWLEDGEMENTS

I crossed paths with Geeta Narlikar very fleetingly when I was 19 in college working on my undergraduate thesis project in Fred Ausubel's lab at the Department of Molecular Biology at Mass General Hospital in Boston, and she was a postdoc in Bob Kingston's lab. I sat three bays down from her bench, but I was generally intimidated by the biochemists in the Kingston Lab who didn't seem to work on anything alive. I still can't quite believe I ended up here at UCSF working in the Narlikar lab. I was convinced when I started college that I wanted to be a botanist or entomologist and I was obsessed with E.O. Wilson, and plant evolution. When I was starting to think about graduate schools, I distinctly remember a person who knew Geeta saying something along the lines of, "Well, you could apply to UCSF to study enzymology in the Narlikar Lab, she is an amazing scientist but that stuff is really hard core!" I didn't exactly follow Geeta to UCSF, but I also didn't forget that comment.

I am so grateful to Geeta for continuously inspiring me to take intellectual risks, and for her thoughtful, dedicated mentorship. Geeta reminds me almost every time I go into her office why science is so much fun. In my first year in the lab, Geeta had a daughter and named her Kalpana, which means "Imagination." Reflecting on my time in the Narlikar lab as graduation approaches, I believe that what really sets Geeta apart as a mentor is the unique way in which she helps students to harness their own imagination. I have felt both deeply intellectually

challenged and also supported in my time in the Narlikar Lab. While I am excited for my own next steps and also to follow the future of the Narlikar Lab, I will miss this special scientific environment.

It has been a real privilege to be a part of the UCSF community. I was fortunate to have the opportunity to collaborate with Roger Cooke's and Yifan Cheng's labs during my time at UCSF. The exchange of ideas, reagents, and excitement across the three research groups has created an incredibly fruitful and nurturing learning environment, and I am thankful for the time and effort Roger and Yifan personally invested both in our collaborative project and also in teaching me. I would like to thank Yifan Cheng for his tireless personal efforts to get the EM structure project off the ground. I still remember the day we first saw earmuffs on our nucleosomes!

Nariman Naber in the Cooke lab in particular has been an incredible resource and mentor. She has an uncanny ability to just make the experiment work, and squeeze every last bit of information out of a sample, whether it be from the miniscule samples of protein I was able to bring to the EPR machine, or the fragile muscle fibers from the legs of tarantulas. It is also just so much fun to work with Nariman, and she has been a great personal resource to me in my time at UCSF. Our 2009 story all started with an EPR observation. In 2005, my labmate Peretz Partensky came up with the creative idea to use EPR to study structural changes in the flexible N-terminal tails of histone proteins upon binding

to chromatin remodeling enzymes. This was the beginning of a long term collaboration between the labs, where we have benefited not only from the EPR know-how but the deep knowledge of motor protein mechanisms in general in the Cooke lab. I am grateful to Roger Cooke for his many insights into our biological questions, for a lot of timely suggestions and handy back of the envelope calculations, and for taking us sailing.

I would like to thank the other members of my thesis committee, Jonathan Weissman and Sandy Johnson for their help. I would particularly like to thank Hiten Madhani for his generous help with our manuscript and discussions about chromatin biology in general over the years.

The Narlikar lab has been both a very supportive as well as exciting environment. I was lucky to work with Janet Yang during my rotation. She's a prankster but she was also remarkably patient with me, even when I did things like spill our entire histone prep onto the lab bench. Looking back, I am struck by how generous and selfless Janet was with me, both in sharing with me a piece of her project to work on, and in giving me her reagents and time. Tina Madrid, Claire Rowe, Georgette Charles, Janet, and Susan Shih were the founding members of the Narlikar lab, and they helped ease the path for the rest of us who came after them and were all very helpful in training me in my first year. Claire, Evelyn Chang, Koy Saeteurn, Kalyan Sinha, and Bassem Al-Sady were great baymates. Claire especially always went out of her way to help me with

calculations and fixing equipment, and I will never forget our epic road and camping trip to Palm Springs for the Helicase Meeting. I am so grateful to our lab managers, Tina Madrid, Elena Sevastopoulos, Amanda Habel, and Julia Tretyakova. Amanda especially went above and beyond the call of duty to help me when I needed massive quantities of histones for the EPR experiments. My lab sibling Peretz has a beautiful mind. He is an instigator and adventurer, and I am grateful for his insights into the ACF project, and for many unpredictable and delightful evenings at Langton Labs. Daniele Canzio started graduate school several years after me, but he is very wise and I look up to him both scientifically and personally for his determination, humility, and tremendous personal integrity. He has helped me through some of my more challenging moment in graduate school, both at the bench and beyond. I am also thankful to have had the chance to work with Coral Zhou and John Leonard during their rotations in the Narlikar Lab. Even though I was supposed to be mentoring them, they are both so talented that I quickly began to learn from them.

I would also like to thank several honorary members of the Narlikar lab. I am thankful to Matt Simon for taking me under his wing in the first year of graduate school and encouraging me, I learned so much from him during our collaboration on the MLA project. I would also like to thank Jesse Zalatan from the Lim Lab, my “academic uncle” in terms of science lineage. He’s a standout surfer and scientist and has taught me a lot and made grad school a lot more fun. Angela Won in the Lim Lab has been a great friend to me over the years. I

appreciate her frankness and her encouragement to think more creatively about less well traveled paths in science.

I would like to thank several critical past mentors, Andy Keech who mentored me during high school at the Smithsonian National Zoo in DC, where I first really got excited about biology. Sarah Mathews at the Harvard Herbarium who taught me about plant evolution, Fred Ausubel, my undergraduate advisor at Harvard who taught me to love genetics and also encouraged me to broaden my outlook beyond plant biology, and Dennis Kim for teaching me *C. elegans* genetics and helping me realize that I could be interested in many areas of science.

I would like to thank the residents of 262 Chattanooga Street for their support as housemates and friends, John Zedlewski, Jairam Ranganathan, Jamey Bass, and most of all Johnvey Hwang who somehow managed to put up with me for almost seven years and counting.

Finally, I would like to thank my parents for believing in me and supporting me on this journey, through thick and thin.

Chapter 2 and sections of Chapter 4, the Methods section of this thesis, are a reprint of material previously published in Nature (2009 Dec 24;462(7276):1016-21.). This material is included here in accordance with Nature's permissions request policies for authors.

The Chromatin remodeller ACF acts as a dimer and exploits the histone H4 tail and flanking DNA substrate cues to move nucleosomes.

by Lisa R. Racki

ABSTRACT

A fundamental mode of gene regulation in eukaryotes is to alter access of the nuclear machinery to DNA through packaging into chromatin. Human ACF, a member of the ISWI-family of chromatin remodeling enzymes, is an ideal model system to study the basic mechanism of moving nucleosomes because it is a small complex and makes one class of products, evenly spaced nucleosomes, thought to be important for heterochromatin formation. ACF kinetically distinguishes between different flanking DNA lengths on either side of a nucleosome, moving the nucleosome toward the longer flanking DNA faster than toward the shorter DNA.

Using electron microscopy and enzymatic assays, we observe that ACF can bind and function as a cooperative homodimer to move nucleosomes. The dimeric partners bind the nucleosome near the N-terminal tails of H4 and face in opposing directions. This unusual architecture raises new questions about how the protomers collaborate rather than compete in a tug of war. We observe nucleotide-dependent changes in contacts of the enzyme with the two H4 tails. In the presence of ADP, the enzyme complex contacts one H4 tail, whereas with a nucleotide analogue thought to mimic an activated ATP state, both H4 tails are

immobilized. These conformational states support a model for allosteric communication between the dimeric partners.

We next focused on how the enzyme interprets and integrates two critical components of the nucleosome that we term ‘substrate cues:’ the H4 tail and flanking DNA. We find that the H4 tail and flanking DNA stimulate remodeling activity non-additively, suggesting that the two cues may either function in two different rate limiting steps, or that the two cues function in a coupled manner in one rate limiting step. Using spin-labeled ATP, we observe that the H4 tail but not flanking DNA is important for formation of a restricted conformation of the nucleotide-binding pocket. The H4 tail and flanking DNA both have larger effects on nucleosome remodeling than on ATP hydrolysis. The H4 tails and flanking DNAs play synergistic roles on remodeling and may be important for coupling ATP hydrolysis to nucleosome remodeling.

TABLE OF CONTENTS

Preface

	Dedication	iii
	Acknowledgements	iv
	Permissions	ix
	Abstract	x
	Table of contents	xii
	List of tables and figures	xiii
	Author contributions	xv
Chapter 1	Introduction	1
Chapter 2	The chromatin remodeller ACF acts as a dimeric motor to space nucleosomes	19
Chapter 3	Synergy between substrate cues of ACF	63
Chapter 4	Methods	110

LIST OF TABLES AND FIGURES

CHAPTER 2

- Figure 1** ATP state regulates immobilization of the histone H4 tail and proximal interactions
- Figure 2** SNF2h and ACF function as dimers of ATPases
- Figure 3** Visualization of SNF2h bound to the nucleosome in the presence of ADP•BeFx using EM
- Figure 4** Simple model for how a dimeric ACF moves nucleosomes
- Figure S1** Nucleosome constructs used in this work
- Figure S2** Deconvolution of spectra to determine the fraction of bound spin probes
- Figure S3** A van't Hoff plot for A15C-MSL nucleosomes with 60 bp of flanking DNA on one side (0-601-60) bound by SNF2h in the apo state
- Figure S4** SNF2h-nucleosome complex
- Figure S5** Random conical tilt 3D reconstruction of SNF2h- nucleosome complex
- Figure S6** Images of negatively stained nucleosomes and SNF2h alone
- Figure S7** Monomeric SNF2h bound to the nucleosome in the presence of ADP•BeFx
- Figure S8** An alternative model for how the two ATPase molecules cooperate to achieve nucleosome movement

CHAPTER 3

- Figure 1** Mechanistic models for how ACF integrates substrate cues into its mechanochemical cycle
- Figure 2** The H4 tail and flanking DNA cues affect nucleosome remodeling as probed by FRET
- Figure 3** The H4 tail and flanking DNA substrate cues affect ATP hydrolysis
- Figure 4** Physical models for Effects of Cues on ATP active site
- Figure 5** Electron Paramagnetic Spin Spectroscopy with 2'3' spin-labeled ATP
- Figure 6** The H4 tail but not flanking DNA is required for SNF2h to induce a constrained conformation in the ATP pocket
- Figure 7** Temperature dependence of the 62G conformation of the nucleotide binding pocket
- Figure 8** The H4 tail can rescue ATP hydrolysis in trans
- Figure 9** The H4 tail does not rescue nucleosome remodeling in trans
- Figure 10** The H4 tail extension mutants have effects on ATP hydrolysis
- Figure 11** The H4 tail extension mutants have effects on nucleosome remodeling
- Figure 12** Physical models for the cues acting in one or two ATP hydrolysis events
- Table 1** Relative rate constants (k_{rel}) for ATP hydrolysis and nucleosome remodeling

AUTHOR CONTRIBUTIONS

For Chapter Two, I worked closely with my my co-first author and labmate Janet G. Yang and members of two other UCSF labs, Yifan Cheng's lab and Roger Cooke's lab, and especially Nariman Naber in the Cooke lab. My labmate Peretz D. Partensky came up with the initial concept to use EPR to study interactions of chromatin remodeling enzymes with the flexible histone tails of nucleosomes and helped to design and initiate the EPR experiments. Nariman Naber and I performed all the EPR-based experiments. Thomas J. Purcell conducted the deconvolution analysis of the EPR data, and Roger Cooke helped to design and analyze the EPR experiments. Yifan Cheng and I designed and performed the electron microscopy-based experiments, and Yifan Cheng and Ashley Acevedo conducted the analysis of the electron microscopy data. Janet G. Yang performed the equilibrium analytical ultracentrifugation and footprinting experiments. I performed the fluorescence-based binding and FRET-based activity assays. I worked with Janet G. Yang, Geeta J. Narlikar to design and interpret most of the experiments.

For Chapter Three, I worked closely with Nariman Naber, Roger Cooke, and Geeta J. Narlikar. I performed the enzymatic assays. The EPR experiments

were possible because Nariman Naber had previously synthesized the spin-labeled nucleotide analogues, and worked with these compounds with other motor proteins, including myosin and kinesin. Nariman Naber and I performed all the EPR experiments. Amanda Habel and Julia Tretyakova purified the wild-type histone proteins for making nucleosomes for these experiments. I worked closely with Nariman Naber, Roger Cooke, and Geeta Narlikar to design the EPR experiments. Geeta Narlikar and I designed the kinetic experiments, with help from John Leonard. I worked with Geeta Narlikar, Roger Cooke, Nariman Naber, and John Leonard to interpret the data.

CHAPTER 1

Introduction

A. Chromatin structure is dynamic

DNA packaging into chromatin regulates all the manipulations of eukaryotic DNA: replication, segregation, transcription, recombination, and repair. The nucleosome itself, which is the fundamental unit of packaging of chromatin, greatly decreases the accessibility of the DNA to transcription factors and can have large effects on gene expression^{1,2}. By the 1920's, different categories of 'euchromatin' and 'heterochromatin' were described based on structural and functional properties of *Drosophila* polytene chromosomes³. As gross descriptors, Euchromatin is more decondensed and transcriptionally active, whereas heterochromatin is more compact and transcriptionally silent. At a more detailed level, nucleosomes in heterochromatin are more regularly spaced on DNA and interact with one another to form higher order structures, first the 30nm fiber and then higher order levels of compaction. More recently, different functional types of heterochromatin have been described, based on functional properties and the types of non-histone proteins that drive higher order compaction⁴. Moreover, temporally distinct forms of heterochromatin have been described. Most generally, constitutive heterochromatin, such as that found at telomeric regions and the centromere are silent, whereas facultative chromatin is temporally regulated by environmental, cell cycle and/or developmental cues⁵. In metazoans, the formation of heterochromatin, sequestering regions of DNA not needed for particular cell types, is important for cellular differentiation. The

nucleosome crystal structure was determined in 1984 at 7Å resolution, providing the first detailed physical picture of the basic unit of chromatin packaging⁶. Before the structure of the nucleosome was solved at even this low resolution, however, electron micrographs of chromatin had been observed with the classic 'beads on a string' conformation and fractionation, sedimentation, and crosslinking studies provided evidence for the composition and stoichiometry of the basic unit of chromatin, the nucleosome⁷⁻⁹. Moreover, it was observed that both active and repressed regions of chromatin contained histones, but that there were organizational differences, most notably DNAase I hypersensitive sites were present in active chromatin, suggesting that the histone proteins were in altered conformations¹⁰. Chromatin remodeling enzymes were discovered to be the major players in driving these structural transitions. The genes encoding several chromatin remodeling enzymes were first discovered in genetic screens for regulators of gene expression. Yeast SWI2/SNF2 was discovered in a genetic screen for mutants unable to grow anaerobically on sucrose^{11,12}. By homology, these proteins were discovered to be ATPases, but how they exerted their effects on gene expression was not understood until later genetic and biochemical studies¹³⁻¹⁵.

B. ATP-dependent Remodeling Enzymes drive different types of structural transitions in chromatin *in vivo* and *in vitro*

i. Discovery of the activating chromatin remodeling enzyme family

SWI2/SNF2

Activating Chromatin remodeling complexes of the SWI2/SNF2 family were first functionally identified, purified and characterized from yeast and human (HeLa cells) through *in vitro* assays with nuclear extracts for factors promoting the ability to enhance Gal4 binding to chromatin template *in vitro* (SWI/SNF), and the ability to disrupt nucleosome structure (hSWI/SNF)^{16,17}. SWI/SNF complexes can introduce changes in superhelicity in closed circular nucleosomal arrays; SWI/SNF complexes can generate nucleosomes containing stable loops of DNA, and dinucleosome- like species; SWI/SNF complexes can also transfer the histone octamer to acceptor DNA and exchange H2A/H2B dimers between nucleosomes¹⁷⁻²³. In contrast, the **A**TP-dependent **c**hromatin **a**ssembly **f**actor (ACF), a member of the ISWI-family of chromatin remodeling complexes can regularly space multiple nucleosomes, while SWI/SNF complexes cannot¹⁹. The ability of SWI/SNF complexes to generate diverse products is consistent with their biological role of locally disrupting histone–DNA interactions at promoters²⁴. Generating stable DNA loops within a nucleosome would allow SWI/SNF complexes to expose nucleosomal DNA in crowded chromatin environments where there is insufficient room to slide the nucleosomes. Removing dimers or octamers could be coupled with the action of a histone chaperone to generate nucleosome-free regions or regions that can exchange regular dimers with variant dimers at promoters²⁵ (Text from this section adapted

from Racki, L. R. & Narlikar, G. J. ATP-dependent chromatin remodeling enzymes: two heads are not better, just different. *Curr Opin Genet Dev* 18, 137-144)

ii. Repressive chromatin remodeling enzyme family ISWI

Another class of remodeling enzymes, the ISWI family can promote dramatically different *in vivo* outcomes, promoting ATP-dependent assembly of regularly spaced chromatin arrays. The complexes **A**TP-dependent **c**hromatin assembly **f**actor (ACF) and **c**hromatin **a**ccessibility **c**omplex (CHRAC) were purified from *Drosophila* nuclear extracts as factors that could promote assembly of periodically spaced nucleosomes *in vitro* (Ito, Kadonaga 1997, Varga-Weiz,Becker 1997). Repressive ISWI-containing complexes were found in yeast and human, but interestingly the yeast homologue of ISWI also participates in transcriptional activation also part of the NURF complex and was identified in a screen for factors promoting the formation of DNAase hypersensitivity sites at promoters²⁶⁻²⁸. ISWI is essential in metazoans but not yeast, and plays an important role in X-inactivation in *Drosophila*²⁹. While the different classes of remodelers can generate different types of products, they share the ability to move nucleosomes from one location on DNA to another.

C. Structural features of chromatin remodeling enzymes and homology to helicases

The enzymatic activity of each complex resides within a catalytic ATPase subunit, which can remodel nucleosomes in the absence of the remaining subunits^{19,24,30}. These ATPase subunits are part of the SF2 superfamily of helicases^{31,32}. They all contain two RecA-like domains or lobes: 1A, which contains the Walker A or p-loop motif and the Walker B or DExx motif, and 2A. ATP binds in the cleft formed by these two domains. Changes in the ATP state during the ATPase cycle are thought to drive movement of 1A relative to 2A³³. Analogous to SF1 and SF2 helicases, these small movements are thought to be amplified by accessory domains that extend out from 1A and 2A. These accessory domains often differ structurally between different classes of helicases, and are generically termed 1B and 2B^{31,32}. Analogous to helicases, the ATPase activity of remodeling complexes is stimulated upon binding substrate, namely nucleosomes or free DNA¹⁹. The ISWI ATPases have a long alpha helical c-terminal accessory domain consisting of three subdomains, HAND, SANT, and SLIDE, respectively, which are thought to bind flanking DNA, based on crosslinking experiments^{34,35}.

Although neither the SWI/SNF nor the ISWI family of remodeling enzyme has detectable DNA helicase activity, both classes do display another hallmark of

helicases, the ability to translocate on DNA. Early studies using a triplex displacement technique had suggested that the ATPase subunits of RSC and ACF complexes can translocate on DNA^{36,37}. Recent elegant studies using single-molecule approaches now directly demonstrate processive movement of yeast SWI/SNF and yeast RSC along DNA^{38,39}. Both classes of complexes thus share fundamental mechano-chemical properties. However, they appear to use the energy of ATP hydrolysis to achieve very different outcomes²⁵ (Text of this section adapted from Racki, L. R. & Narlikar, G. J. ATP-dependent chromatin remodeling enzymes: two heads are not better, just different. *Curr Opin Genet Dev* 18, 137-144).

D. ACF as a model system for studying the task of moving nucleosomes

This fundamental task of moving the histone octamer on DNA is still not well understood. Little is known about what transient changes in nucleosome structure occur during movement, and how the enzyme uses ATP to catalyze these changes. While the motor protein has high homology to well characterized helicases, a detailed description of the mechanism of action of these enzymes has been hindered by a number of hurdles: First, the complexity and size of the nucleosome substrate. For the nucleosome to move even the smallest imaginable stepsize of one base pair, many contacts between the histone

octamer and 147bp of DNA would have to be broken and reformed, presumably in an ordered manner. Unlike motor proteins such as kinesin which traverse a polymeric track carrying cargo, the cargo for remodeling enzymes, the histone octamer, is physically wrapped by the polymeric track. Additional hurdles that hinder a detailed description of nucleosome remodeling mechanisms include a lack of structural data for the enzyme-bound nucleosome substrate, the large size of many of the multi-protein remodeling complexes, in which the ATPase subunit alone is often not well behaved. Finally, the diversity of products these molecular motors produce, as described above for SWI/SNF complicates their study.

Human ACF, a member of the ISWI family of chromatin remodeling enzymes, is an ideal model system to study the basic mechanism of moving nucleosomes. The complex is small, consisting of only two subunits, the catalytic ATPase SNF2h, and Acf1, and the catalytic subunit is active alone and recapitulates all of the major features of the complex. Moreover, ACF creates only one class of products, translationally repositioned nucleosomes, rather than the many additional types of products produced by some other remodeling enzymes, making it more amenable to *in vitro* assays. Further, the additional mechanistic feature of ACF, the ability to regularly spacing nucleosomes, is important to understand as it is thought to be critical for a significant biological outcome, the forming of heterochromatin. And finally, the catalytic subunit SNF2h and its homologues in yeast and *Drosophila* can also form additional classes of

complexes with other subunits that have alternative *in vitro* outcomes and associated biological roles. For example, CHRAC contains a topoisomerase, and NURF does not regularly space nucleosomes but is important for transcriptional activation rather than silencing. Understanding the basic mechanism of the catalytic subunit SNF2h will thus be important for understanding these additional, biologically significant functions at the biochemical level.

E. Dynamic flanking DNA length sensing model for ACF

To regularly spacing nucleosomes, ACF must be able to sense flanking DNA length on both sides of nucleosomes. In addition to being able to space nucleosomes in the context of an array of nucleosomes, ACF can equalize the length of DNA on both sides of a mononucleosome on a short piece of DNA *in vitro*^{40,41}. This centering activity can be used as a proxy for studying spacing activity. Previous work in the Narlikar lab has determined that SNF2h catalytically senses flanking DNA length up to 40 base pairs, and the whole ACF complex senses flanking DNA length up to 60 base pairs. The Narlikar lab has previously developed an *in vitro* FRET remodeling assay, where a fluorescent donor dye is attached on the short end of the DNA of a mononucleosome, and an acceptor fluorescent dye is attached to the histone octamer such that the construct starts at high FRET and loss of FRET as a function of time, ATP, and

enzyme concentrations can be measured to determine rate constants. Using this assay, it was observed that the rate of movement of nucleosomes is proportional to flanking DNA length under saturating concentrations of enzyme, indicating that flanking DNA affects k_{cat} for remodeling⁴⁰. Additional experiments showed that ACF continues to move nucleosomes back and forth, even once centering is achieved, in the presence of ATP. These observations led to a model where the enzyme samples flanking DNA length on either side of the nucleosome but moves the nucleosome towards the longer piece of DNA faster than the shorter piece of DNA, such that centered nucleosomes accumulate. Such a model requires that ACF be able to sense flanking DNA length on both sides of the nucleosome, either by falling off one side and rebinding the other side, or being able to processively reverse directions while remaining bound.

F. A role for the H4 tail in ACF mechanism

i. H4 tail implicated in ISWI mechanism

The N-terminal tail of histone H4, but not the other histone tails, plays an important role in the mechanism of ISWI family remodeling enzymes. The histone H4 tail emerges from the nucleosome core particle at about 2 superhelical turns of DNA from the nucleosome dyad or center point of the nucleosomal DNA sequence¹. This nucleosomal location, Superhelical Location

2, is abbreviated as “SHL(\pm 2)” to indicate the two pseudosymmetric locations in the nucleosome at this distance from the Dyad. Removing the first 19 amino acids of histone H4, or more specifically the basic patch (K16R17H18R19) of amino acids that constitute the critical epitope important for ISWI motors, causes a dramatic effect on remodeling rates *in vitro*, but not on nucleosome binding⁴²⁻⁴⁴. Moreover, genetic studies in flies have demonstrated a genetic interaction with histone H4 acetylation at lysine 16 and ACF, and *in vitro* studies show that lysine 16 acetylation abrogates ISWI function^{29,44}. It is not known which step of the ATPase cycle the H4 tail participates in, or structurally what part of the enzyme interacts with it. Previous studies have hypothesized that the basic patch interacts with an acidic patch on the helicase domain of ISWI³⁵. It is also possible that the c-terminal domain of ACF interacts with the H4 tail, as it contains a SANT domain which has been implicated in other systems with histone tail binding^{45,46}.

ii. H4 tail implicated in heterochromatin formation

Interestingly, the same basic patch residues important for ACF function are also thought to play a role in mediating nucleosome-nucleosome interactions in compacted chromatin. Crosslinking and structural studies suggest that the H4 tail basic patch interacts with an acidic patch on Histone H2A of another nucleosome^{47,48}.

G. ACF Integrates Substrate Cues

Two critical elements of the nucleosomal substrate, or substrate cues, are required for ACF to move nucleosomes: flanking DNA and the histone H4 tail. However, it is not known when these cues are used during the ATP hydrolysis cycle of the enzyme, or physically how they are recognized. Both cues are critical for ACF to act in a context appropriate manner on the substrate. The same basic patch residues for ACF function play a structural role in mediating nucleosome-nucleosome interactions in folding of arrays of nucleosomes into higher order structures. The basic patch interacts with an acidic patch of amino acids on the globular domain of H2A of a neighboring nucleosome during folding^{47,48}. Acetylation of lysine 16 in the basic patch is a post translational modification associated with transcriptional activation^{49,50}. Both of these physical changes in the H4 tail structure and accessibility signal biological contexts in which ACF is not needed. Thus the H4 tail acts as a dynamic signal or cue which ACF must recognize. Similarly, in the context of folded heterochromatin, flanking DNA is occluded in structural models of the 30nm fiber, the first level of folding of arrays of nucleosomes. In order to act appropriately, ACF must interpret and integrate these two types of cues. Thus understanding how ACF reads these cues is central to understanding the basic mechanism of moving nucleosomes.

H. Work presented here

a. A Dimer Model for nucleosome spacing

In Chapter Two, we describe a dimer model for nucleosome spacing by ACF. We observe that ACF binds nucleosomes as a cooperative dimer, and that dimerization is important for remodeling activity. We observe evidence for allostery between the dimeric partners in their interactions with the H4 tails of the nucleosome. Our Negative stain EM structure indicates that the two protomers bind on opposite sides of the nucleosome and appear to face in opposite directions, which may be mechanistically important for sampling flanking DNA on both sides of the nucleosomes, but raises new questions about how the protomers collaborate rather than competing in a tug of war.

b. Synergistic Integration of Substrate Cues on nucleosome remodeling

In Chapter Three, we explore how ACF interprets and integrates two substrate cues, the H4 tail and flanking DNA. We observe that the two substrate cues act non-additively to promote both ATP hydrolysis and nucleosome remodeling. We also find that the H4 tail but not the flanking DNA is required for a conformational change in the ATP binding pocket of the enzyme. These observations lead to two classes of models to explain how the enzyme reads

these signals from the substrate: One model where both cues act in a cooperative manner in the same rate limiting step to promote ATP hydrolysis, and a second model where there are two types of ATP hydrolysis, and flanking DNA participates in one ATP hydrolysis event while the H4 tail participates in the other ATP hydrolysis event.

We also find that the H4 tail and flanking DNA both appear to play a role in coupling ATP hydrolysis to nucleosome remodeling. The H4 tail and flanking DNA have smaller effects on ATP hydrolysis than on nucleosome remodeling. We observe that the H4 tail can rescue ATP hydrolysis when added in trans as a peptide, but does not rescue nucleosome remodeling. Additionally, mutants extending the flexible linker length between the critical basic patch epitope of the H4 tail and the nucleosome core, demonstrate length-dependent defects on both ATP hydrolysis and proportional (uncoupled) defects on nucleosome repositioning. This data suggests that the H4 tail may play a role either in positioning the enzyme in a productive binding mode on the nucleosome, or possibly acting as a point of attachment the nucleosome may use to apply force to break histone-DNA contacts.

- 1 Luger, K., Mäder, A. W., Richmond, R. K., Sargent, D. F. & Richmond, T. J. Crystal structure of the nucleosome core particle at 2.8 Å resolution. *Nature* **389**, 251-260, doi:10.1038/38444 (1997).
- 2 Davey, C. A., Sargent, D. F., Luger, K., Maeder, A. W. & Richmond, T. J. Solvent mediated interactions in the structure of the nucleosome core particle at 1.9 Å resolution. *J Mol Biol* **319**, 1097-1113, doi:S0022-2836(02)00386-8 [pii] 10.1016/S0022-2836(02)00386-8 (2002).
- 3 Heitz, E. Das heterochromatin der moose. *Jahrb Wiss Bot* **69**, 762-818 (1928).
- 4 Fillion, G. J. *et al.* Systematic protein location mapping reveals five principal chromatin types in *Drosophila* cells. *Cell* **143**, 212-224, doi:S0092-8674(10)01057-3 [pii] 10.1016/j.cell.2010.09.009 (2010).
- 5 Trojer, P. & Reinberg, D. Facultative heterochromatin: is there a distinctive molecular signature? *Mol Cell* **28**, 1-13, doi:S1097-2765(07)00623-5 [pii] 10.1016/j.molcel.2007.09.011 (2007).
- 6 Richmond, T. J., Finch, J. T., Rushton, B., Rhodes, D. & Klug, A. Structure of the nucleosome core particle at 7 Å resolution. *Nature* **311**, 532-537 (1984).
- 7 Kornberg, R. D. Chromatin structure: a repeating unit of histones and DNA. *Science* **184**, 868-871 (1974).
- 8 Kornberg, R. D. & Thomas, J. O. Chromatin structure; oligomers of the histones. *Science* **184**, 865-868 (1974).
- 9 Olins, A. L. & Olins, D. E. Spheroid chromatin units (v bodies). *Science* **183**, 330-332 (1974).
- 10 Krebs, J. E. & Peterson, C. L. Understanding "active" chromatin: a historical perspective of chromatin remodeling. *Crit Rev Eukaryot Gene Expr* **10**, 1-12 (2000).
- 11 Carlson, M., Osmond, B. C. & Botstein, D. Mutants of yeast defective in sucrose utilization. *Genetics* **98**, 25-40 (1981).
- 12 Abrams, E., Neigeborn, L. & Carlson, M. Molecular analysis of SNF2 and SNF5, genes required for expression of glucose-repressible genes in *Saccharomyces cerevisiae*. *Mol Cell Biol* **6**, 3643-3651 (1986).
- 13 Peterson, C. L. & Herskowitz, I. Characterization of the yeast SWI1, SWI2, and SWI3 genes, which encode a global activator of transcription. *Cell* **68**, 573-583, doi:0092-8674(92)90192-F [pii] (1992).
- 14 Henikoff, S. Transcriptional activator components and poxvirus DNA-dependent ATPases comprise a single family. *Trends Biochem Sci* **18**, 291-292 (1993).
- 15 Travers, A. A. The reprogramming of transcriptional competence. *Cell* **69**, 573-575, doi:0092-8674(92)90218-2 [pii] (1992).

- 16 Côté, J., Quinn, J., Workman, J. L. & Peterson, C. L. Stimulation of GAL4 derivative binding to nucleosomal DNA by the yeast SWI/SNF complex. *Science* 265, 53-60 (1994).
- 17 Kwon, H., Imbalzano, A. N., Khavari, P. A., Kingston, R. E. & Green, M. R. Nucleosome disruption and enhancement of activator binding by a human SW1/SNF complex. *Nature* 370, 477-481, doi:10.1038/370477a0 (1994).
- 18 Havas, K. et al. Generation of superhelical torsion by ATP-dependent chromatin remodeling activities. *Cell* 103, 1133-1142, doi:S0092-8674(00)00215-4 [pii] (2000).
- 19 Narlikar, G. J., Fan, H. Y. & Kingston, R. E. Cooperation between complexes that regulate chromatin structure and transcription. *Cell* 108, 475-487, doi:S0092867402006542 [pii] (2002).
- 20 Bruno, M. et al. Histone H2A/H2B dimer exchange by ATP-dependent chromatin remodeling activities. *Mol Cell* 12, 1599-1606, doi:S1097276503004994 [pii] (2003).
- 21 Lorch, Y., Cairns, B. R., Zhang, M. & Kornberg, R. D. Activated RSC-nucleosome complex and persistently altered form of the nucleosome. *Cell* 94, 29-34, doi:S0092-8674(00)81218-0 [pii] (1998).
- 22 Guyon, J. R., Narlikar, G. J., Sullivan, E. K. & Kingston, R. E. Stability of a human SWI-SNF remodeled nucleosomal array. *Mol Cell Biol* 21, 1132-1144, doi:10.1128/MCB.21.4.1132-1144.2001 (2001).
- 23 Jaskelioff, M., Gavin, I. M., Peterson, C. L. & Logie, C. SWI-SNF-mediated nucleosome remodeling: role of histone octamer mobility in the persistence of the remodeled state. *Mol Cell Biol* 20, 3058-3068 (2000).
- 24 Fan, H. Y., Narlikar, G. J. & Kingston, R. E. Noncovalent modification of chromatin: different remodeled products with different ATPase domains. *Cold Spring Harb Symp Quant Biol* 69, 183-192, doi:10.1101/sqb.2004.69.183 (2004).
- 25 Racki, L. R. & Narlikar, G. J. ATP-dependent chromatin remodeling enzymes: two heads are not better, just different. *Curr Opin Genet Dev* 18, 137-144, doi:S0959-437X(08)00011-7 [pii] 10.1016/j.gde.2008.01.007 (2008).
- 26 Tsukiyama, T., Becker, P. B. & Wu, C. ATP-dependent nucleosome disruption at a heat-shock promoter mediated by binding of GAGA transcription factor. *Nature* 367, 525-532, doi:10.1038/367525a0 (1994).
- 27 Tsukiyama, T., Daniel, C., Tamkun, J. & Wu, C. ISWI, a member of the SWI2/SNF2 ATPase family, encodes the 140 kDa subunit of the nucleosome remodeling factor. *Cell* 83, 1021-1026, doi:0092-8674(95)90217-1 [pii] (1995).
- 28 Tsukiyama, T. & Wu, C. Purification and properties of an ATP-dependent nucleosome remodeling factor. *Cell* 83, 1011-1020, doi:0092-8674(95)90216-3 [pii] (1995).
- 29 Corona, D. F., Clapier, C. R., Becker, P. B. & Tamkun, J. W. Modulation of ISWI function by site-specific histone acetylation. *EMBO Rep* 3, 242-247, doi:3/3/242 [pii] 10.1093/embo-reports/kvf056 (2002).

- 30 Gangaraju, V. K. & Bartholomew, B. Mechanisms of ATP dependent chromatin remodeling. *Mutat Res* 618, 3-17, doi:S0027-5107(07)00024-3 [pii]
10.1016/j.mrfmmm.2006.08.015 (2007).
- 31 Dürr, H., Körner, C., Müller, M., Hickmann, V. & Hopfner, K. P. X-ray structures of the *Sulfolobus solfataricus* SWI2/SNF2 ATPase core and its complex with DNA. *Cell* 121, 363-373, doi:S0092-8674(05)00298-9 [pii]
10.1016/j.cell.2005.03.026 (2005).
- 32 Thomä, N. H. et al. *Structure* of the SWI2/SNF2 chromatin-remodeling domain of eukaryotic Rad54. *Nat Struct Mol Biol* 12, 350-356, doi:nsmb919 [pii]
10.1038/nsmb919 (2005).
- 33 Lewis, R., Dürr, H., Hopfner, K. P. & Michaelis, J. Conformational changes of a Swi2/Snf2 ATPase during its mechano-chemical cycle. *Nucleic Acids Res* 36, 1881-1890, doi:gkn040 [pii]
10.1093/nar/gkn040 (2008).
- 34 Grüne, T. et al. *Crystal* structure and functional analysis of a nucleosome recognition module of the remodeling factor ISWI. *Mol Cell* 12, 449-460, doi:S1097276503002739 [pii] (2003).
- 35 Dang, W. & Bartholomew, B. Domain architecture of the catalytic subunit in the ISW2-nucleosome complex. *Mol Cell Biol* 27, 8306-8317, doi:MCB.01351-07 [pii]
10.1128/MCB.01351-07 (2007).
- 36 Whitehouse, I., Stockdale, C., Flaus, A., Szczelkun, M. D. & Owen-Hughes, T. Evidence for DNA translocation by the ISWI chromatin-remodeling enzyme. *Mol Cell Biol* 23, 1935-1945 (2003).
- 37 Saha, A., Wittmeyer, J. & Cairns, B. R. Chromatin remodeling by RSC involves ATP-dependent DNA translocation. *Genes Dev* 16, 2120-2134, doi:10.1101/gad.995002 (2002).
- 38 Zhang, Y. et al. DNA *translocation* and loop formation mechanism of chromatin remodeling by SWI/SNF and RSC. *Mol Cell* 24, 559-568, doi:S1097-2765(06)00731-3 [pii]
10.1016/j.molcel.2006.10.025 (2006).
- 39 Lia, G. et al. *Direct observation* of DNA distortion by the RSC complex. *Mol Cell* 21, 417-425, doi:S1097-2765(05)01896-4 [pii]
10.1016/j.molcel.2005.12.013 (2006).
- 40 Yang, J. G., Madrid, T. S., Sevastopoulos, E. & Narlikar, G. J. The chromatin-remodeling enzyme ACF is an ATP-dependent DNA length sensor that regulates nucleosome spacing. *Nat Struct Mol Biol* 13, 1078-1083, doi:nsmb1170 [pii]
10.1038/nsmb1170 (2006).
- 41 Eberharter, A. et al. Acf1, *the largest* subunit of CHRAC, regulates ISWI-induced nucleosome remodelling. *EMBO J* 20, 3781-3788, doi:10.1093/emboj/20.14.3781 (2001).
- 42 Clapier, C. R., Längst, G., Corona, D. F., Becker, P. B. & Nightingale, K. P. Critical role for the histone H4 N terminus in nucleosome remodeling by

- ISWI. *Mol Cell Biol* 21, 875-883, doi:10.1128/MCB.21.3.875-883.2001 (2001).
- 43 Hamiche, A., Kang, J. G., Dennis, C., Xiao, H. & Wu, C. Histone tails modulate nucleosome mobility and regulate ATP-dependent nucleosome sliding by NURF. *Proc Natl Acad Sci U S A* 98, 14316-14321, doi:251421398 [pii] 10.1073/pnas.251421398 (2001).
- 44 Ferreira, H., Flaus, A. & Owen-Hughes, T. Histone modifications influence the action of Snf2 family remodelling enzymes by different mechanisms. *J Mol Biol* 374, 563-579, doi:S0022-2836(07)01201-6 [pii] 10.1016/j.jmb.2007.09.059 (2007).
- 45 Boyer, L. A. et al. Essential *role* for the SANT domain in the functioning of multiple chromatin remodeling enzymes. *Mol Cell* 10, 935-942, doi:S1097276502006342 [pii] (2002).
- 46 Boyer, L. A., Latek, R. R. & Peterson, C. L. The SANT domain: a unique histone-tail-binding module? *Nat Rev Mol Cell Biol* 5, 158-163, doi:10.1038/nrm1314 (2004).
- 47 Dorigo, B. et al. Nucleosome *arrays* reveal the two-start organization of the chromatin fiber. *Science* 306, 1571-1573, doi:306/5701/1571 [pii] 10.1126/science.1103124 (2004).
- 48 Schalch, T., Duda, S., Sargent, D. F. & Richmond, T. J. X-ray structure of a tetranucleosome and its implications for the chromatin fibre. *Nature* 436, 138-141, doi:nature03686 [pii] 10.1038/nature03686 (2005).
- 49 Turner, B. M., Birley, A. J. & Lavender, J. Histone H4 isoforms acetylated at specific lysine residues define individual chromosomes and chromatin domains in *Drosophila* polytene nuclei. *Cell* 69, 375-384, doi:0092-8674(92)90417-B [pii] (1992).
- 50 Suka, N., Luo, K. & Grunstein, M. Sir2p and Sas2p opposingly regulate acetylation of yeast histone H4 lysine16 and spreading of heterochromatin. *Nat Genet* 32, 378-383, doi:ng1017 [pii] 10.1038/ng1017 (2002).

CHAPTER 2

The chromatin remodeler ACF acts as a dimeric motor to space nucleosomes

The chromatin remodeler ACF acts as a dimeric motor to space nucleosomes

Lisa R. Racki^{1,3}, Janet G. Yang^{1,3}, Nariman Naber¹, Peretz D. Partensky¹, Ashley Acevedo¹, Thomas J. Purcell¹, Roger Cooke¹, Yifan Cheng^{1,2}, & Geeta J. Narlikar¹

¹*Department of Biochemistry and Biophysics, University of California, 600 16th Street, San Francisco, CA 94158, USA.* ²*The W.M. Keck Advanced Microscopy Laboratory, Department of Biochemistry and Biophysics, University of California San Francisco, CA 94158, USA.* ³*These authors contributed equally to this work*

Evenly spaced nucleosomes directly correlate with condensed chromatin and gene silencing. The ATP-dependent chromatin assembly factor (ACF) forms such structures *in vitro* and is required for silencing *in vivo*. ACF generates and maintains nucleosome spacing by constantly moving a nucleosome towards the longer flanking DNA faster than the shorter flanking DNA. But how the enzyme rapidly moves back and forth between both sides of a nucleosome to accomplish bidirectional movement is unknown. We show that nucleosome movement depends cooperatively on two ACF molecules, suggesting that ACF functions as a dimer of ATPases. Further, the nucleotide state determines whether the dimer closely engages one vs. both sides of the nucleosome. Three-dimensional reconstruction by single particle electron microscopy of the ATPase-nucleosome complex in an activated

ATP state reveals a dimer architecture in which the two ATPases face each other. Our results suggest a model in which the two ATPases work in a coordinated manner, taking turns to engage either side of a nucleosome, thereby allowing processive bidirectional movement. This novel dimeric motor mechanism differs from that of dimeric motors such as kinesin and dimeric helicases that processively translocate unidirectionally and reflects the unique challenges faced by motors that move nucleosomes.

Chromatin-remodeling motors play essential roles in organizing the chromatin state for regulating eukaryotic genomes, yet how they carry out their myriad activities is poorly understood. Their substrate, the nucleosome, contains 147 bp of DNA wrapped in ~1.5 turns around an octamer of histone proteins. Even the smallest movement of the histone octamer relative to the DNA presumably requires a coordinated process of breaking and reforming the many histone-DNA contacts. The ACF chromatin-remodeling complex exemplifies the task, as it is able to move nucleosomes to create evenly spaced nucleosomal arrays that contain equal DNA on either side of each nucleosome¹⁻¹⁰. These evenly spaced arrays are important for packaging the underlying DNA into silent chromatin structures *in vivo*¹⁻¹⁰.

ACF is part of the ISWI family of remodeling complexes. The ATPase subunits of ISWI complexes can move nucleosomes by themselves while the accessory subunits modulate this basic activity¹¹⁻¹⁵. The human ACF complex consists of one ATPase subunit, SNF2h and one accessory subunit, Acf1^{6,7}.

SNF2h is part of the SF2 family of DExx box proteins that includes helicases and nucleic acid translocases¹⁶. The ATPase domain of SNF2h has two RecA-like domains, which are thought to form a cleft within which ATP binds. SNF2h also has an alpha-helical extension comprised of three additional domains, HAND, SANT and SLIDE which are thought to play a role in binding flanking DNA^{17,18}. We showed previously that ACF generates a dynamic equilibrium in which nucleosomes with equal flanking DNA on either side accumulate⁸. Our data implied that ACF achieves the dynamic equilibrium by constantly sampling either side of the nucleosome. This sampling mechanism raised the question of how ACF efficiently switches back and forth between both sides of a nucleosome. We hypothesized that understanding how the ATP state affects interactions of the enzyme with the nucleosome would provide insight into the sampling process.

Previous work has shown that ISWI enzymes require a basic patch, K₁₆R₁₇H₁₈R₁₉, on N-terminal tail of histone H4 for maximal activity¹⁹⁻²³. The role of the H4 tail is not known, but it has been hypothesized that an acidic patch on the ATPase domain of ISWI enzymes may interact with the basic patch on the H4 tail. These previous observations imply that the ATPase subunit contacts the H4 tail and that the contacts may change during the ATPase cycle. We therefore used changes in the mobility of the H4 tail as a handle to follow how changes in the nucleotide state alter interactions between SNF2h and the nucleosome. We used electron paramagnetic resonance (EPR) spectroscopy for these studies²⁶. We covalently attached a

maleimide spin label to a cysteine introduced in place of an alanine at position 15 on the H4 tail (A15C-MSL, Supplementary Fig.1b), which is directly adjacent to the basic patch. Thermal fluctuations cause a spin label attached to a protein to undergo motion in a spatial region defined by the adjacent protein surface. The resulting EPR spectrum is a highly sensitive measure of the region accessible to the probe. Conformational changes can thus be detected via changes in probe mobility, and these are monitored as changes in the EPR spectrum. EPR can also resolve and quantify multiple states and is particularly powerful in monitoring transitions between unstructured and structured regions of proteins. The A15C-MSL nucleosomes were assembled using an asymmetric DNA template comprising the 601 positioning sequence with 60 bp of flanking DNA on one side (0-601-60, Fig. 1a and Supplementary Fig. 1a)²⁷. The presence of the probe did not alter the maximal rate of nucleosome remodeling by SNF2h (data not shown).

In the absence of SNF2h, the EPR spectrum of the A15C-MSL probe indicated a highly mobile probe (Fig. 1a, top spectrum). The high mobility of the probe in unbound nucleosomes suggested that the H4 N-terminal tails are largely unstructured. Next, we determined how binding of SNF2h altered the mobility of the H4 tail. When the nucleosomes were saturated with SNF2h in the absence of nucleotide (apo state), the EPR spectrum shows two sets of spectral components as indicated by the arrows (Fig 1a, middle spectrum). The inner spectral components (blue arrows) are indicative of a highly mobile probe whereas the wider set of spectral components (highlighted by the red

dashed lines) and the broadening of the central peak are indicative of a second state with more restricted mobility. A given peak height in the left-most immobilized spectral component represents 4.1 times more spins than the same peak height for the mobile component. Deconvolution of the spectra indicated that about half of the H4 tails were in each of the two states ($56\pm 5.4\%$ in the immobilized state, see Supplementary Fig. 2 for fitting and quantification method)²⁸. In the presence of ADP, the immobilized subpopulation also constituted half of the probes (spectra not shown). Our attempts to trap the SNF2h-nucleosome complex in the ATP state using ATP analogs were unsuccessful as these analogs either supported low levels of remodeling (AMP-PNP, ATP γ S) or did not detectably inhibit remodeling (AMP-PCP). We were however able to mimic an activated ATP state using the analog, ADP•BeF_x. In contrast to the data in the apo state and with ADP, almost all of the probe on the H4 tail became immobilized in the presence of SNF2h and ADP•BeF_x ($91.5\pm 2.6\%$ of probe in the immobilized peak). This change is shown by the increase in spectral intensity of the immobilized component (left-most peak, Fig. 1a, bottom spectrum). This dramatic increase in the amount of probes immobilized indicated that both H4 tails were bound by SNF2h in the presence of ADP•BeF_x. Together, these data indicate that SNF2h induces nucleotide-dependent changes in the H4 tail conformation such that in the apo and ADP states, half the H4 tails are immobilized and in an activated ATP state mimicked by ADP•BeF_x, all H4 tails are bound.

The EPR data raised two possibilities for how SNF2h binds the nucleosome in the apo and ADP states: (a) SNF2h symmetrically binds both H4 tails and each H4 tail exists in a two-state equilibrium between mobile and immobile states (with an equilibrium constant of 1) or, (b) SNF2h asymmetrically binds only one of the two H4 tails. For model (a), we expect immobilization to increase upon lowering temperature as the highly mobile state is entropically favored whereas the structured immobile state is enthalpically favored, as seen for docking of the kinesin neck linker²⁹. The fraction of H4 tails immobilized was unchanged, within error, from 23°C to 4°C (Fig. 1d, 54.6% immobilized at 4°C and 23°C). A van't Hoff plot of the equilibrium constant for H4 tail mobility as a function of temperature yields a ΔH of 0.76 kJ/mol, and ΔS of 4.4×10^{-3} kJ/mol-K (Supplementary Fig. 3), values that are substantially smaller than the favorable ΔH of 50 kJ/mol and unfavorable ΔS of 0.17 kJ/mol-K for docking of the kinesin neck linker²⁹. These data rule out model (a) and provide strong support for the asymmetric binding of model (b). To further test model (b) we used hydroxyl radical footprinting of the same nucleosome construct to follow changes in ACF contacts as a function of nucleotide state (Fig. 1c). In the apo state, ACF binding induces asymmetric protection of nucleosomal DNA: protection is observed in the SHL(-2) region, but not the SHL(+2) region, consistent with other ISWI complexes and with model (b)^{9,30}. In contrast, in the ADP•BeF_x state, ACF binding results in significant protection in both SHL(-2) and SHL(+2) regions, consistent with the EPR data.

The asymmetry with respect to H4 tail binding observed in the apo state could arise either (a) due to the presence of asymmetric flanking DNA or (b) due to structural constraints placed by the apo state. To distinguish between these possibilities we repeated the EPR experiment using nucleosomes with 60bp of flanking DNA on both sides (60-601-60 template). Apo-SNF2h still bound only one of the two H4 tails in the context of this symmetric nucleosome (Fig. 1b). These data strongly support a model in which apo-SNF2h can only bind one H4 tail at a time, and the availability of flanking DNA biases which side of the nucleosome the enzyme binds preferentially. Together the above data suggest that the enzyme switches between an asymmetric conformation where it interacts with one H4 tail at a time in the apo state and a more symmetric conformation where it binds both H4 tails in the ADP•BeF_x state.

The observation that SNF2h binds both H4 tails in the presence of ADP•BeF_x suggests that either (a) one SNF2h molecule bridges both H4 tails or, (b) SNF2h binds as a dimer such that each ATPase contacts an H4 tail. To distinguish between these models we first investigated the oligomeric state of SNF2h alone. Using equilibrium analytical ultra-centrifugation we found that unbound SNF2h is a monomer (data not shown). Because several well-studied dimeric helicases dimerize upon binding their DNA substrates, we next determined if SNF2h dimerizes on nucleosomes³¹. If dimerization of SNF2h is tightly coupled to nucleosome binding we expected to see cooperative SNF2h binding. We measured the binding to nucleosomes by taking advantage of our observation that the fluorescence of a Cy3 dye

attached near the entry site of the DNA increases upon SNF2h binding (Fig. 2a). We find that in the apo state, SNF2h binds to the nucleosome cooperatively, consistent with previous observations of cooperative binding by the *Drosophila* ISWI protein³². The Hill Coefficient of 1.8 suggests that at least two molecules of SNF2h bind in a manner such that binding of one molecule is strongly coupled to binding of the second (Fig. 2b). The EPR data from Figure 1 and the Hill Coefficient of 1.8, together suggest that in the apo state, SNF2h binds as a dimer but only one of the two SNF2h molecules engages an H4 tail.

To determine whether two SNF2h molecules were necessary to mediate maximal nucleosome remodeling, we measured the dependence of chromatin remodeling activity on SNF2h concentration using a FRET-based method (Fig. 2c). The rate constant of remodeling also depends cooperatively on SNF2h concentration with a Hill Coefficient of 1.8 (Fig. 2d, left panel). We next determined if the entire ACF complex also functions most effectively as a dimer. We analogously saw a cooperative dependence of the remodeling rate constant on ACF concentration with a Hill Coefficient of 1.9 (Fig. 2d, right panel). Together, these data strongly suggest that the predominant functional form of ACF is a dimer of ATPases.

A hallmark of dimeric motors such as kinesin and the *E. coli* Rep helicase is that they cycle between states in which one motor subunit is engaged with the substrate and states in which both motor subunits are transiently engaged³¹.

By working in coordinated pairs, one motor subunit can serve as an anchor to the other moving motor to prevent dissociation from the substrate. The ATP state helps regulate the affinity of the motor for the substrate. Our EPR results suggest that a SNF2h dimer analogously cycles between at least two states, one in which only one ATPase engages an H4 tail and another in which both ATPases engage the two H4 tails. To determine if these different conformational states reflect states with different affinities, we measured the affinity of SNF2h for the nucleosome in different ATP states (Fig. 2e). In the presence of ADP, SNF2h bound cooperatively but with slightly weaker affinity than in the apo state. In both the apo and ADP states, the high cooperativity of binding indicates that binding of one SNF2h molecule by itself is very weak and requires the presence of another SNF2h molecule to increase its overall affinity. The cooperativity could arise either from direct SNF2h-SNF2h contacts or could be mediated through a conformational change in the nucleosome without direct SNF2h-SNF2h contacts. In the presence of ADP•BeF_x, the K_{1/2} for SNF2h binding is ~3-fold lower than that in the apo state indicating a stronger binding affinity. Further, SNF2h binding in the presence of ADP•BeF_x is not cooperative (Hill Coefficient =1). These data suggest that in presence of ADP•BeF_x the affinity of each SNF2h molecule is sufficiently high such that binding of one SNF2h molecule is no longer highly dependent on the presence of the other.

Our finding that two ATPases are required for maximal nucleosome remodeling raises the question of how the nucleosome structure accommodates two SNF2h molecules. Other dimeric motors, such as kinesin and helicases, are oriented such that each ATPase subunit can take turns

translocating on the polymeric substrate in the same direction³¹. We used negative stain electron microscopy to visualize the complex of SNF2h with nucleosomes in the presence of ADP•BeF_x (Fig. 3 and Supplementary Fig. 4 and Supplementary Methods). Nucleosomes with 60bp of flanking DNA (0-601-60) were incubated with SNF2h concentrations comparable to the $K_{1/2}$ for nucleosomes in the presence of ADP•BeF_x, adsorbed to a glow discharged carbon film, and negatively stained with uranyl formate. The specimen was imaged at tilt angles of 60° and 0° (Supplementary Fig. 5). A total of 10,059 pairs of particles were interactively selected from 100 image pairs.

Classification of particles from images of untilted specimen shows three distinct classes (Fig. 3a, b) that can be clearly recognized as a nucleosome by itself and a nucleosome with either one or two SNF2h molecules bound. On average ~70% of the complexes contained two SNF2h molecules bound. The singly bound SNF2h molecules could reflect the use of non-saturating SNF2h, a technical necessity to prevent particle crowding on the grid. In the complexes with two SNF2h molecules bound, the flanking DNA was not clearly visible in the two-dimensional (2D) class averages, possibly because the flanking DNA is flexible and gets averaged out. An alternative possibility is that in most of the complexes, the flanking DNA is rearranged due to interaction with a domain of SNF2h. Consistent with this possibility we do not clearly observe the extended HAND-SANT-SLIDE domain that has been shown to interact with flanking DNA in the apo state¹⁷. We hypothesize that there may be a conformational rearrangement of the HAND-SANT-SLIDE domain in the presence of ADP•BeF_x. Further, no large region of direct

contact between the two SNF2h molecules is apparent, consistent with the Hill Coefficient of 1.0 in this state (Fig. 2e).

In the 2D class averages, the region of each SNF2h monomer that interacts with the nucleosome appears to contain two globular lobes (Fig. 3a). These lobes may represent the two RecA-related ATP binding folds observed in SF2 family motors^{33,34}. The two lobes are also apparent in the 2D class averages of SNF2h alone (Fig. 3c and Supplementary Fig. 6). Three-dimensional (3D) reconstructions of the nucleosome with two (or one) SNF2h bound were calculated using the well-established random conical tilt approach to a resolution of ~ 27 Å without the explicit application of any two-fold symmetry (Fig. 3a and Supplementary Figs 5 and 7)³⁵. The two SNF2h molecules face each other on the nucleosome, and seem to obey the 2-fold symmetry of the nucleosome with one putative ATPase domain at SHL(+2) and one at SHL(-2) (Fig. 3a, 2-fold or opposing symmetry most apparent in the middle panel). Consistent with the EPR and footprinting data in Figure 1, each SNF2h monomer seems to directly contact one H4 N-terminal tail and the SHL(-2)/(+2) regions in the ADP•BeF_x state. While the overall architecture appears almost symmetric, given the 27 Å resolution, any local structural asymmetries that may exist between the two SNF2h molecules cannot be resolved.

The above architecture raises the question of how the dimeric partners cooperate rather than compete in a “tug of war.” Our findings suggest an “alternating action” model schematized in Figure 4. In this model, each

ATPase takes turns in engaging the flanking DNA on either side and the corresponding H4 tail at SHL(-2) or (+2)^{9,17}. An ability of the two ATPases to take turns, as suggested by our observation that the apo state of the enzyme engages only one H4 tail at a time, would help avoid a “tug of war” situation. The ATPase that engages the longer DNA hydrolyzes ATP faster, as previously shown^{8,36}. This ATPase becomes the leading ATPase and sets the direction of nucleosome movement by translocating on nucleosomal DNA^{37,38}. The leading ATPase generates a DNA loop/wave that can propagate across the histone octamer as suggested previously³⁹⁻⁴¹. The second, subordinate ATPase could then further act as another anchor to stabilize the intermediate while the leading ATPase is translocating (Fig. 4, mimicked by ADP•BeF_x). Interaction with the second H4 tail may help in the binding of the subordinate ATPase. In the simplest version of this model, the subordinate ATPase does not bind or hydrolyze ATP once the leading ATPase fires⁴². This division of labor between identical subunits is analogous to hexameric helicases where occupancy of one ATPase subunit regulates the affinity of an adjacent subunit for nucleotide⁴³. Whether the communication between the two ATPases is direct or through the nucleosome remains an important future question. A variation of this model in which the non-leading ATPase also hydrolyzes ATP is described in Supplementary Figure 8. Successive rounds of sampling and translocation would then equalize the DNA on either side of a nucleosome. A dimer-based mechanism is also indicated by single-molecule data showing that dimeric ACF complexes can switch the direction of nucleosome translocation several times without dissociation (supporting manuscript by Blosser et al.). Our results help explain the significance of previous

observations that two *Drosophila* ACF molecules can bind in the context of DNA and provide a mechanistic explanation for the processive action of ISWI complexes^{3,44,45}.

We hypothesize that in contrast to kinesin and dimeric helicases, whose biological functions require unidirectional translocation along a largely uniform polymeric substrate, the biological functions of chromatin-remodeling enzymes like ACF place very different demands on motor architecture. The opposing architecture of the two motors in ACF may enable ACF to rapidly and processively change the direction of nucleosome movement in order to achieve a defined spacing. It will be interesting to investigate whether bidirectional movement via dimerization is a general feature of enzymes that space nucleosomes, and whether remodeling enzymes with other activities use different strategies.

Methods Summary

EPR measurements were performed with an EMX EPR spectrometer from Bruker Instruments (Billerica, MA). First derivative, X-band spectra were recorded in a high-sensitivity microwave cavity using 50-s, 100-Gauss wide magnetic field sweeps. EM samples were adsorbed to a glow-discharged copper grid coated with carbon film for 30 seconds followed by conventional negative stain with 0.75% uranyl formate. Images were collected using a Tecnai T12 microscope (FEI company, Hillsboro, OR) and recorded at a magnification of 52,000X with an UltraScan 4096 x 4096 pixel CCD camera (Gatan Inc, USA). Full methods are described in Supplementary Methods.

Supplementary Information accompanies the paper on www.nature.com/nature.

Acknowledgements. We thank J. Widom (Northwestern University) for the 601 plasmid. We thank H. Madhani, M.D. Simon, and members of the Narlikar Lab for helpful discussion and comments on the manuscript. We thank R. Howard for help with AUC; W. Ross, J. Lin, S. Hota and B. Bartholomew for advice on footprinting; and C. Cunningham for assistance with nucleosome depiction. This work was supported by grants from the Sandler Family Supporting Foundation (Sandler Opportunity Award and New Technology Award in Basic Science to Y.C, Program for Breakthrough Biomedical Research (PBBR) Award to G.J.N.), UCSF Academic Senate Shared Equipment Grant (to Y.C), grants from the National Institutes of Health

(to R.C. and G.J.N) and by the Beckman Foundation (to G.J.N.). P.P. and J.G.Y. were supported by US National Science Foundation Graduate Research Fellowships. G.J.N is a Leukemia and Lymphoma Society Scholar. G.J.N. wishes to acknowledge D. Herschlag's productive mentorship.

Author Information. Correspondence and requests for materials should be addressed to

G.J.N. (e-mail: Geeta.Narlikar@ucsf.edu) and Y.C. (e-mail: YCheng@ucsf.edu)

REFERENCES

- ¹ Corona, D. F. *et al.* ISWI regulates higher-order chromatin structure and histone H1 assembly in vivo. *PLoS Biol* **5**, e232 (2007).
- ² Fyodorov, D. V., Blower, M. D., Karpen, G. H. & Kadonaga, J. T. Acf1 confers unique activities to ACF/CHRAC and promotes the formation rather than disruption of chromatin in vivo. *Genes Dev* **18**, 170-183 (2004).
- ³ Ito, T., Bulger, M., Pazin, M. J., Kobayashi, R. & Kadonaga, J. T. ACF, an ISWI-containing and ATP-utilizing chromatin assembly and remodeling factor. *Cell* **90**, 145-155 (1997).
- ⁴ Varga-Weisz, P. D. *et al.* Chromatin-remodelling factor CHRAC contains the ATPases ISWI and topoisomerase II. *Nature* **388**, 598-602 (1997).
- ⁵ Deuring, R. *et al.* The ISWI chromatin-remodeling protein is required for gene expression and the maintenance of higher order chromatin structure in vivo. *Mol Cell* **5**, 355-365 (2000).
- ⁶ Poot, R. A. *et al.* HuCHRAC, a human ISWI chromatin remodelling complex contains hACF1 and two novel histone-fold proteins. *Embo J* **19**, 3377-3387 (2000).
- ⁷ Bochar, D. A. *et al.* A family of chromatin remodeling factors related to Williams syndrome transcription factor. *Proc Natl Acad Sci U S A* **97**, 1038-1043 (2000).
- ⁸ Yang, J. G., Madrid, T. S., Sevastopoulos, E. & Narlikar, G. J. The remodeling enzyme ACF is an ATP-dependent DNA length sensor that

- regulates nucleosome spacing. *Nat Struct Mol Biol* **13**, 1078-1083 (2006).
- ⁹ Kagalwala, M. N., Glaus, B. J., Dang, W., Zofall, M. & Bartholomew, B. Topography of the ISW2-nucleosome complex: insights into nucleosome spacing and chromatin remodeling. *Embo J* **23**, 2092-2104 (2004).
- ¹⁰ Sun, F. L., Cuaycong, M. H. & Elgin, S. C. Long-range nucleosome ordering is associated with gene silencing in *Drosophila melanogaster* pericentric heterochromatin. *Mol Cell Biol* **21**, 2867-2879 (2001).
- ¹¹ Corona, D. F. *et al.* ISWI is an ATP-dependent nucleosome remodeling factor. *Mol Cell* **3**, 239-245 (1999).
- ¹² Aalfs, J. D., Narlikar, G. J. & Kingston, R. E. Functional differences between the human ATP-dependent nucleosome remodeling proteins BRG1 and SNF2H. *J Biol Chem* **276**, 34270-34278 (2001).
- ¹³ Eberharter, A. *et al.* Acf1, the largest subunit of CHRAC, regulates ISWI-induced nucleosome remodelling. *Embo J* **20**, 3781-3788 (2001).
- ¹⁴ Langst, G., Bonte, E. J., Corona, D. F. & Becker, P. B. Nucleosome movement by CHRAC and ISWI without disruption or trans-displacement of the histone octamer. *Cell* **97**, 843-852 (1999).
- ¹⁵ Ito, T. *et al.* ACF consists of two subunits, Acf1 and ISWI, that function cooperatively in the ATP-dependent catalysis of chromatin assembly. *Genes Dev* **13**, 1529-1539 (1999).
- ¹⁶ Durr, H., Flaus, A., Owen-Hughes, T. & Hopfner, K. P. Snf2 family ATPases and DExx box helicases: differences and unifying concepts

- from high-resolution crystal structures. *Nucleic Acids Res* **34**, 4160-4167 (2006).
- ¹⁷ Dang, W. & Bartholomew, B. Domain architecture of the catalytic subunit in the ISW2-nucleosome complex. *Mol Cell Biol* **27**, 8306-8317 (2007).
- ¹⁸ Grune, T. *et al.* Crystal structure and functional analysis of a nucleosome recognition module of the remodeling factor ISWI. *Mol Cell* **12**, 449-460 (2003).
- ¹⁹ Clapier, C. R., Langst, G., Corona, D. F., Becker, P. B. & Nightingale, K. P. Critical role for the histone H4 N terminus in nucleosome remodeling by ISWI. *Mol Cell Biol* **21**, 875-883 (2001).
- ²⁰ Clapier, C. R., Nightingale, K. P. & Becker, P. B. A critical epitope for substrate recognition by the nucleosome remodeling ATPase ISWI. *Nucleic Acids Res* **30**, 649-655 (2002).
- ²¹ Hamiche, A., Kang, J. G., Dennis, C., Xiao, H. & Wu, C. Histone tails modulate nucleosome mobility and regulate ATP-dependent nucleosome sliding by NURF. *Proc Natl Acad Sci U S A* **98**, 14316-14321 (2001).
- ²² Fazio, T. G., Gelbart, M. E. & Tsukiyama, T. Two distinct mechanisms of chromatin interaction by the Isw2 chromatin remodeling complex in vivo. *Mol Cell Biol* **25**, 9165-9174 (2005).
- ²³ Ferreira, H., Flaus, A. & Owen-Hughes, T. Histone modifications influence the action of Snf2 family remodelling enzymes by different mechanisms. *J Mol Biol* **374**, 563-579 (2007).

- ²⁴ Zofall, M., Persinger, J. & Bartholomew, B. Functional role of extranucleosomal DNA and the entry site of the nucleosome in chromatin remodeling by ISW2. *Mol Cell Biol* **24**, 10047-10057 (2004).
- ²⁵ Langst, G. & Becker, P. B. ISWI induces nucleosome sliding on nicked DNA. *Mol Cell* **8**, 1085-1092 (2001).
- ²⁶ Rice, S. *et al.* A structural change in the kinesin motor protein that drives motility. *Nature* **402**, 778-784 (1999).
- ²⁷ Lowary, P. T. & Widom, J. New DNA sequence rules for high affinity binding to histone octamer and sequence-directed nucleosome positioning. *J Mol Biol* **276**, 19-42 (1998).
- ²⁸ Naber, N., Purcell, T. J., Pate, E. & Cooke, R. Dynamics of the nucleotide pocket of myosin measured by spin-labeled nucleotides. *Biophys J* **92**, 172-184 (2007).
- ²⁹ Rice, S. *et al.* Thermodynamic properties of the kinesin neck-region docking to the catalytic core. *Biophys J* **84**, 1844-1854 (2003).
- ³⁰ Schwanbeck, R., Xiao, H. & Wu, C. Spatial contacts and nucleosome step movements induced by the NURF chromatin remodeling complex. *J Biol Chem* **279**, 39933-39941 (2004).
- ³¹ Lohman, T. M., Thorn, K. & Vale, R. D. Staying on track: common features of DNA helicases and microtubule motors. *Cell* **93**, 9-12 (1998).
- ³² Chin, J., Langst, G., Becker, P. B. & Widom, J. Fluorescence anisotropy assays for analysis of ISWI-DNA and ISWI-nucleosome interactions. *Methods Enzymol* **376**, 3-16 (2004).

- 33 Durr, H., Korner, C., Muller, M., Hickmann, V. & Hopfner, K. P. X-ray structures of the *Sulfolobus solfataricus* SWI2/SNF2 ATPase core and its complex with DNA. *Cell* **121**, 363-373 (2005).
- 34 Thoma, N. H. *et al.* Structure of the SWI2/SNF2 chromatin-remodeling domain of eukaryotic Rad54. *Nat Struct Mol Biol* **12**, 350-356 (2005).
- 35 Radermacher, M. *et al.* Cryo-electron microscopy and three-dimensional reconstruction of the calcium release channel/ryanodine receptor from skeletal muscle. *J Cell Biol* **127**, 411-423 (1994).
- 36 Stockdale, C., Flaus, A., Ferreira, H. & Owen-Hughes, T. Analysis of nucleosome repositioning by yeast ISWI and Chd1 chromatin remodeling complexes. *J Biol Chem* **281**, 16279-16288 (2006).
- 37 Zofall, M., Persinger, J., Kassabov, S. R. & Bartholomew, B. Chromatin remodeling by ISW2 and SWI/SNF requires DNA translocation inside the nucleosome. *Nat Struct Mol Biol* **13**, 339-346 (2006).
- 38 Whitehouse, I., Stockdale, C., Flaus, A., Szczelkun, M. D. & Owen-Hughes, T. Evidence for DNA translocation by the ISWI chromatin-remodeling enzyme. *Mol Cell Biol* **23**, 1935-1945 (2003).
- 39 Cairns, B. R. Chromatin remodeling: insights and intrigue from single-molecule studies. *Nat Struct Mol Biol* **14**, 989-996 (2007).
- 40 Strohner, R. *et al.* A 'loop recapture' mechanism for ACF-dependent nucleosome remodeling. *Nat Struct Mol Biol* **12**, 683-690 (2005).
- 41 Langst, G. & Becker, P. B. Nucleosome remodeling: one mechanism, many phenomena? *Biochim Biophys Acta* **1677**, 58-63 (2004).

- ⁴² Racki, L. & Narlikar, G. ATP-dependent chromatin remodeling enzymes: two heads are not better, just different. *Curr Opin Genet Dev* **18**, 137-144 (2008).
- ⁴³ Enemark, E. J. & Joshua-Tor, L. On helicases and other motor proteins. *Curr Opin Struct Biol* **18**, 243-257 (2008).
- ⁴⁴ Fyodorov, D. V. & Kadonaga, J. T. Dynamics of ATP-dependent chromatin assembly by ACF. *Nature* **418**, 897-900 (2002).
- ⁴⁵ Gangaraju, V., Prasad, P., Srour, A., Kagalwala, M. & Bartholomew, B. Conformational changes associated with template commitment in ATP-dependent chromatin remodeling by ISW2. *Mol Cell* **35**, 58-69 (2009).
- ⁴⁶ He, X., Fan, H. Y., Narlikar, G. J. & Kingston, R. E. Human ACF1 alters the remodeling strategy of SNF2h. *J Biol Chem* **281**, 28636-28647 (2006).

FIGURE LEGENDS

Figure 1. ATP state regulates immobilization of the histone H4 tail and proximal interactions. (a) Left panels: EPR spectra of MSL labeled 0-601-60 nucleosomes. Right panels: Schematic interpretation of EPR spectra, based on data from (a), (c), & (d). Binding of Apo SNF2h to the nucleosome decreases the mobility of half the H4 tails. SNF2h binding in the presence of ADP•BeF_x decreases the mobility of both H4 tails. (b) EPR spectrum of Apo SNF2h bound to spin-labeled 60-601-60 nucleosomes reveals that only one of the two H4 tails is immobilized. (c) Hydroxyl radical foot-printing of ACF on 0-601-60 nucleosomes. Top panel: schematic of mononucleosome structure with 12 bp of flanking DNA on one side, with dyad in green, histone H4 in blue, and the region surrounding SHL (-2) and (+2) in red. Middle panel: Protection patterns for nucleosomes alone (black line, N) compared to nucleosomes bound by Apo-ACF (red line, N+ACF). Bottom panel: nucleosomes alone (black line, N) compared to nucleosomes bound by ACF in the presence of ADP•BeF_x (red line, N+ACF+ ADP•BeF_x). Yellow bars highlight protection in the SHL (-2) and (+2) regions. (d) Temperature dependence of probe immobilization in the Apo SNF2h-nucleosome complex. Slope of the straight line = $2.1 \times 10^{-4} \pm 8 \times 10^{-4}$ immobilized fraction/°C. Error represents s.e.m.

Figure 2. SNF2h and ACF function as dimers of ATPases. (a) Schematic of nucleosome structure with dye attachment sites for (b) and (d). The DNA is end-labeled with Cy3 (blue) on the shorter flanking DNA. The octamer is

labeled with Cy5 at H2A-120C (yellow). (b) Cy3 fluorescence intensity of the construct shown in (a) as a function of SNF2h concentration, using nucleosomes with 78bp of flanking DNA on one side. A representative replicate curve is shown. Data are fit to the general equation for cooperative binding (see Methods). Hill Coefficient (n) = 1.8 ± 0.17 ; $K_{1/2} = 353 \pm 30$ nM. (c) Schematic of FRET-based nucleosome remodeling assay. Rate constant of remodeling is measured by following the decrease in FRET between Cy3 and Cy5 in the presence of ATP. (d) Left panel: Nucleosome remodeling rate constant as a function of SNF2h concentration for nucleosomes with 78bp of flanking DNA. Right panel: Nucleosome remodeling rate constant as a function of ACF concentration for nucleosomes with 20 bp of flanking DNA. Hill Coefficient (n) = 1.8 ± 0.1 ; $K'_{1/2} = 281 \pm 32$ nM for SNF2h and Hill Coefficient (n) = 1.9 ± 0.3 ; $K'_{1/2} = 26 \pm 3$ nM for ACF. Each panel represents global fits to data obtained from three independent experiments. (e) SNF2h binds as a cooperative dimer to the nucleosome in the absence of nucleotide (black circles), and in the presence of ADP (blue squares). In the presence of ADP•BeF_x, SNF2h binds non-cooperatively (red triangles). These binding measurements were carried out with nucleosomes containing 40bp of flanking DNA on one side and a Cy3 label on the short DNA end. Binding of SNF2h to these nucleosomes is ~2-fold weaker relative to the nucleosomes used in (b)^{9,46}. A representative replicate curve with each nucleotide analogue is shown (left panel), and the average $K_{1/2}$ and Hill Coefficient from three replicates is shown (table). Errors represent s.e.m.

Figure 3. Visualization of SNF2h bound to the nucleosome in the presence of ADP•BeF_x using EM. (a) three different views of the 3-D reconstruction of dimeric SNF2h bound to the nucleosome (left panels) and corresponding representative 2-D class averages (right panels). The crystal structure of the core mononucleosome was placed manually into the 3D reconstruction. Histone H4 is highlighted in red. The isosurface of the 3-D reconstruction at high threshold is shown in blue, and low threshold in grey. (b) Left panel: representative 2-D class average of negative stain EM images of unbound nucleosomes. Right panel: representative 2-D class average of one SNF2h bound to a nucleosomes. Numbers used to calculate a particular class average shown in lower left corner in (a) and (b). (c) Representative 2-D class averages of SNF2h alone.

Figure 4. Simple model for how a dimeric ACF moves nucleosomes. H4 tail is in red and the two ATPases in ACF are shown in blue and purple. Only one subunit binds ATP at a time. In the ATP state, each ATPase subunit takes turns in binding the flanking DNA. The ATPase that binds the longer flanking DNA (purple) hydrolyzes ATP faster and starts translocating DNA across the nucleosome. During and post hydrolysis, the second ATPase (blue) also engages the nucleosome, preventing loss of the DNA loop-containing intermediate (mimicked by ADP•BeF_x). In the ADP state, the non-translocating monomer disengages and the translocating monomer remains engaged with the nucleosome. ATP state may also regulate the extent of any direct contacts

between the two ATPase subunits and such contacts may be substantially fewer in the ADP-BeFx state than in other ATP states.

FIGURE 1

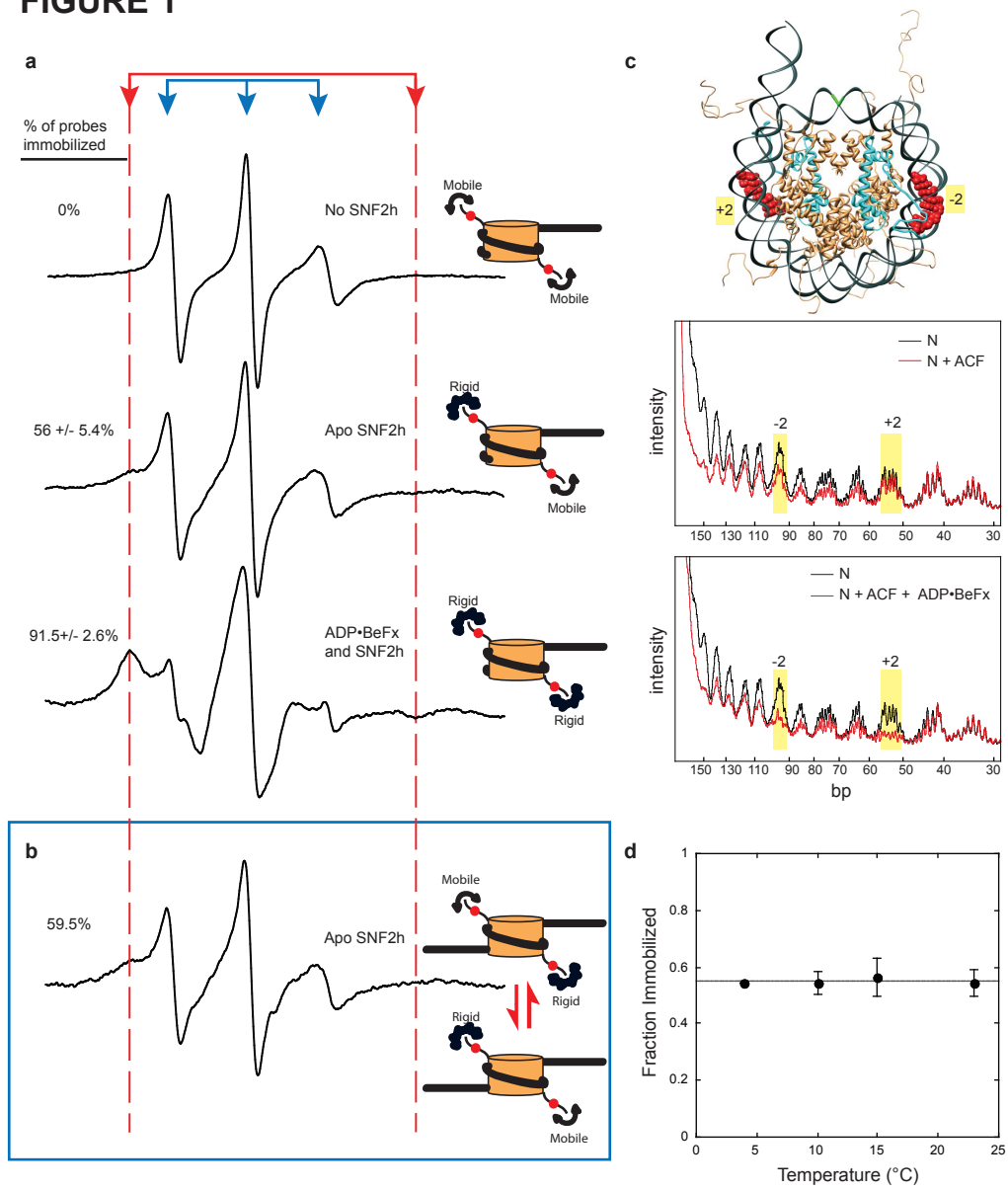


FIGURE 2

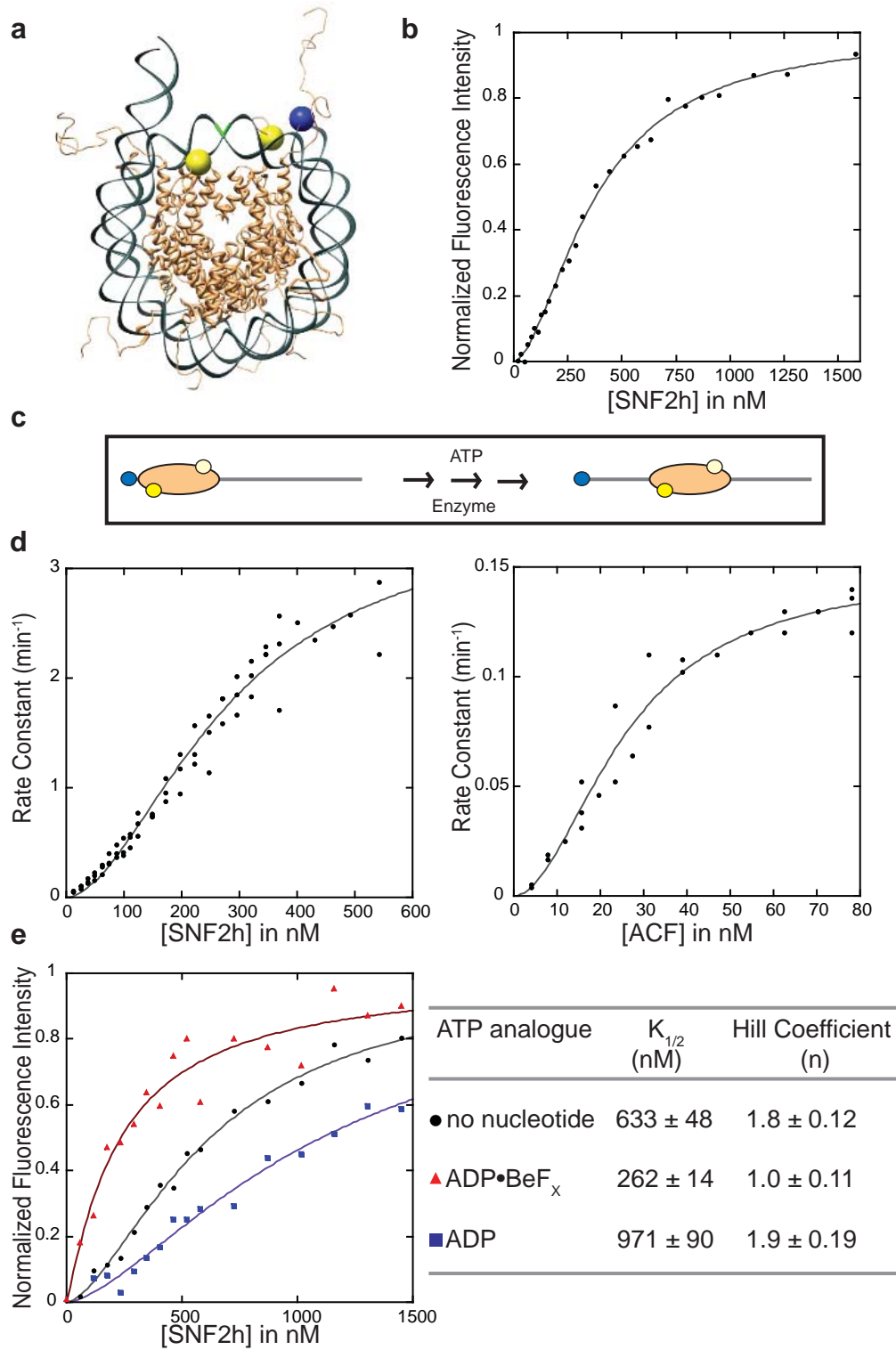


Figure 3

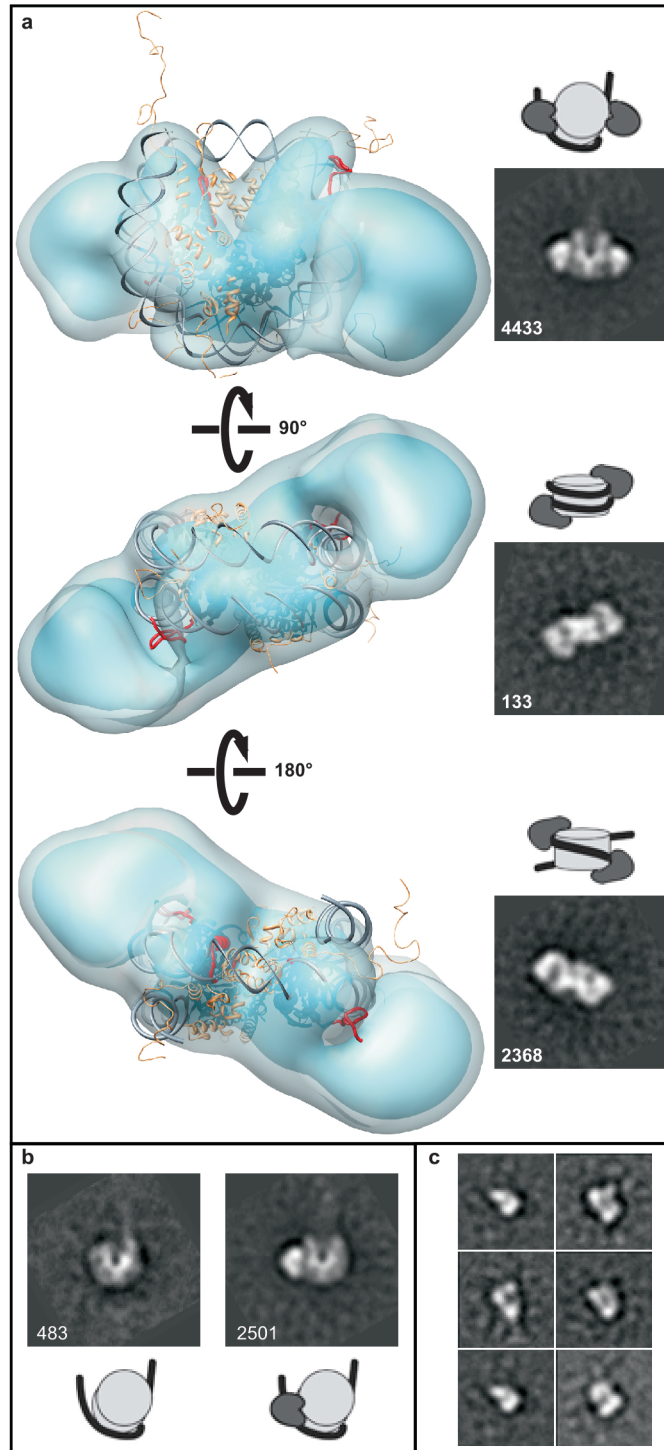
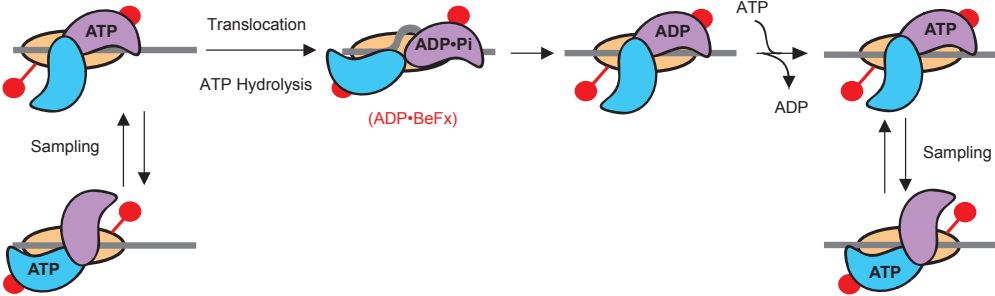


FIGURE 4



Supplementary Information

The chromatin remodeler ACF acts as a dimeric motor to space nucleosomes

Lisa R. Racki, Janet G. Yang, Nariman Naber, Peretz Partensky, Ashley Acevedo, Thomas J. Purcell, Roger Cooke, Yifan Cheng, & Geeta J. Narlikar

Supplementary Information Contents:

- Supplementary Figure 1: DNA sequences used to construct nucleosomes in this work.
- Supplementary Figure 2: Deconvolution of spectra to determine the fraction of bound spin probes.
- Supplementary Figure 3: A van't Hoff plot for A15C-MSL nucleosomes with 60 bp of flanking DNA on one side (0-601-60) bound by SNF2h in the apo state.
- Supplementary Figure 4: SNF2h-nucleosome complex.
- Supplementary Figure 5: Random conical tilt 3D reconstruction of SNF2h-nucleosome complex.
- Supplementary Figure 6: Images of negatively stained nucleosomes and SNF2h alone.
- Supplementary Figure 7: Monomeric SNF2h bound to the nucleosome in the presence of ADP•BeF_x.
- Supplementary Figure 8: An alternative model for how the two ATPase molecules cooperate to achieve nucleosome movement.

References for SI

SUPPLEMENTARY FIGURES

Supplementary Figure 1. a. Schematic of nucleosomal constructs. The locations of SHL(-2) and (+2) with reference to the linker DNA are shown. b. Maleimide spin labelling of histone H4 tail of the nucleosome. Left panel: nucleosome structure with histone H4 in blue and the site of attachment of the spin label (MSL) in red (residue A15 of H4 is mutated to cysteine). Superhelical locations (SHL) -2, 0, and +2 (black arrows) are defined relative to the flanking DNA on one side. Right panel: structure of MSL.

Supplementary Figure 2. Deconvolution of spectra to determine the fraction of bound spin probes. The fraction of immobilized probe was calculated by deconvolution of spectra into a mobile and immobilized component. a. Representative mobile (blue) and immobilized (green) spectra were added so that the sum (red) best matched the sample spectrum (black in part b.) by least squares minimization. The spectra of spin labeled nucleosomes alone contained no evidence of the immobilized component and the average of three such spectra was taken as 100% mobile compound. The spectra from spin-labeled nucleosomes with SNF2h and ADP•BeF_x are primarily immobilized with a small mobile component, approximately 90% and 10% respectively. The representative immobilized spectrum was derived by averaging 3 samples, followed by subtraction of 9.4% representative mobile spectrum to yield a pure immobilized spectrum. c. Residuals (grey) from fitting in b.

Supplementary Figure 3. A van't Hoff plot for A15C-MSL nucleosomes with 60 bp of flanking DNA on one side (0-601-60) bound by SNF2h in the apo state. Deconvolution of spectra into mobile and immobile components as described in supplementary methods was used to obtain values for the equilibrium constant for H4 tail mobility as a function of temperature (4°C to 23°C): $K = [(\text{immobile fraction})/(\text{mobile fraction})]$. These data are displayed as a plot of $-\text{Rln}(K)$ in kJ/(Kelvin-mol) vs. $1/T$ in Kelvin⁻¹. A fit to the van't Hoff equation gives a ΔH of -0.76 ± 2.3 kJ/mol, and ΔS of $4.4 \times 10^{-3} \pm 8.1 \times 10^{-3}$ kJ/mol K. For comparison, the ΔH and ΔS values associated with the classic example of the unstructured to structured transition of the kinesin neck-linker are respectively -50 kJ/mol and -0.17 kJ/mol K, which are two orders of magnitude greater in absolute value¹.

Supplementary Figure 4. SNF2h-nucleosome complex. (a) An image of negatively stained SNF2h-nucleosome complex. Indicated by arrowhead in the raw image are three types of particles: nucleosomes alone (1), nucleosomes with one SNF2h bound (2), and two SNF2h bound (3). Class averages calculated from images of untilted specimen. (b) Nucleosome with monomeric SNF2h bound and (c) Nucleosome with dimeric SNF2h bound. Only particles with SNF2h bound were selected for multiple rounds of multi-reference alignment and classification. Numbers in b and c indicate the total number of particles in each class.

Supplementary Figure 5. Random conical tilt 3D reconstruction of SNF2h-nucleosome complex. (a) and (b): raw images of a typical tilt pair images. (c) Fourier Shell Correlation (FSC) curve of 3D reconstructions calculated by standard random conical tilt approach. FSC=0.5 criteria is used to estimate the resolution of the 3D reconstruction as $\sim 27\text{\AA}$.

Supplementary Figure 6. Images of negatively stained nucleosomes and SNF2h alone. (a) Negative stain electron microscopy images of nucleosomes with 60bp of flanking DNA on one side alone. 2-D Class average shows two top views (insert). (b) images of SNF2h monomers alone; (c) 2-D Class averages show multiple views of SNF2h monomers. (d) 2-D Class average of SNF2h dimer bound to the nucleosome as a reference for size.

Supplementary Figure 7. Monomeric SNF2h bound to the nucleosome in the presence of ADP•BeF_x. (a) Top view of 3-D reconstruction by random conical tilt of 1454 particle pair images of monomeric SNF2h bound to the nucleosome with 60bp of flanking DNA on one side, docked manually onto the core mononucleosome crystal structure. Histone H4 is highlighted in red. Isosurface with higher threshold is in blue, and lower threshold is in grey. (b) and (c) alternate views. (d) 2-D class average of singly bound nucleosome. (e) resolution of the 3-D reconstruction is estimated from FCS=0.5 as ~ 30 angstroms.

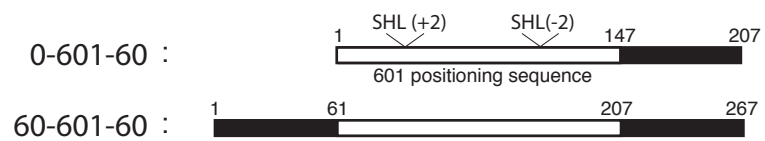
Supplementary Figure 8. An alternative model for how the two ATPase molecules cooperate to achieve nucleosome movement. In this model, different ATP hydrolysis events occur in the two ATPase sites. The dimeric ATPase samples both sides of the nucleosome such that at any point only one ATPase subunit engages one of the two flanking DNAs. The ATPase that engages the longer flanking DNA (purple) more often hydrolyzes ATP first and thereby determines the directionality of subsequent nucleosome movement. This hydrolysis event loosens a small stretch of DNA from the histone octamer making it available for translocation. The second ATPase (blue) then hydrolyzes ATP and translocates the DNA to generate a DNA loop. At this stage both the ATPase subunits closely engage the nucleosome to prevent loss of the loop containing intermediate. In this model, the two ATPase subunits cooperate through a division of labor. One subunit hydrolyzes ATP to loosen DNA and the other hydrolyzes ATP during translocation. The direction of nucleosome movement is switched when the division of labor is switched based on which subunit engages the longer flanking DNA. Such coordination is achieved by ATPase cycles that are offset. One way in which these cycles can be offset is shown in the Figure. As shown, ADP•BeF_x may mimic a state in which one ATPase has ADP•Pi (blue) and the other (purple) has ADP. Because ADP•BeF_x is formed by mixing ADP and BeF_x, it is possible that one subunit is occupied by ADP and the other is occupied by ADP•BeF_x.

REFERENCES FOR SUPPLEMENTARY FIGURES

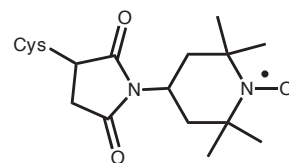
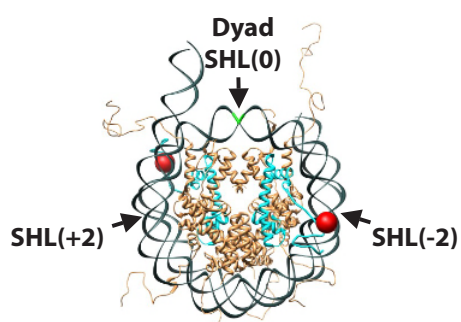
- 1 **Rice, S. *et al.* Thermodynamic properties of the kinesin neck-region docking to the catalytic core. *Biophys J* 84, 1844-1854 (2003).**

FIGURE S1

a



b



Maleimide Spin Label (MSL)

Figure S2

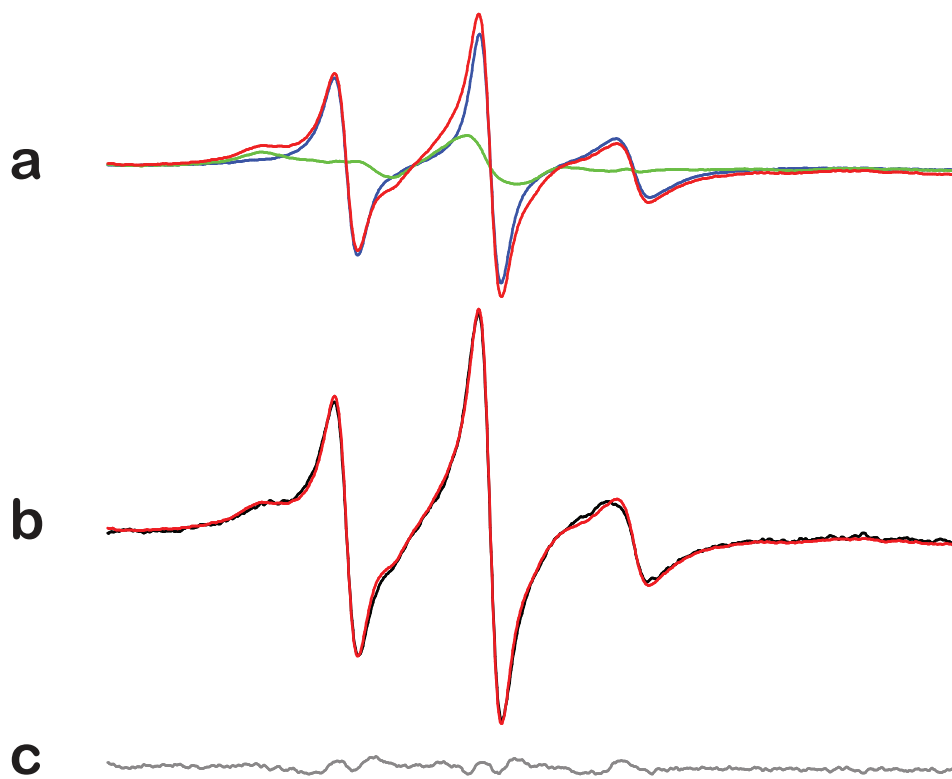


FIGURE S3

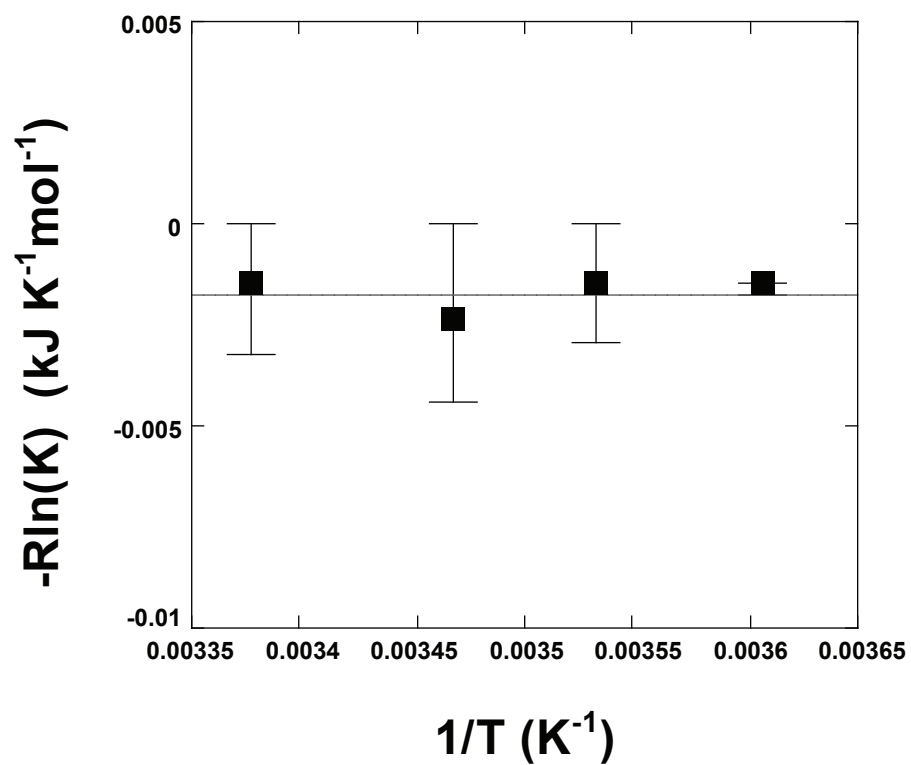


Figure S4

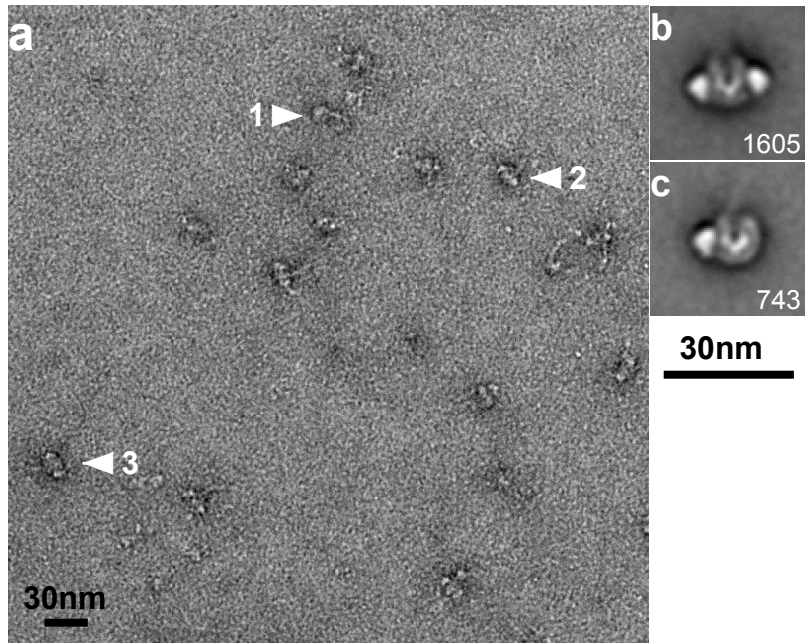


Figure S5

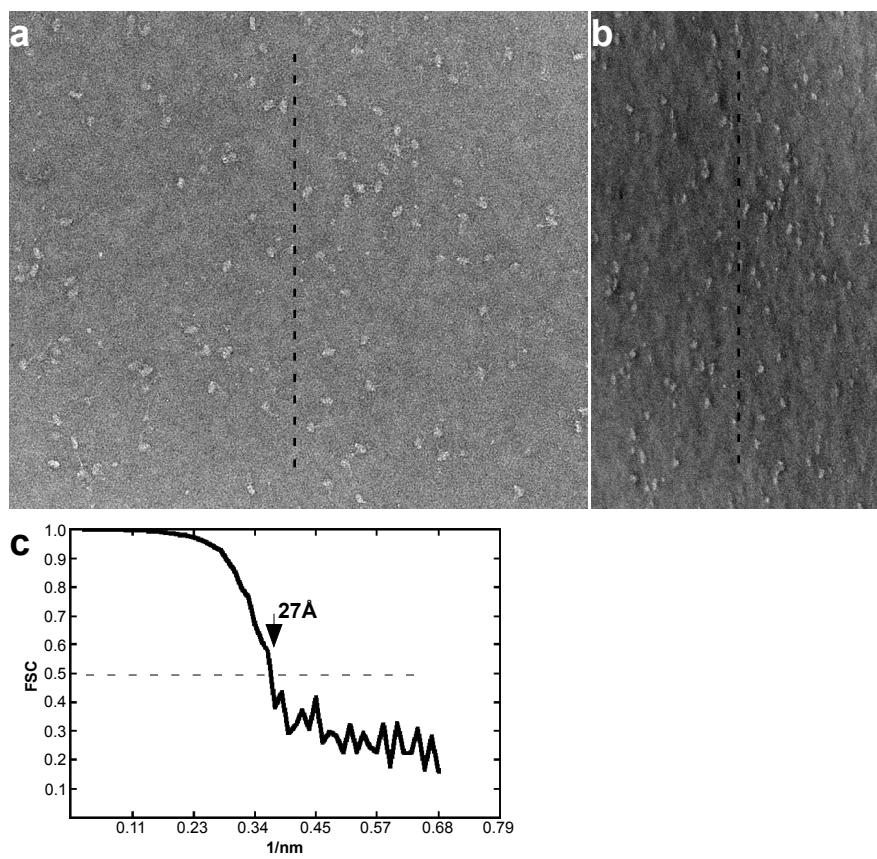


Figure S6

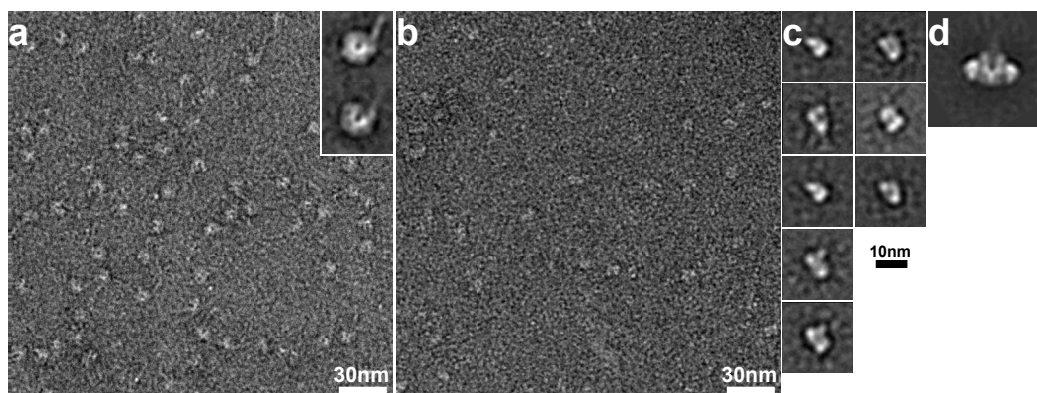


Figure S7

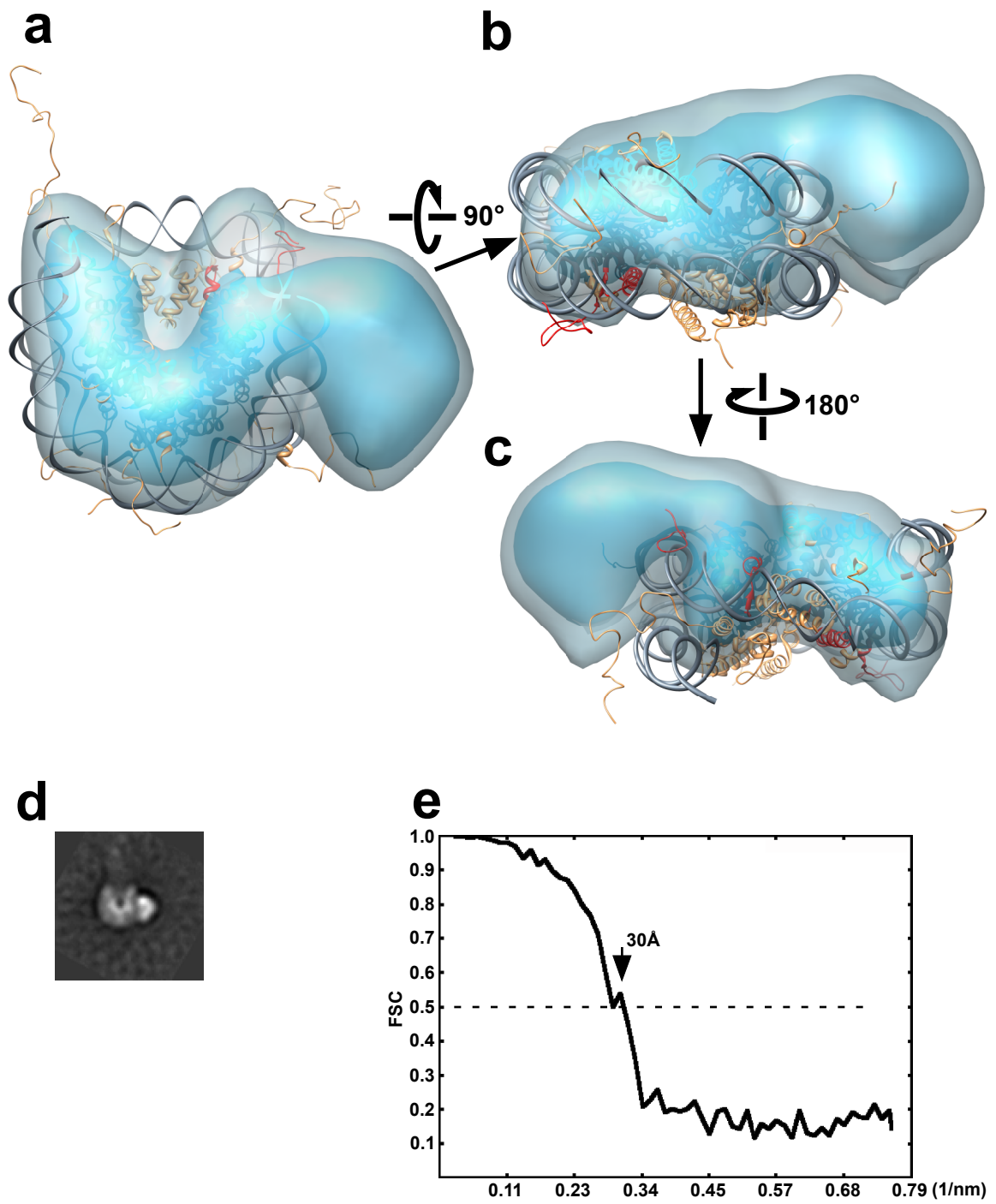
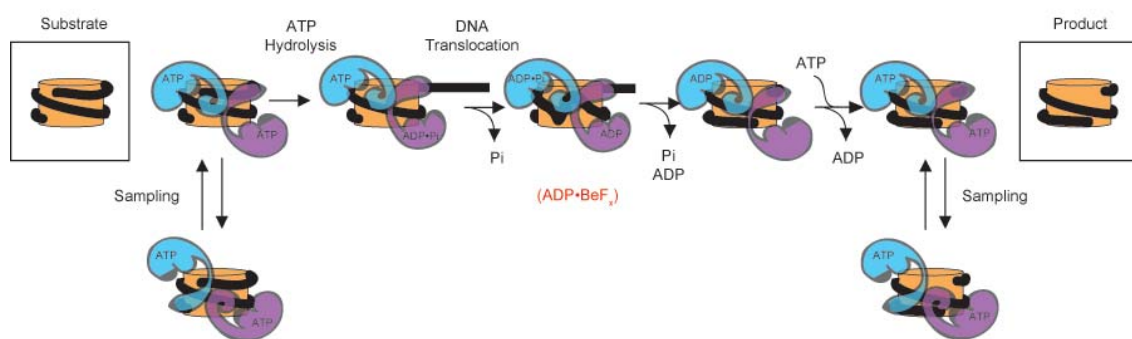


Figure S8



Chapter 3

Synergy Between Substrate Cues of ACF

1. Introduction

ACF uses two key components of the substrate to move nucleosomes: Flanking DNA and the histone H4 tail. Both substrate cues have been shown to promote ATP hydrolysis and remodeling by ACF¹⁻⁶. These epitopes thus play critical roles, though the physical and mechanistic basis for their interaction with the enzyme is not well understood. The H4 tail and flanking DNA act as dynamic signals which the enzyme must recognize and integrate in order to act appropriately, thus we call them 'substrate cues.' Footprinting and crosslinking studies suggest that in the apo-state (no nucleotide), the ATPase domain of ACF interacts with the nucleosome at SHL(±2) on the nucleosomal DNA, where the flexible histone H4 tail emerges from the nucleosome core particle, and the SLIDE domain of ACF interacts with flanking DNA^{3,5,7}. While these data provide basic information about which domains of ACF interact with the substrate cues, neither flanking DNA nor the H4 tail appear to exert their effects on ground state affinity of the enzyme for nucleosomes, as observed by several groups. The H4 tail has been shown not to have a large effect on the K_m of the enzyme for nucleosomes, and while K_m/K_d effects have been observed for flanking DNA length, the magnitude of these effects is smaller than their effects on k_{cat} ^{4,8,9}. Thus both cues play a role in catalysis, and serve as useful handles to probe ACF mechanism and potentially identify intermediate steps in the reaction cycle of ACF. This study is focused on elucidating how dimeric ACF interprets and integrates the H4 tail and flanking DNA cues.

2. The H4 tail and flanking DNA cues affect remodeling as probed by FRET

Both the H4 tail and flanking DNA have previously been shown to affect nucleosome remodeling rates of ACF, but it is not known how ACF integrates these two cues into its mechanochemical cycle. Two broad classes of mechanistic models are possible: ACF could use the two cues in separate rate-limiting steps (Model 1), or ACF could use the two cues in the same rate limiting step (Models 2a and 2b) (Figure 1). If ACF uses the two cues in the same rate-limiting step, the two cues could function additively (Model 2a) or cooperatively (Model 2b). Model 2a predicts that the effects of the two cues will be additive on activity, whereas Models 1 and 2b both predict that the effects of the cues on enzyme activity will be non-additive.

To distinguish between these classes of models, we measured remodeling rates for ACF with nucleosome substrates containing neither, one, or both of the cues. Nucleosomes lacking the H4 tails (termed gH4 for globular domain of histone H4, see Figure 2a), and containing 20 base pairs of flanking DNA on one side of the nucleosome (termed +20), move nucleosomes with a k_{\max} of $0.54 \pm 0.022 \text{ min}^{-1}$ under single turnover (STO) conditions with saturating ATP and ACF. In comparison, gH4 nucleosomes containing 80 base pairs of flanking DNA, which is longer than the maximal length sensing of ACF, move

nucleosomes 4.6-fold faster than the gH4+20 nucleosomes. Similarly, nucleosomes with 20 base pairs of DNA but containing the wild type H4 tails move nucleosomes 3.7-fold faster than the gH4+20 nucleosomes. However, wt+80 nucleosomes, which contain both 80 base pairs of flanking DNA and the H4 tail, move the nucleosomes 149-fold faster than gH4+20 nucleosomes. Thus the cues function non-additively, but rather in a cooperative manner to promote nucleosome remodeling (See Table 1).

This observation of the cooperative effects of the cues supports Models 1 and 2b over Model 2a. ACF functions as a dimer to move nucleosomes, however it is not known whether both protomers must hydrolyze ATP to get efficient nucleosome remodeling. Single molecule experiments indicate that moving the nucleosome a single step requires at least two ATP-hydrolysis dependent steps, suggesting that more than one ATP may be hydrolyzed to move the nucleosome a single step¹⁰. One possibility is that there are two types of ATP hydrolysis, corresponding to the two rate-limiting steps in Model 1. Alternatively, both ATP hydrolysis events use both cues, consistent with Model 2b. We therefore wanted to examine the effect of the H4 tail and flanking DNA on ATP hydrolysis.

3. The H4 tail and flanking DNA cues both stimulate ATP hydrolysis in the context of the nucleosome.

The H4 tail and flanking DNA have both previously been shown to affect ATP hydrolysis rates as well as nucleosome remodeling^{2,4,5,8,9,11}. We sought to determine the magnitude of these effects on ATP hydrolysis. Neither the H4 tail nor the flanking DNA appeared to have significant effects on the K_m of enzyme for ATP in the context of the nucleosome (Figure 2b, 3b and data not shown). To compare the effects of the H4 tail and flanking DNA cues on maximal ATP hydrolysis rates, we used slightly different nucleosome constructs: Nucleosomes lacking both flanking DNA and the H4 tail (termed gH4 core), lacking the H4 tail but containing 60bp of DNA flanking both sides of the nucleosome (termed gH4 60-60), nucleosomes with the H4 tail but no flanking DNA (termed Wt core), and nucleosomes with both the H4 tail and 60bp of flanking DNA on both sides (Wt 60-60) (Figure 3a). The rationale for using core and 60-60 DNA constructs instead of the +20 and +80 constructs used in the FRET remodeling assay was to maximize the window of potential effects of the cues, because in general the cues have smaller effects on ATP hydrolysis than on remodeling. SNF2h is stimulated by extranucleosomal or flanking DNA, and this stimulation is proportional to flanking DNA length⁴. Under STO nucleosome conditions, with saturating concentrations of ACF and multiple turnover (MTO), saturating concentrations of ATP, gH4 6060 nucleosomes stimulate ATP hydrolysis only 1.2-fold more than gH4 core nucleosomes. Wt core nucleosomes stimulate ATP hydrolysis 1.4-fold more than gH4 core nucleosomes. However, wt 60-60 nucleosomes stimulate ATP hydrolysis 5.5-fold more than gH4 core

nucleosomes. The effects of the H4 tail and flanking DNA on ATP hydrolysis thus appear to be non-additive (Table 1).

The STO nucleosome conditions used in this experiment to match the conditions used in FRET remodeling assays pose a practical constraint: The rate constants measured in this manner are very sensitive to error in the concentrations of the four types of nucleosome constructs. To address this practical concern, we also measured ATPase rate constants under MTO, saturating nucleosome conditions to minimize any variability in measured rate constants due to subtle differences in concentrations of the four nucleosome constructs (Figure 3d). Interestingly, we also observe that the measured rate constants under MTO, saturating nucleosome and ATP concentrations are significantly larger than observed under the STO nucleosome conditions (188 min⁻¹ under MTO conditions for wt 60-60 nucleosomes instead of 9.2min⁻¹ under STO conditions). Nucleosomes lacking flanking DNA but containing the H4 tail (termed wt core) are stimulated 3.4-fold more than nucleosomes lacking both the H4 tail and flanking DNA (termed gH4 core, meaning globular H4) under saturating, MTO ATP and nucleosome concentrations (Figure 3a,b). Nucleosomes with 60 bp of DNA on both sides of the nucleosome (termed gH4 60-60) are stimulated 2.1-fold more than nucleosomes without flanking DNA (termed gH4 core). Nucleosomes with both flanking DNA and the H4 tail (termed wt 6060) are stimulated 40-fold more than gH4 core nucleosomes. The effects of the H4 tail and flanking DNA on ATP hydrolysis are thus non-additive.

It is possible that there are two ATP hydrolysis events in nucleosome remodeling, and each cue plays a role in one of these events (Model 1), or that the two cues act in a coupled manner (Model 2).

In an attempt to distinguish between these models, we looked at the effect of the cues on ATP hydrolysis under STO ATP conditions, but with MTO, saturating nucleosomes. ATP binding to ACF is not cooperative (Figure 2d,3b). We reasoned that given that ATP binding is not cooperative in the enzyme dimer, under STO conditions we might be able to observe the first ATP hydrolysis event. If only one of the substrate cues, the flanking DNA or the H4 tail, affects ATP hydrolysis under STO ATP conditions, this may rule out that the cue act in the same step. We observe that both cues have effects under STO ATP conditions, but of smaller magnitude (on the order of 2-fold slower than with with Wt 60-60 nucleosomes) than observed under MTO, saturating ATP conditions (Figure 3e). This observation is initially hard to reconcile with a two-step model, and is most easily explained by both steps acting in the same step. However, additional experiments and thinking is needed to distinguish between these models.

4. Physical Models for how H4 tail and Flanking DNA may promote ATP hydrolysis

While it is thought that the N-terminal ATPase domain of SNF2h interacts with the H4 tail and the c-terminal HAND/SANT/SLIDE alpha helical domain interacts with flanking DNA, how these interactions promote ATP hydrolysis is not known. Moreover, the contacts between the enzyme dimer and the nucleosome likely change as a function of nucleotide state. For example, in the apo and ADP states of the complex, only one H4 tail is bound by SNF2h, whereas in the presence of the nucleotide analogue ADP BeFx, both H4 tails are immobilized¹².

i. ATPase pocket closure

In many SF1 and SF2 family helicases, binding of DNA or RNA promotes closure of the two RecA lobes of the ATPase domain onto ATP, thus promoting catalysis^{13,14}. The ATPase domain of chromatin remodeling enzyme consists of two RecA like lobes separated by a flexible linker, and ATP binds in a cleft between these lobes. While the WalkerA and WalkerB catalytic motifs both are on the 1A RecA lobe, the arginine finger is often on lobe 1B, which is displaced from bound ATP. Pocket closure thus drives the arginine finger into position to promote catalysis. Interestingly, structural studies with the related remodeling enzyme Rad54 suggest that the two lobes can rotate 180° with respect to each other¹⁵⁻¹⁷. One possible role for the substrate cues is that binding of one or both of them could help promote the closed conformation of the ATPase domain. If the ATPase pocket is in a two state equilibrium between open and closed

conformations, it is possible that binding of the substrate cues could preferentially stabilize the closed conformation of the pocket. For example, if one RecA lobe makes strong contacts with nucleosomal DNA, but the other RecA-lobe makes fewer contacts with the nucleosome core particle, but can bind the H4 tail, binding of the tail could stabilize the closed state (Figure 4a). An acidic patch on the ATPase domain has been hypothesized to potentially interact with the basic patch of the H4 tail¹⁸.

ii. Relief from autoinhibition

A variation of the pocket closure model comes from recent findings with another family of chromatin remodeling enzymes, Chd1, where the two RecA lobes of the enzyme are physically propped open by a third domain, and thus in an autoinhibited state where they cannot close onto ATP¹⁹. The third autoinhibitory domain can bind to the histone H3 n-terminal tail, relieving inhibition. It is possible that the short N-terminal domain of SNF2h before the ATPase domain binds the H4 tail, or that the C-terminal HAND/SANT/SLIDE domain of SNF2h which is thought to bind flanking DNA could also serve as an autoinhibitory domain in the absence of flanking DNA (Figure 4b).

iii. The Arginine finger hypothesis

One potential role for the H4 tail could be to participate in catalysis by directly stabilizing the transition state during ATP hydrolysis. One of the arginines of the H4 tail basic patch, K16R17H18R19 could act as an arginine finger, substituting for the enzyme's endogenous arginine finger on RecA-like lobe 2A (Figure 4c).

5. The H4 tail but not flanking DNA is required for a restricted conformation of the ATP binding pocket

i. SNF2h binds to spin labeled nucleotide analogues

In order to better understand how the H4 tail and flanking DNA cues affect the ATP binding pocket, we used a nucleotide analogue with a nitroxide moiety to probe the active site²⁰. A spin labeled ATP analogue with the spin probe on the 2'3' hydroxyls of ATP (2'3'SLATP) supports remodeling by SNF2h (Figures 5a,b). Moreover, 2'3'SLADP binds to SNF2h alone, with an affinity of 3.3uM (Figure 5c). Binding of SNF2h also induced a restricted conformation of the spin probe of 47.4G, corresponding to a cone angle of mobility for the probe of 118.8°²¹. The cone angle of mobility is defined by a region of space the probe can sample due to thermal motion. This tumbling space is determined by the adjacent protein surface of the enzyme in the nucleotide binding pocket.

Beryllium fluoride is thought to mimic the gamma phosphate of ATP in an activated intermediate in ATP hydrolysis²².

i. A new conformational state of the ATP binding pocket in the presence of nucleosomes

In the presence of wild-type nucleosomes with 60 base pairs of flanking DNA (wt +60), SNF2h induces a restricted conformation of the 2'3'probe on ADP of 47.7G corresponding to 117.8°, as is observed with SNF2h alone (Figures 5, 6a, black spectrum). In the presence of Beryllium Fluoride (BeFx) and wt+60 nucleosomes, SNF2h induces a dramatic conformational change in the ATP-binding pocket that further restricts the cone angle of mobility for 2'3'SLADP from 117.8° to 68.8°*(62G*). Note that these values have asterixes because the precise splitting could not be determined from this spectrum. The equilibrium between the 48G and 62G conformations of 2'3'SLADP shows a temperature dependence. With Wt 60-60 nucleosomes, we observe that the 62G restricted conformation is favored at higher temperature (30°C), but the 48G less restricted conformation is favored at lower temperature (2°C) indicating that this conformational restriction is entropically driven (Figure 7).

ii. The H4 tail but not flanking DNA are required for the conformational restriction of the ATP binding pocket of SNF2h

In order to determine how the H4 tail and flanking DNA cues affect ATP hydrolysis, we examined the effects of the cues on the conformational state of the ATP binding pocket of SNF2h. SNF2h in the presence of nucleosomes with flanking DNA but lacking the H4 tail (gH4+60) bound 2'3' SLADP and induced a 48.1G conformation corresponding to a cone angle of mobility of 116.4°(Figure 6b). In the presence of beryllium fluoride, however, the 62G conformation was not obtained. These data indicate that the H4 promotes a more restricted conformation of the ATP binding pocket of SNF2h.

SNF2h with nucleosomes lacking flanking DNA but containing the H4 tail (wt core) bind 2'3'SLADP and can induce a 47.2G conformation of the nucleotide binding pocket corresponding to a 116.4° cone angle (Figure 6c). However, flanking DNA appears to be dispensable for inducing the more restricted conformation of the nucleotide binding pocket (61.9G, or 68.8°). This result indicates that the H4 tail but not flanking DNA plays a role in this conformational state of the enzyme. This result supports a model in which the H4 tail and flanking DNA act in different steps during the mechanochemical cycle of dimeric enzyme (Model 1). However, the 2'3' spin probe is only sensitive to very local conformational changes, thus it is possible that flanking DNA may play an EPR-invisible role on the conformation of the nucleotide pocket. In this scenario, the flanking DNA and H4 tail cues could still act in a coupled fashion in the same step (Model 2b).

5. The H4 tail and flanking DNA play a role in coupling ATP hydrolysis to nucleosome remodeling.

The flanking DNA and H4 tail cues have disproportionate effects on ATP hydrolysis and nucleosome remodeling rates, as measured by the FRET remodeling assay. Removal of flanking DNA or the H4 tail causes a 3.9 and 4.9-fold defect on ATP hydrolysis respectively, but causes an order of magnitude more deleterious effects on nucleosome remodeling rates under comparable conditions (40-fold for flanking DNA, and 33-fold for the H4 tail) (Table 1). These data suggest that the substrate cues may play a role not only in ATP hydrolysis, but also coupling ATP hydrolysis to nucleosome remodeling.

The nucleosome remodeling rates obtained from bulk FRET experiments, however, reflect multiple translocation steps. Thus it is possible that the substrate cues may have an uncoupled effect on measured remodeling rates because they act at each of several FRET-sensitive translocation steps. The FRET dye pair we used reports on at least three nucleosome translocation steps, based on single molecule FRET experiments¹⁰. Gel upshift data, however, suggests that removal of the H4 tail has a comparable magnitude effect on the first translocation step visible by gel for ACF as we observe for the bulk FRET assay (Figure 11). Single molecule FRET experiments with a chase indicate that nucleosomes having moved the first 7bp step, collapse to the 10.5bp step size

observed by gel upshift.¹⁰ This data is consistent with the H4 tail playing a role in coupling ATP hydrolysis to remodeling. The parallel gel upshift experiment with shortened flanking DNA has not yet been performed and is technically challenging because it is difficult to resolve intermediate bands on a native gel with such short linker DNA. The H4 tail cue thus seems to play two roles in nucleosome remodeling: a catalytic role in driving ATP hydrolysis, and a role in coupling ATP hydrolysis to remodeling.

6. The H4 tail peptide can rescue ATP hydrolysis in trans, but not nucleosome remodeling.

We observe that the defect in ATP hydrolysis rates in nucleosomes lacking the H4 tail can be rescued by addition of exogenous peptide. Addition of a peptide containing the sequence of the first 19 amino acids deleted in the globular H4 tail mutant (H4T peptide) rescues ATP hydrolysis (Figure 8a). However, exogenous H4T peptide inhibits ATP hydrolysis at higher concentrations (Figure 8b).

The H4 tail peptide also promotes ATP hydrolysis in the context of naked DNA. However, the peptide alone cannot promote ATP hydrolysis¹¹. It is possible that the H4 tail forms a DNA-H4T epitope with local nucleosomal DNA at

SHL(± 2), which the enzyme contacts. It has been previously suggested that DNA-binding may drive a region of the H4 tail (residues 16-24) containing the basic patch (16-19) into an alpha-helical conformation^{23,24}. The potential DNA-binding activity of the H4T peptide alone, however, raises the possibility that the rescue of ATP hydrolysis we observe with nucleosomes is due to enzyme binding to peptide that is in contact with flanking DNA. To distinguish between these possibilities, we measured ATP hydrolysis rates as a function of H4T peptide concentration in the context of gH4 core nucleosomes, which lack flanking DNA. We see partial rescue of ATP hydrolysis in this context (Figure 8c). It is still possible, however, that the H4T peptide binds to nucleosomal DNA at different locations from SHL(± 2) and rescues ATP hydrolysis.

In contrast to the observed rescue of ATP hydrolysis by exogenous H4T peptide, nucleosome remodeling is not rescued (Figure 9). The correct attachment of the H4 tail thus appears to matter for nucleosome repositioning. It is possible that the H4 tail serves as a signal to direct the ATPase domain of ACF to bind the nucleosome at SHL(± 2) such that the enzyme can perform translocation in the correct orientation to get productive remodeling. In this model, the lack of physical connection to the histone octamer prevents the exogenous peptide from orienting the enzyme correctly. Alternatively, if the enzyme uses the H4 tail as a lever arm to exert force, the lack of physical connection to the histone octamer would also abrogate nucleosome remodeling.

7. Physical Models for how H4 tail and Flanking DNA may promote coupling of ATP hydrolysis to nucleosome remodeling.

i. Decrease alternative binding modes

Substrate cues could function to position the enzyme in a productive binding mode on the nucleosome. The nucleosome as a substrate is larger than the enzyme protomers, and likely offers alternative binding surfaces for the enzyme where it cannot hydrolyze ATP effectively. The flanking DNA and H4 tail may function to position the enzyme in the productive binding mode. One study suggests that removing either the H4 tail or flanking DNA decreases the footprint of the enzyme on nucleosomal DNA at SHL(± 2), where it is thought to bind, without dramatically altering the affinity for the nucleosome¹. Moreover, the H4 tail cannot rescue ATP hydrolysis or remodeling when grafted onto one of the other histone globular domains, suggesting that the H4 tail has a position-specific role at SHL(± 2) of the nucleosome^{11,25}.

ii. Point of attachment for force application

The H4 tail and flanking DNA could have a physical role as points of contact the enzyme may use to apply force to break histone-DNA contacts. For example, one commonly cited model for nucleosome remodeling is the 'loop propagation' model, where the enzyme reels in a region of flanking DNA onto the surface of

the octamer, and propagates this loop or bulge of distorted DNA around the histone octamer surface²⁶. Thus the enzyme may apply force during ATP hydrolysis to flanking DNA to pull it inwards.

It is also thought that ISWI family enzymes translocate along nucleosomal DNA at SHL(± 2). Nicks and gaps on nucleosomal DNA at SHL(± 2) have been shown to block nucleosome remodeling^{7,27}. These observations have been interpreted to suggest that ISWI remodeling enzymes are DNA translocases. The H4 tail, which is adjacent to SHL(± 2) could serve as a point of attachment that the translocating enzyme protomer uses to orient and maintain its position at SHL(± 2) as it moves along nucleosomal DNA and breaks histone-DNA contacts.

8. Extending the length of the H4 tail linker causes proportional defects on ATP hydrolysis and nucleosome remodeling rates.

To learn more about why the connection between the H4 tail and the histone octamer appears to matter for nucleosome remodeling, we made nucleosomes with histone H4 tail mutants where the distance between the globular domain and the basic patch has been increased by seven or 12 amino acids of either unstructured (Gly-Gly-Ser-Gly)_n linkers or linkers designed to have the propensity to form alpha-helices Ala(Glu-Ala-Ala-Ala-Lys)_nAla²⁸. We included the linkers with alpha-helical propensity because of previous observations and

speculation that amino acids 16-24 of the H4 tail may form an alpha helix upon interaction with local DNA rather than be unstructured as suggested by crystal structures generated under conditions of high divalent cation or spermine which could competitively shield these interactions^{23,24,29,30}. The formation of an alpha helix of amino acids 16-24 could result in an extension of a long alpha helix within the globular domain of H4 from residues 24-40 which is kinked at proline 32³¹. We hoped to potentially distinguish between the effects of linker extension and disruption of the putative alpha helix. From this preliminary experiment, we observe that there is an apparent length-dependent defect in both ATP hydrolysis and remodeling for the ser-gly extension mutants. (Figures 10,11) Moreover, these mutants have roughly proportional effects on both ATP hydrolysis and remodeling, rather than the uncoupling effect we observed for nucleosomes lacking the H4 tail completely. The lack of uncoupling effects is consistent with both possible models for the role of the H4 tail in coupling ATP hydrolysis to nucleosome repositioning. For the non-productive-binding model, the local concentration of the basic patch epitope is very high, and longer H4 tail linkers still bind to DNA at SHL(± 2) with high efficiency and orient the enzyme appropriately. For the force-bearing lever model, the linker lengths we chose may still be short enough to allow ACF to exert force on the nucleosome. In the case of the putative alpha-helical linker mutants, both the seven and 12 amino acid extensions have intermediate defects on ATP hydrolysis and nucleosome remodeling, and an apparent lack of length dependence in this preliminary experiment, but the differences are small(Figure 10,11). More experiments will

need to be done to determine what this difference in behavior of the flexible linker and the putative alpha helical linker means, but this result suggests that length and secondary structure of the H4 tail linker can alter the effects of the basic patch on ACF function in different ways.

9. Conclusions and Speculations

We observe synergy between the H4 tail and flanking DNA in promoting nucleosome remodeling. The non-additive effects of the cues on both nucleosome remodeling and ATP hydrolysis raise two classes of models for how the enzyme integrates these two kinds of information: In Model 1, each cue acts in a separate ATP hydrolysis event during nucleosome remodeling. In Model 2, both cues act cooperatively in the same ATP hydrolysis event. We observe that the H4 tail and flanking DNA are both required for ATP hydrolysis, but only the H4 tail and not the flanking DNA is required for a conformational change in the ATP binding pocket. This observation is consistent with Model 1, where two ATP hydrolysis events of the enzyme complex are qualitatively different (Figure 12a). But it is also possible that the effects of flanking DNA on the ATP binding pocket are not detectable by the spin probe which senses local environmental changes near the 2'3'hydroxyls of ATP. Our observation that under STO ATP conditions, both substrate cues matter, in conjunction with the observation that ATP binding is non-cooperative in the dimer, appear to be consistent with a model in which both cues act in the same ATP hydrolysis event (Model 2). In such a model, the

interactions between each cue and the enzyme are coupled, either allosterically or via direct interaction with each other (Figure 12b). More experiments will be needed to distinguish between these two classes of models.

We also observe an apparent uncoupling of the effects of the cues on ATP hydrolysis and nucleosome remodeling. Moreover, physical attachment of the H4 tail to the nucleosomes is dispensable for ATP hydrolysis, but vital for nucleosome remodeling. H4 tail extension mutants cause proportional length-dependent defects in both ATP hydrolysis and nucleosome remodeling. Taken together, these observations suggest that the substrate cues may play a role either in correctly orienting the enzyme on the nucleosome and thus decrease non-productive binding modes, or that the cues are used as physical points of attachment to exert physical force on the nucleosome and break histone-DNA contacts. The observations of non-additivity and uncoupling of the effects of the substrate cues must also be reconciled with the dimer hypothesis, where two protomers must communicate and integrate cue information on both sides of the nucleosome.

The observation that the substrate cues of flanking DNA and the H4 tail cooperatively stimulate enzyme activity raise the question as to why this might be biologically advantageous. Such coupled stimulation may help ensure high substrate specificity, and prevent ACF from acting on chromatin in the wrong context. When only one of the cues is available, very little stimulation occurs. So

for example in compacted chromatin, transient exposure of short stretches of flanking DNA or the H4 tail would not stimulate ACF. Only when both cues are simultaneous available, does the enzyme act at maximal capacity.

- 1 Dang, W., Kagalwala, M. N. & Bartholomew, B. Regulation of ISW2 by concerted action of histone H4 tail and extranucleosomal DNA. *Mol Cell Biol* **26**, 7388-7396, doi:26/20/7388 [pii] 10.1128/MCB.01159-06 (2006).
- 2 Clapier, C. R., Längst, G., Corona, D. F., Becker, P. B. & Nightingale, K. P. Critical role for the histone H4 N terminus in nucleosome remodeling by ISWI. *Mol Cell Biol* **21**, 875-883, doi:10.1128/MCB.21.3.875-883.2001 (2001).
- 3 Zofall, M., Persinger, J. & Bartholomew, B. Functional role of extranucleosomal DNA and the entry site of the nucleosome in chromatin remodeling by ISW2. *Mol Cell Biol* **24**, 10047-10057, doi:24/22/10047 [pii] 10.1128/MCB.24.22.10047-10057.2004 (2004).
- 4 Yang, J. G., Madrid, T. S., Sevastopoulos, E. & Narlikar, G. J. The chromatin-remodeling enzyme ACF is an ATP-dependent DNA length sensor that regulates nucleosome spacing. *Nat Struct Mol Biol* **13**, 1078-1083, doi:nsmb1170 [pii] 10.1038/nsmb1170 (2006).
- 5 Whitehouse, I., Stockdale, C., Flaus, A., Szczelkun, M. D. & Owen-Hughes, T. Evidence for DNA translocation by the ISWI chromatin-remodeling enzyme. *Mol Cell Biol* **23**, 1935-1945 (2003).
- 6 Stockdale, C., Flaus, A., Ferreira, H. & Owen-Hughes, T. Analysis of nucleosome repositioning by yeast ISWI and Chd1 chromatin remodeling complexes. *J Biol Chem* **281**, 16279-16288, doi:M600682200 [pii] 10.1074/jbc.M600682200 (2006).
- 7 Schwanbeck, R., Xiao, H. & Wu, C. Spatial contacts and nucleosome step movements induced by the NURF chromatin remodeling complex. *J Biol Chem* **279**, 39933-39941, doi:M406060200 [pii] 10.1074/jbc.M406060200 (2004).
- 8 Ferreira, H., Flaus, A. & Owen-Hughes, T. Histone modifications influence the action of Snf2 family remodelling enzymes by different mechanisms. *J Mol Biol* **374**, 563-579, doi:S0022-2836(07)01201-6 [pii] 10.1016/j.jmb.2007.09.059 (2007).
- 9 He, X., Fan, H. Y., Narlikar, G. J. & Kingston, R. E. Human ACF1 alters the remodeling strategy of SNF2h. *J Biol Chem* **281**, 28636-28647, doi:M603008200 [pii] 10.1074/jbc.M603008200 (2006).
- 10 Blosser, T. R., Yang, J. G., Stone, M. D., Narlikar, G. J. & Zhuang, X. Dynamics of nucleosome remodelling by individual ACF complexes. *Nature* **462**, 1022-1027, doi:nature08627 [pii] 10.1038/nature08627 (2009).

- 11 Clapier, C. R., Nightingale, K. P. & Becker, P. B. A critical epitope for substrate recognition by the nucleosome remodeling ATPase ISWI. *Nucleic Acids Res* 30, 649-655 (2002).
- 12 Racki, L. R. et al. *The chromatin remodeller ACF acts as a dimeric motor to space nucleosomes.* *Nature* 462, 1016-1021, doi:nature08621 [pii] 10.1038/nature08621 (2009).
- 13 Lee, J. Y. & Yang, W. UvrD helicase unwinds DNA one base pair at a time by a two-part power stroke. *Cell* 127, 1349-1360, doi:S0092-8674(06)01601-1 [pii] 10.1016/j.cell.2006.10.049 (2006).
- 14 Singleton, M. R., Dillingham, M. S. & Wigley, D. B. Structure and mechanism of helicases and nucleic acid translocases. *Annu Rev Biochem* 76, 23-50, doi:10.1146/annurev.biochem.76.052305.115300 (2007).
- 15 Lewis, R., Dürr, H., Hopfner, K. P. & Michaelis, J. Conformational changes of a Swi2/Snf2 ATPase during its mechano-chemical cycle. *Nucleic Acids Res* 36, 1881-1890, doi:gkn040 [pii] 10.1093/nar/gkn040 (2008).
- 16 Dürr, H., Körner, C., Müller, M., Hickmann, V. & Hopfner, K. P. X-ray structures of the *Sulfolobus solfataricus* SWI2/SNF2 ATPase core and its complex with DNA. *Cell* 121, 363-373, doi:S0092-8674(05)00298-9 [pii] 10.1016/j.cell.2005.03.026 (2005).
- 17 Thomä, N. H. et al. Structure of the SWI2/SNF2 chromatin-remodeling domain of eukaryotic Rad54. *Nat Struct Mol Biol* 12, 350-356, doi:nsmb919 [pii] 10.1038/nsmb919 (2005).
- 18 Dang, W. & Bartholomew, B. Domain architecture of the catalytic subunit in the ISW2-nucleosome complex. *Mol Cell Biol* 27, 8306-8317, doi:MCB.01351-07 [pii] 10.1128/MCB.01351-07 (2007).
- 19 Hauk, G., McKnight, J. N., Nodelman, I. M. & Bowman, G. D. The chromodomains of the Chd1 chromatin remodeler regulate DNA access to the ATPase motor. *Mol Cell* 39, 711-723, doi:S1097-2765(10)00622-2 [pii] 10.1016/j.molcel.2010.08.012 (2010).
- 20 Naber, N. et al. Closing of the nucleotide pocket of kinesin-family motors upon binding to microtubules. *Science* 300, 798-801, doi:300/5620/798 [pii] 10.1126/science.1082374 (2003).
- 21 Griffith, O. H. & Jost, P. C. *Spin Labeling Theory and Applications.* (Academic Press, 1976).
- 22 Petsko, G. A. Chemistry and biology. *Proc Natl Acad Sci U S A* 97, 538-540 (2000).
- 23 Johnson, L. M., Fisher-Adams, G. & Grunstein, M. Identification of a non-basic domain in the histone H4 N-terminus required for repression of the yeast silent mating loci. *EMBO J* 11, 2201-2209 (1992).

- 24 Banères, J. L., Martin, A. & Parello, J. The N tails of histones H3 and H4 adopt a highly structured conformation in the nucleosome. *J Mol Biol* 273, 503-508, doi:S0022-2836(97)91297-3 [pii] 10.1006/jmbi.1997.1297 (1997).
- 25 Hamiche, A., Kang, J. G., Dennis, C., Xiao, H. & Wu, C. Histone tails modulate nucleosome mobility and regulate ATP-dependent nucleosome sliding by NURF. *Proc Natl Acad Sci U S A* 98, 14316-14321, doi:251421398 [pii] 10.1073/pnas.251421398 (2001).
- 26 Strohner, R. et al. A 'loop recapture' mechanism for ACF-dependent nucleosome remodeling. *Nat Struct Mol Biol* 12, 683-690, doi:nsmb966 [pii] 10.1038/nsmb966 (2005).
- 27 Zofall, M., Persinger, J., Kassabov, S. R. & Bartholomew, B. Chromatin remodeling by ISW2 and SWI/SNF requires DNA translocation inside the nucleosome. *Nat Struct Mol Biol* 13, 339-346, doi:nsmb1071 [pii] 10.1038/nsmb1071 (2006).
- 28 Marqusee, S. & Baldwin, R. L. Helix stabilization by Glu-...Lys+ salt bridges in short peptides of de novo design. *Proc Natl Acad Sci U S A* 84, 8898-8902 (1987).
- 29 Richmond, T. J., Finch, J. T., Rushton, B., Rhodes, D. & Klug, A. Structure of the nucleosome core particle at 7 Å resolution. *Nature* 311, 532-537 (1984).
- 30 Luger, K., Mäder, A. W., Richmond, R. K., Sargent, D. F. & Richmond, T. J. Crystal structure of the nucleosome core particle at 2.8 Å resolution. *Nature* 389, 251-260, doi:10.1038/38444 (1997).
- 31 Davey, C. A., Sargent, D. F., Luger, K., Maeder, A. W. & Richmond, T. J. Solvent mediated interactions in the structure of the nucleosome core particle at 1.9 Å resolution. *J Mol Biol* 319, 1097-1113, doi:S0022-2836(02)00386-8 [pii] 10.1016/S0022-2836(02)00386-8 (2002).

Figure Legends

Figure 1. Mechanistic models for how ACF integrates substrate cues into its mechanochemical cycle. a. Two step model (Model 1). In this model, ACF could have two rate-limiting steps of similar magnitude. Each cue acts to catalyze one of the two rate-limiting steps. As it is drawn, the flanking DNA promotes k_1 (blue), and the H4 tail promotes k_2 (red). In this model, the defect of one cue in the double mutant is partially masked by the effect of the other cue. b. Same step model (Model 2). In this model, there is one rate-limiting step in the reaction cycle in which both cues can act, k_2 (purple). If the cues act in the same step, they could act additively, or cooperatively.

Figure 2. The H4 tail and flanking DNA cues affect nucleosome remodeling as probed by FRET. a. Nucleosome constructs. gH4+20 nucleosomes have 20bp of DNA flanking the nucleosome on one side, and lack the H4 tail. gH4+80 nucleosomes have 80bp of DNA flanking the nucleosome on one side, and lack the H4 tail. Wt+20 nucleosomes have 20bp of flanking DNA on one side, and wild-type histone tails. Wt+80 nucleosomes have 80bp of flanking DNA on one side, and wild-type histone tails. b. Representative FRET traces of nucleosome remodeling rates with saturating [ACF], saturating [ATP] (2mM), and under single-turnover conditions for nucleosomes (5nM). FRET reactions performed as described previously and in Methods^{1,2}. Rate constants: Wt+80 $k_{obs} = 11 \text{ min}^{-1}$ with 25nM ACF; wt+20 $k_{obs} = 0.185 \text{ min}^{-1}$ with 25nM ACF; gH4+80 $k_{obs} =$

0.289min⁻¹ with 25nM ACF; gH4+20 kobs = 0.059 with 100nM ACF. c. Average kmax values for nucleosome remodeling. Wt+80 8.03min⁻¹ (The value is extrapolated from the Km curve for [ATP] in Figure 2d, as rate constants for this nucleosome construct are too fast to measure accurately with saturating ATP and ACF); wt+20 0.198±0.038 min⁻¹; gH4+80 0.247±0.087min⁻¹; gH4+20 0.054±0.022min⁻¹. d. FRET remodeling as a function of [ATP]. With 25nM ACF, single-turnover Wt+80 nucleosomes, and varying [ATP], kmax = 8.03, Km (ATP) = 24.5uM, Hill Coefficient n = 0.854. Errors represent s.d.m.

Figure 3. The H4 tail and flanking DNA substrate cues affect ATP

hydrolysis. The experiments in this figure are preliminary and have been done once (n=1). ATPases were performed as described previously and in the Methods section¹. a. Nucleosome constructs. gH4 core nucleosomes lack flanking DNA and the H4 tail. gH4 60-60 nucleosomes have 60bp of DNA flanking both sides of the nucleosome core particle, but lack the H4 tail. Wt core nucleosomes lack flanking DNA but have the H4 tail. Wt 60-60 nucleosomes have 60bp of DNA flanking both sides of the nucleosome core particle, and contain the H4 tail. b. Under single turnover nucleosome conditions (250nM nucleosomes, 500nM SNF2h), fixing the Hill Coefficient in the fit to n=1, the Km of SNF2h for ATP with gH4 60-60 nucleosomes is 53uM, and with gH4 core nucleosomes it is 56uM. c. Effects of cues on ATP hydrolysis under single turnover nucleosome (5nM), multiple turnover saturating ATP (200uM), and saturating ACF conditions (25nM). For gH4 core nucleosomes kcat=1.68min⁻¹;

for gH4 60-60 nucleosomes $k_{cat}=1.88\text{min}^{-1}$; for wt core nucleosomes $k_{cat}=2.39$, for wt 60-60 nucleosomes $k_{cat} = 9.24$. d. Effects of cues on ATP hydrolysis under multiple turnover saturating nucleosome (200nM) and ATP concentrations (200uM) with 25nM ACF. For gH4 core nucleosomes $k_{cat}= 4.7\text{min}^{-1}$, for gH4 60-60 nucleosomes $k_{cat}=9.73$, for wt core nucleosomes $k_{cat} = 16\text{min}^{-1}$, for wt 60-60 nucleosomes $k_{cat} = 188\text{min}^{-1}$. e. Effects of cues on ATP hydrolysis under single turnover subsaturating ATP concentrations (1nM) as a function of nucleosome concentration with 5nM ACF. f. Time courses of single turnover ATPase assays from (e) at saturating [Nucleosomes]. For gH4 core nucleosomes at 75nM, $k_{obs} = 0.061\text{min}^{-1}$, for gH4 60-60 nucleosomes at 10nM, $k_{obs}=0.073\text{min}^{-1}$, for wt core nucleosomes at 50nM $k_{obs}= 0.053\text{min}^{-1}$, for wt 60-60 nucleosomes at 25nM $k_{obs} = 0.13\text{min}^{-1}$.

Figure 4. Physical Models for Effects of Cues on ATP active site. a. ATPase pocket closure. The substrate cues may promote closure of the two RecA-like lobes of the enzyme onto ATP. b. Relief from autoinhibition. A variation of the pocket closure model in which an autoinhibitory domain (yellow) props open the two RecA-like lobes of the ATP binding pocket. Binding of a substrate cue, the H4 tail in the illustrated example, releases this autoinhibitory domain, allowing for pocket closure. c. Arginine Finger hypothesis. In this model, one of the arginines in the basic patch of the H4, Arginine 17 or 19, substitutes for the endogenous arginine finger, and directly coordinates ATP in the active site.

Figure 5. Electron Paramagnetic Spin Spectroscopy with 2'3' Spin-labeled ATP. a. Structure of 2'3'SLATP. The nitroxide moiety is on the 2'3' hydroxyls. b. 2'3' SLATP and 2' SLATP support nucleosome remodeling by SNF2h. Endpoint gel upshift remodeling assay under single turnover nucleosome conditions with 20nM Wt+60 nucleosomes and 120nM SNF2h. 67uM of ATP, 2'3'SLATP, or 2'SLATP, 20 minute endpoint. c. 2'3' SLADP binds SNF2h alone and induces a 47.4G splitting, corresponding to a cone angle of mobility of 118.8°. EPR spectrum of 10uM 2'3'SLADP alone (black) and 10uM 2'3'SLADP in the presence of 16uM SNF2h (pink).

Figure 6. The H4 tail but not flanking DNA is required for SNF2h to induce a constrained conformation in the ATP binding pocket. Note that values with an asterisk indicate that the exact splitting could not be determined from the spectrum. Also note that for the spectra in this figure, we used 2'3'SLADP, which is hydrolyzed rapidly (on the order of minutes) under these conditions and before the sample goes into the EPR machine. a. In the presence of 12uM wt+60 nucleosomes, 30uM SNF2h induces a 47.7G splitting for the probe on 2'3'SLADP, corresponding to a cone angle of 117.8° (black spectrum). Addition of 0.5mM Beryllium Fluoride induces a more restricted conformation of the nucleotide binding pocket of 62G, corresponding to a cone angle of mobility of 68.8° (pink spectrum). b. In the presence of 11.2uM gH4+60 nucleosomes, 30uM SNF2h induces the 48.1G splitting for the probe on 2'3'SLADP, but the

addition of beryllium fluoride does not result in the more restricted conformation of the nucleotide binding pocket, indicating that the H4 tail promotes this conformation. c. In the presence of wt core nucleosomes, SNF2h induces a 47.2G splitting for the probe on 2'3'SLADP and the addition of beryllium fluoride induces the more restricted conformation of the nucleotide binding pocket (61.9G), indicating that flanking DNA is not required for this conformational change.

Figure 7. Temperature dependence of the 62G conformation of the nucleotide binding pocket. The experiments in this figure are preliminary and have been done once (n=1). Also note that values with an asterix indicate that the exact splitting could not be determined from the spectrum. Lowering the temperature from 30°C to 2°C shifts the equilibrium of 2'3'SLADP in the presence of beryllium fluoride from the 62G restricted conformation to the more open 48G conformation. At 2°C (blue spectrum), in the presence of 8uM Wt 60-60 nucleosomes, 10uM 2'3'SLADP and 0.5mM BeFx, 16uM SNF2h induces both a 50.7G splitting (107.8° cone angle) and the 62G* (68.4°* cone angle). At 30°C (red spectrum), the fraction of spins in the 48G* conformation decreases, while the more restricted 62.3G population increases (67.2° cone angle).

Figure 8. The H4 tail can rescue ATP hydrolysis in trans. The experiments in this figure are preliminary and have been done once (n=1). a. The H4 tail rescues ATP hydrolysis by SNF2h in the presence of gH4+78 nucleosomes.

Under MTO nucleosome and ATP conditions (100nM nucleosomes, 50nM SNF2h, 13uM ATP), 50uM H4 tail peptide (amino acids 1-19) rescues ATP hydrolysis. Rate constants: Wt+78 nucleosomes kobs = 7.49 ± 0.042 min⁻¹, Wt+78 nucleosomes with 50uM H4 tail peptide (1-19) kobs = 8.1 ± 0.54 min⁻¹, gH4+78 nucleosomes kobs = 0.68 ± 0.29 min⁻¹, gH4+78 nucleosomes with 50uM H4 tail peptide kobs = 7.02 ± 0.69 min⁻¹. b. The H4 tail partially rescues ATP hydrolysis by SNF2h in the presence of of gH4 60-60 nucleosomes under STO nucleosome, MTO subsaturating ATP conditions (250nM nucleosomes and 500nM SNF2h, 10uM ATP) Rate constants: Wt 60-60 nucleosomes kobs = 13.6 min⁻¹; gH4 60-60 nucleosomes kobs = 2.11; gH4 60-60 nucleosomes + 10uM H4 peptide kobs = 4.83 min⁻¹; gH4 60-60 nucleosomes + 25uM H4 peptide kobs = 8.23 min⁻¹; gH4 60-60 nucleosomes + 50uM H4 peptide kobs = 5.03 min⁻¹. c. The H4 tail partially rescues ATP hydrolysis by SNF2h in the presence of gH4 core nucleosomes under single turnover nucleosome, MTO subsaturating ATP conditions (250nM nucleosomes, 500nM SNF2h, 10uM ATP). Rate Constants: Wt core nucleosomes kobs = 10.3 min⁻¹; gH4 core nucleosomes kobs = 2.11; gH4 core nucleosomes + 10uM H4 peptide kobs = 4.27 min⁻¹; gH4 core nucleosomes + 25uM H4 peptide kobs = 3.85 min⁻¹; gH4 core nucleosomes + 50uM H4 peptide kobs = 0.681 min⁻¹. Errors represent s.d.m.

Figure 9. The H4 tail does not rescue nucleosome remodeling in trans. The experiments in this figure are preliminary and have been done once (n=1). Under STO nucleosome, MTO ATP conditions with gH4+78 nucleosomes and

SNF2h, exogenously added peptide does not rescue nucleosome remodeling but rather inhibits remodeling at concentrations that stimulate ATP hydrolysis. Rate constants were measured with 10nM gH4+78 nucleosomes, 200nM SNF2h, 2mM ATP and varying concentrations of the H4 peptide (a.a. 1-19). Note that the H4 tail peptides used in this experiment contained one remaining F-moc group from synthesis, which could contribute to stickiness and non-productive interactions. Rate constants were then normalized to the value of the rate constant obtained for gH4+78 nucleosomes without peptide (0.008 min⁻¹). An apparent K_i of 6.8uM was obtained from fitting the inhibition of remodeling as a function of peptide concentration.

Figure 10. The H4 tail extension mutants have effects on ATP hydrolysis.

a. H4 tail extension constructs. Histones mutants were created with four types of linkers between the globular domain and the basic patch, the critical epitope of the H4 tail: seven or 12 amino acids of (GGSG)_n, and seven or 12 amino acids of an alpha helix-promoting sequence, A(EAAAK)_nA. These histones, along with Wild-type H4 and H4 tailless (Δ 1-19 amino acids) were used to assemble nucleosomes with a Cy3 dye on one side of the nucleosome and 60bp of flanking DNA on the other side of the nucleosome b. ATPase assays were performed previously and as described in Methods¹. In this preliminary experiment performed once, the H4 tail extension mutants decreased ATPase activity under STO nucleosome conditions (5nM) with saturating ACF (25nM) and MTO subsaturating ATP (4uM). The longer 12sergly linker has a more deleterious

effect than the 7sergly linker compared to Wt, but not as severe as the gH4 (tailless) mutant. Both putative alpha helical linker lengths had intermediate but similar defects. Rate constants: Wt+60 kobs = 14.7min⁻¹; 7sg+60 kobs = 9.76min⁻¹; 12sg+60 kobs = 4.77min⁻¹; 7alpha+60 kobs = 6.61min⁻¹; 12alpha+60 kobs = 6.05 min⁻¹; gH4+60 kobs = 2.38min⁻¹.

Figure 11. The H4 tail extension mutants have effects on nucleosome remodeling. a. Nucleosomes end-labeled on the DNA with a Cy3 dye on one side of the nucleosome and 60bp of DNA on the other side were used in gel mobility shift assays as described previously and in Methods¹. The H4 tail extension mutants decreased remodeling rates under STO nucleosome conditions with saturating ACF and MTO, subsaturating ATP (identical conditions to the ATPase assays in Figure 10). b. Quantification of the gel upshift assays in (a) by measuring the decrease in the fraction of nucleosomes from the unremodeled band with time. The data fit best to a double exponential. Rate constants for the fast phase: Wt+60 kobs = 0.9min⁻¹; 7sg+60 kobs = 0.51min⁻¹; 12sg+60 kobs = 0.37min⁻¹; 7alpha+60 kobs = 0.48; 12alpha+60 kobs = 0.44; gH4+60 kobs not determined.

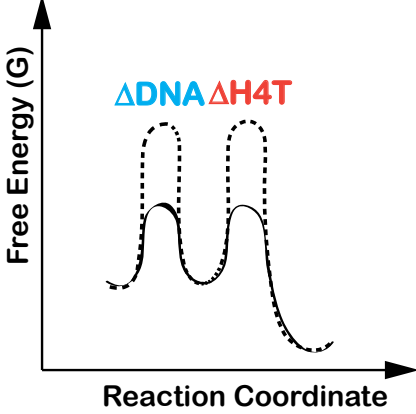
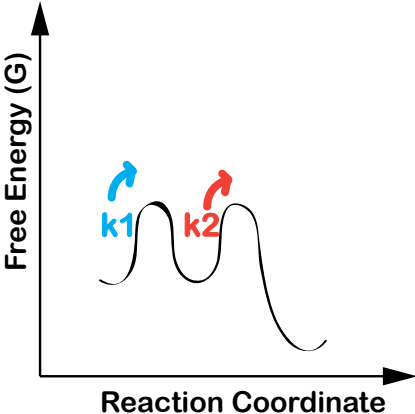
Figure 12. Physical models for the cues acting in one or two ATP hydrolysis events. a. In Model 1, the two types of ATP hydrolysis may be carried out by the two promoters in the dimeric complex. The first protomer may sample flanking DNA length and hydrolyze the first ATP, while the second

protomer may sense the H4 tail and hydrolyze the second ATP. b. In Model 2b, the two substrate cues act in a coupled manner to promote the same ATP hydrolysis event. In such a model, contacts between the H4 tail and the enzyme (green) in an activated intermediate, such as a closed pocket conformation, are stabilized by interactions of DNA with the enzyme (yellow), either allosterically or directly as shown in this example (pink contacts between the H4 tail and flanking DNA).

- 1 Yang, J. G., Madrid, T. S., Sevastopoulos, E. & Narlikar, G. J. The chromatin-remodeling enzyme ACF is an ATP-dependent DNA length sensor that regulates nucleosome spacing. *Nat Struct Mol Biol* **13**, 1078-1083, doi:nsmb1170 [pii] 10.1038/nsmb1170 (2006).
- 2 Yang, J. G. & Narlikar, G. J. FRET-based methods to study ATP-dependent changes in chromatin structure. *Methods* **41**, 291-295, doi:S1046-2023(06)00205-2 [pii] 10.1016/j.ymeth.2006.08.015 (2007).

FIGURE 1

a.



b.

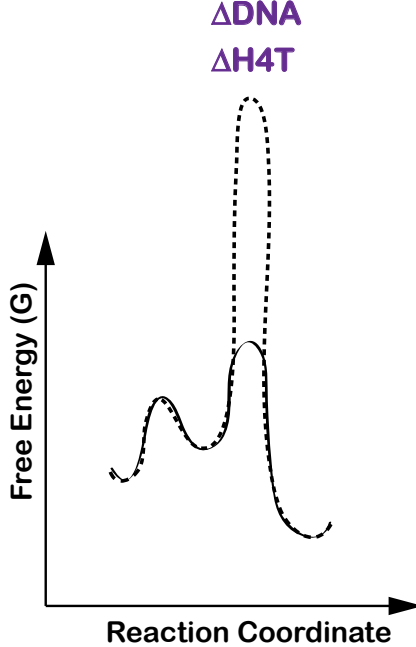
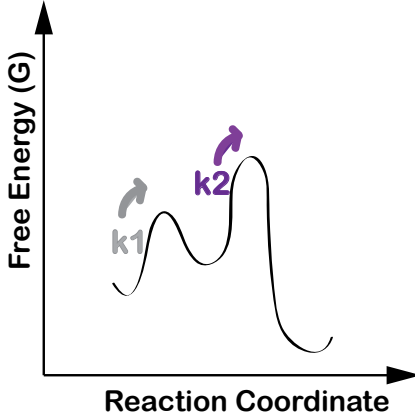
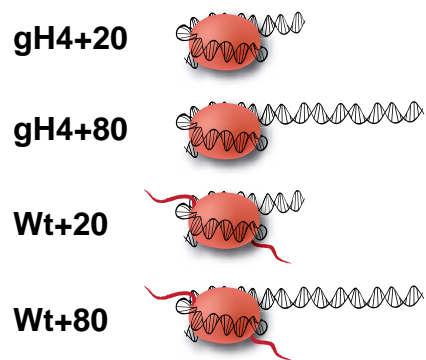
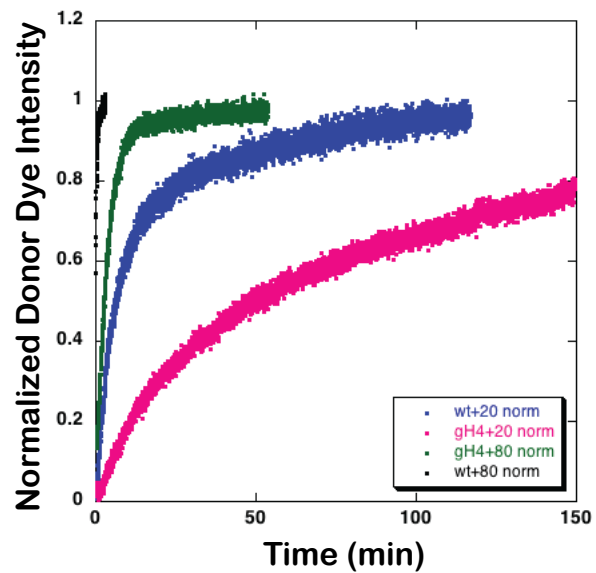


FIGURE 2

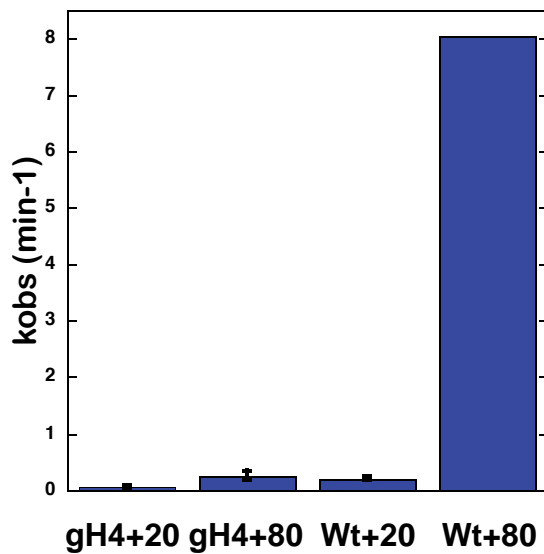
a.



b.



c.



d.

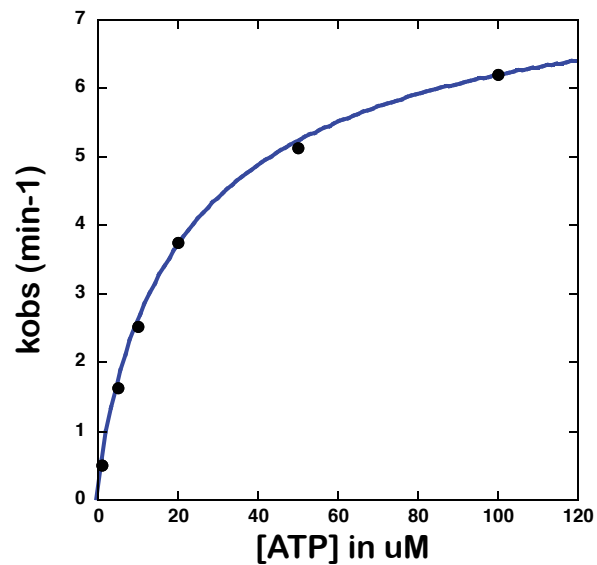
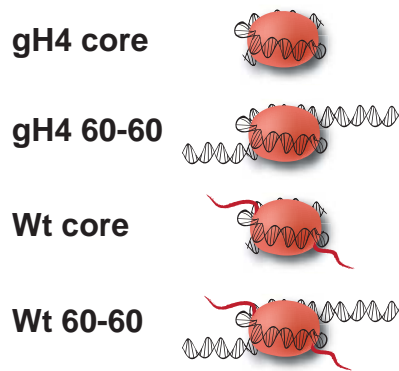
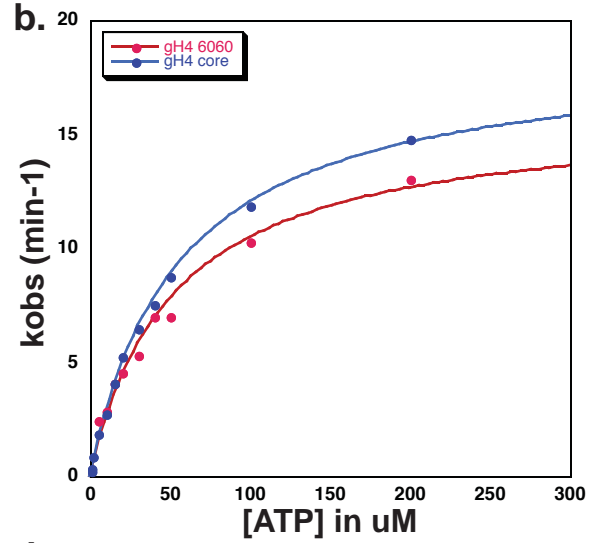


FIGURE 3

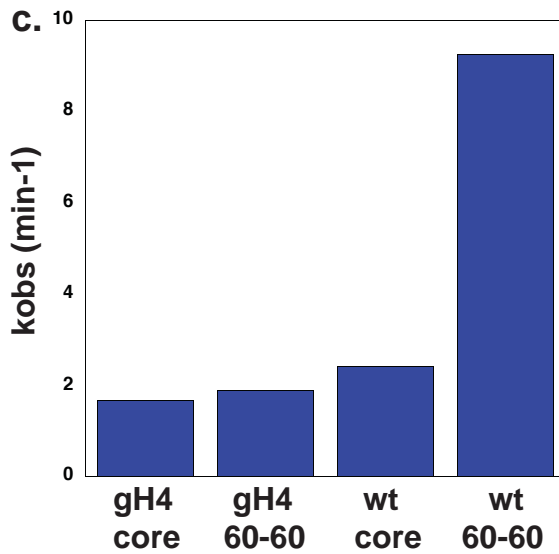
a.



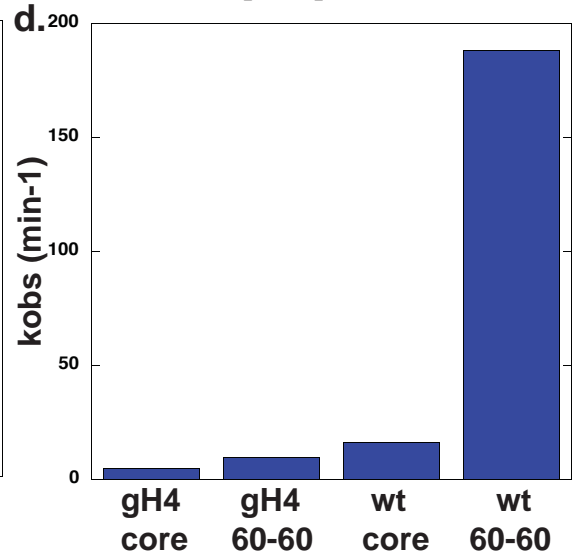
b.



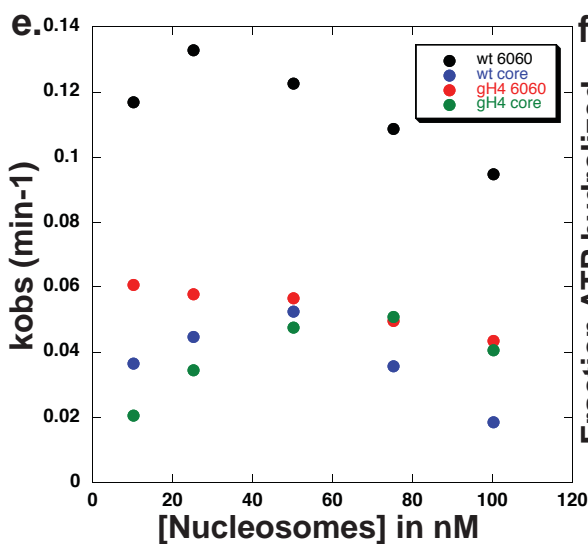
c.



d.



e.



f.

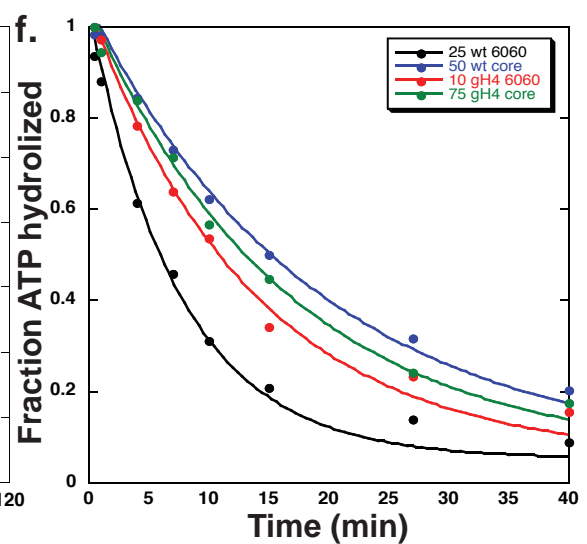
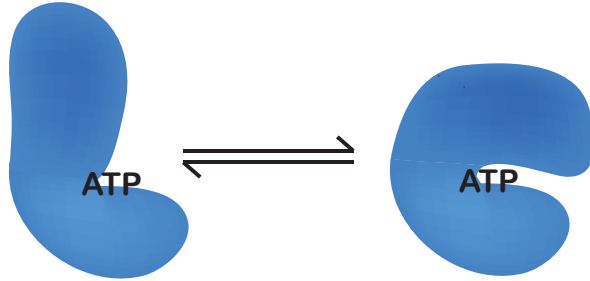
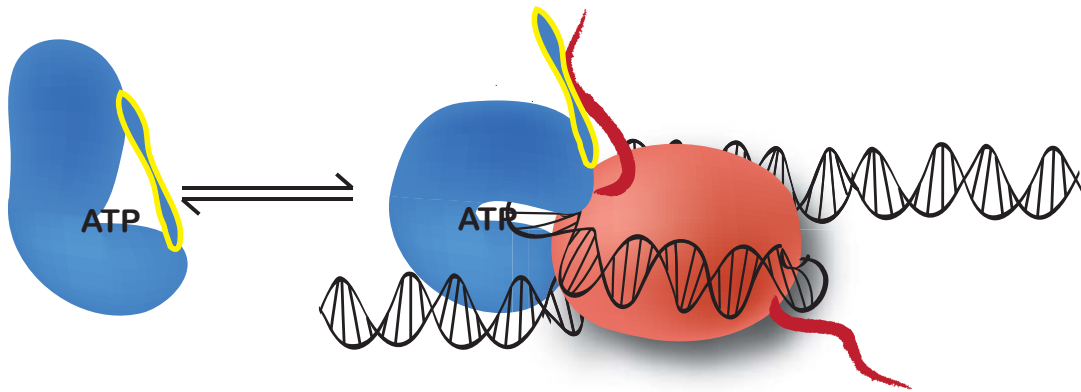


FIGURE 4

a. ATPase pocket closure

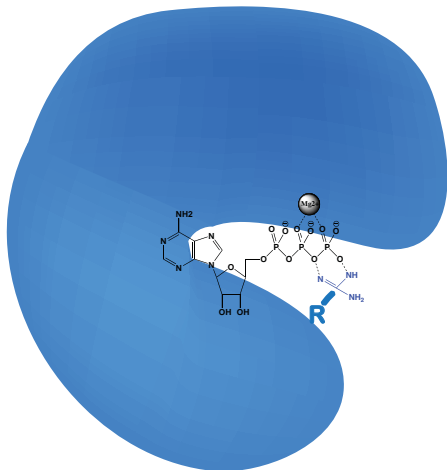


b. Relief from autoinhibition



c. Arginine finger hypothesis

Endogenous Arginine Finger



H4 Arginine Finger

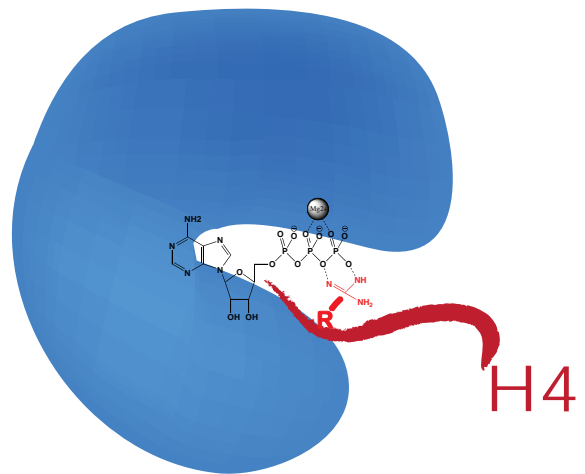
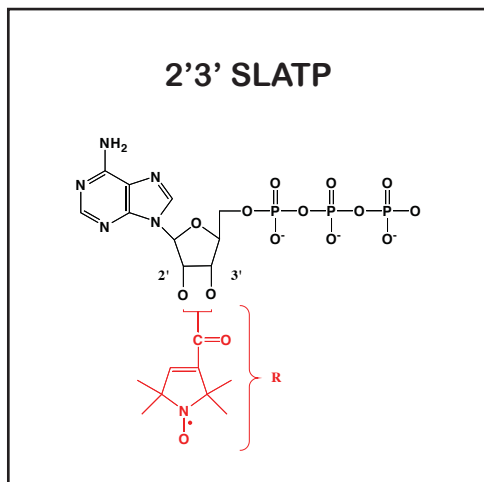


FIGURE 5

a.

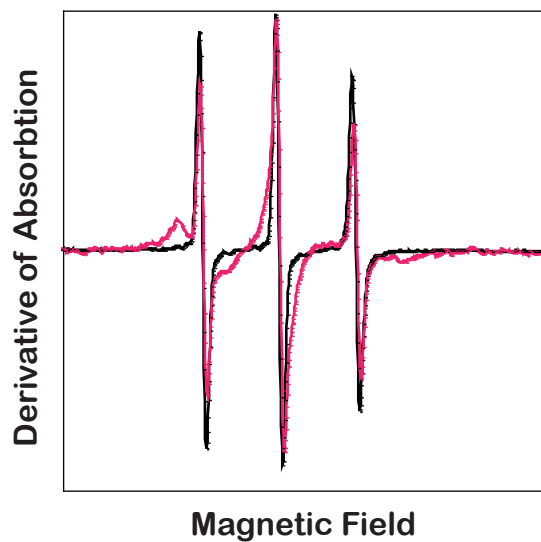


b.



(-) (+) (+) (+)
 ATP ATP 2'3'SLATP 2'SLATP

c.



SNF2h	Splitting	Cone Angle
(-)	32G	Free
(+)	47.4G	118.8°

FIGURE 6

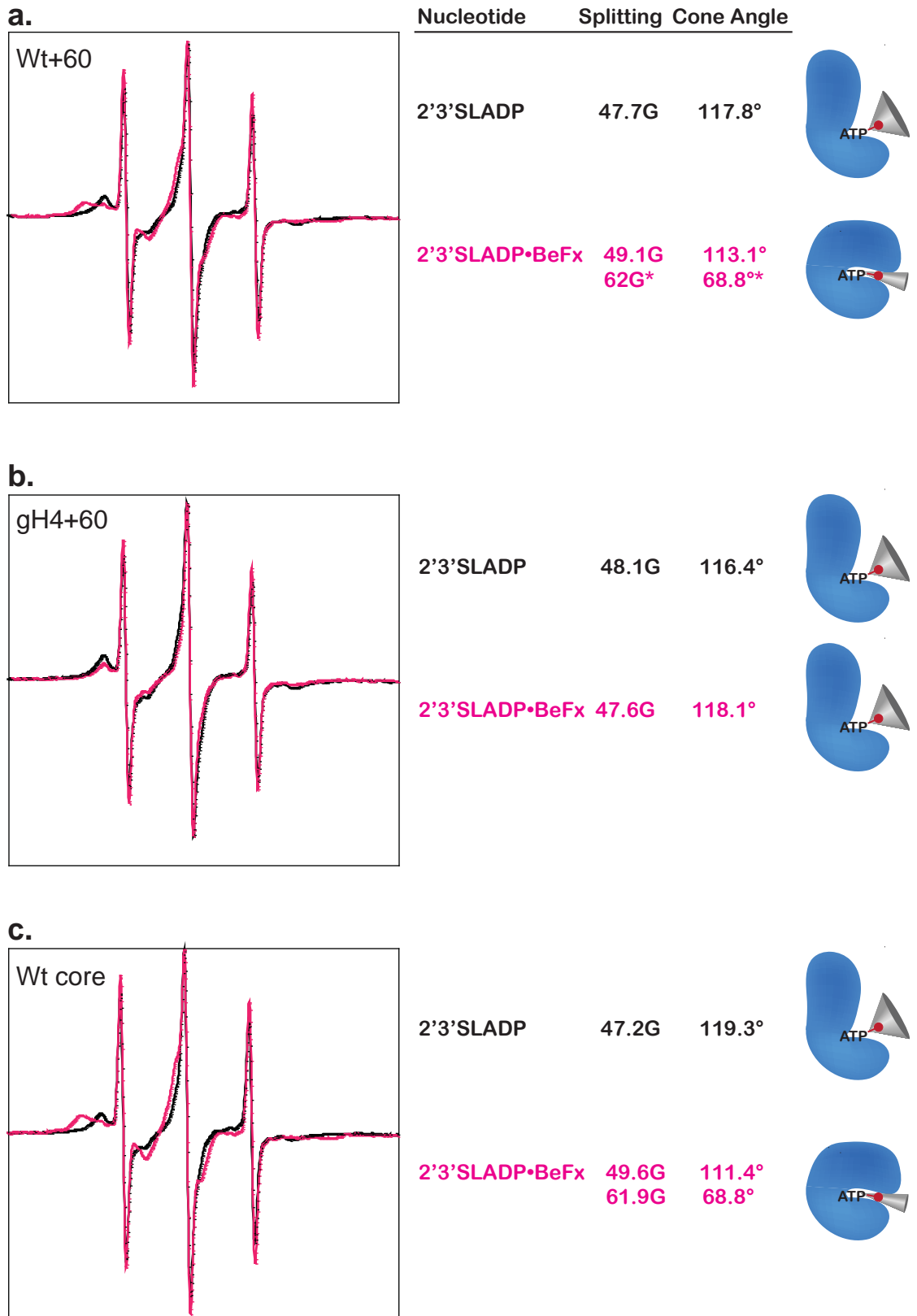
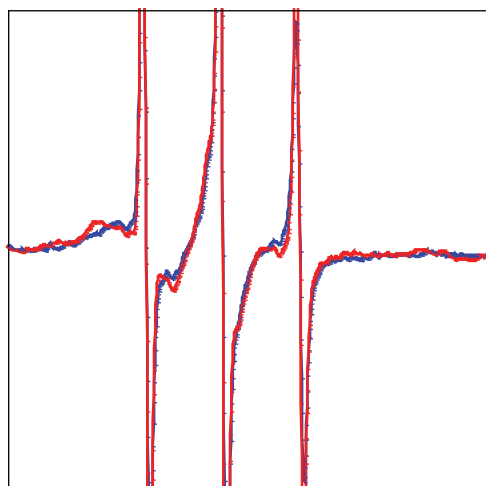


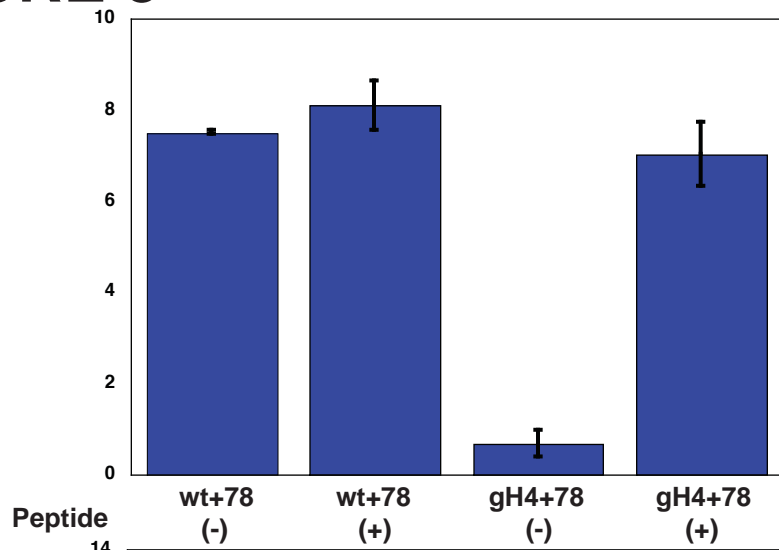
FIGURE 7



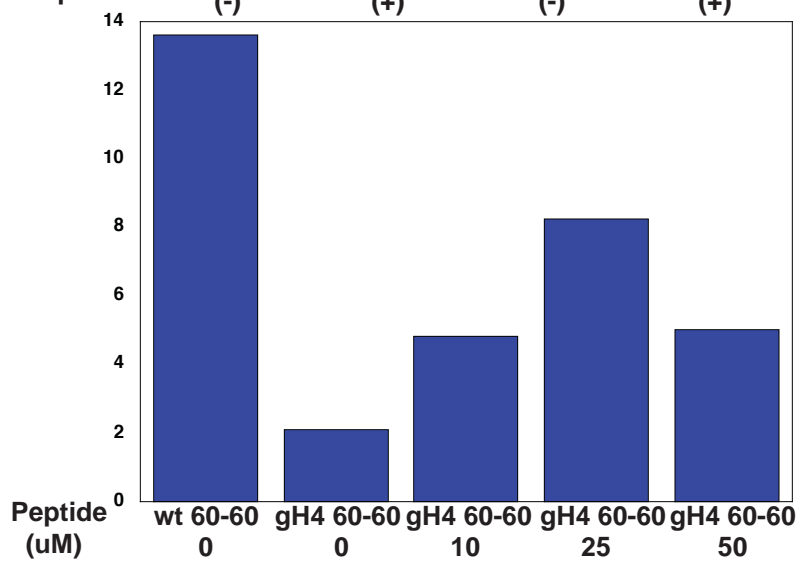
Temperature	Splitting	Cone Angle
2°C	50.7G 62G*	107.8° 68.4°*
30°C	48G* 62.3G	116.8°* 67.2°

FIGURE 8

a.



b.



c.

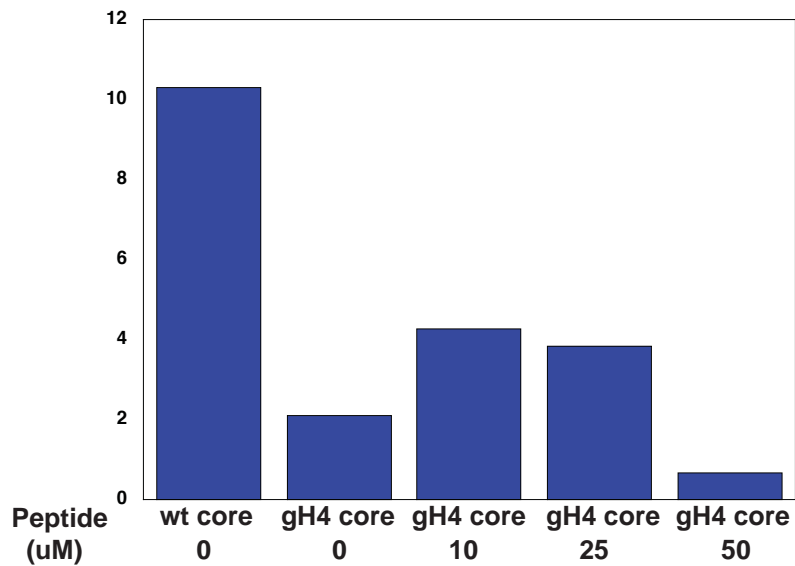


FIGURE 9

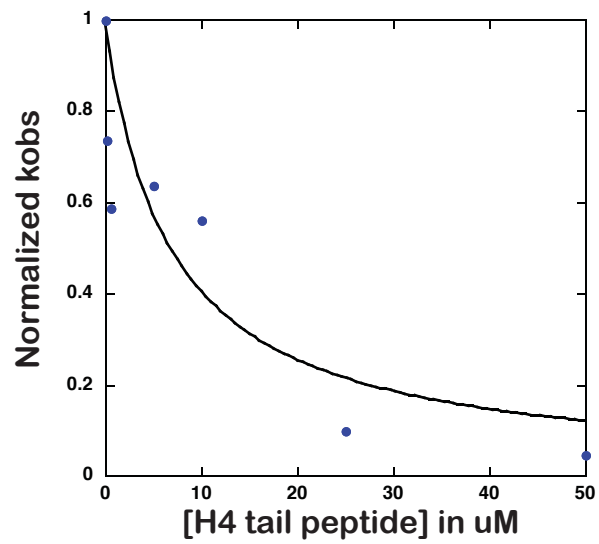
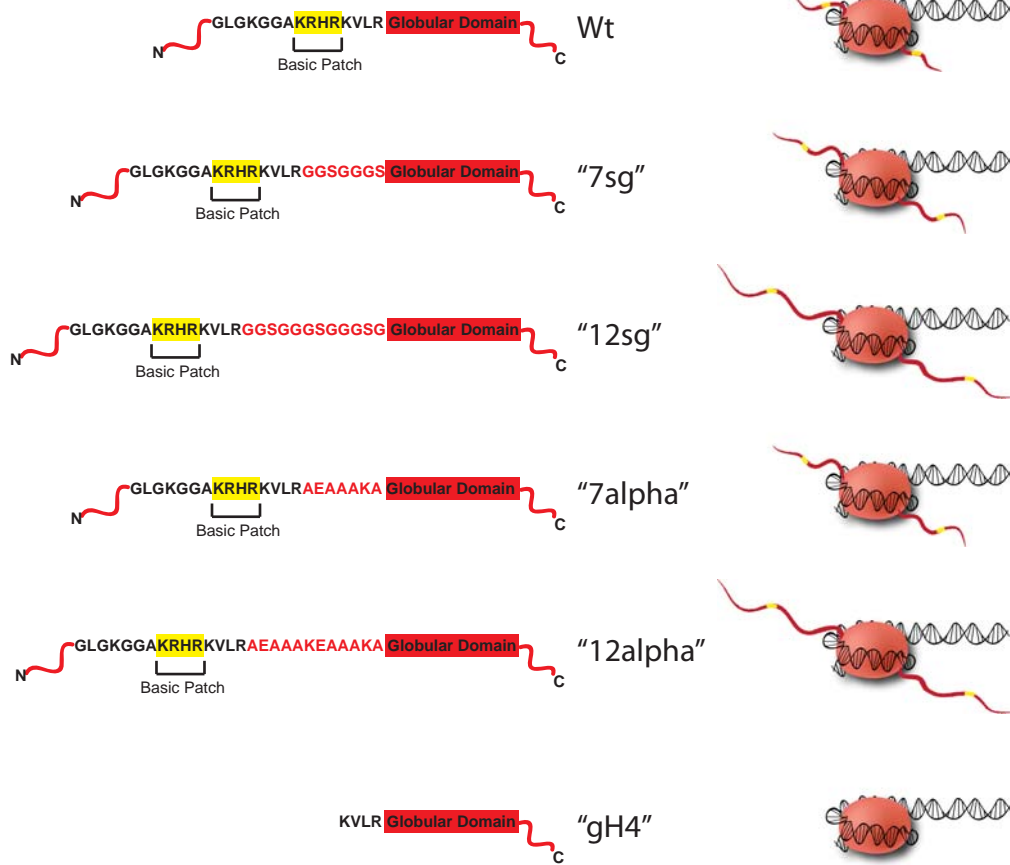


FIGURE 10

a.



b.

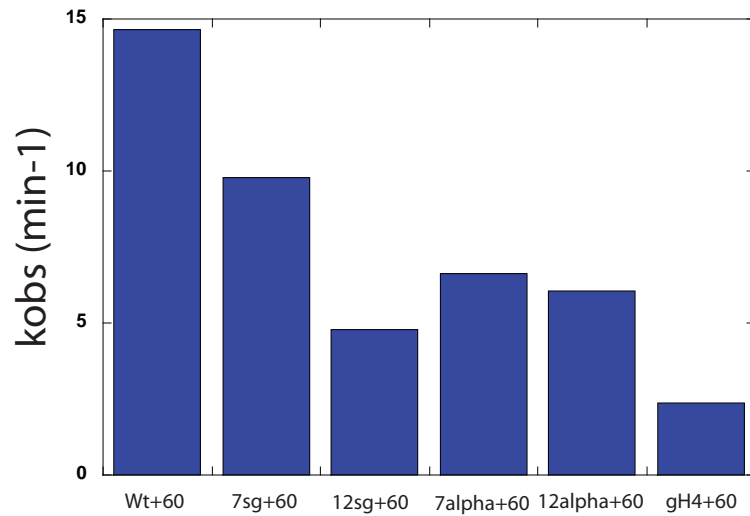
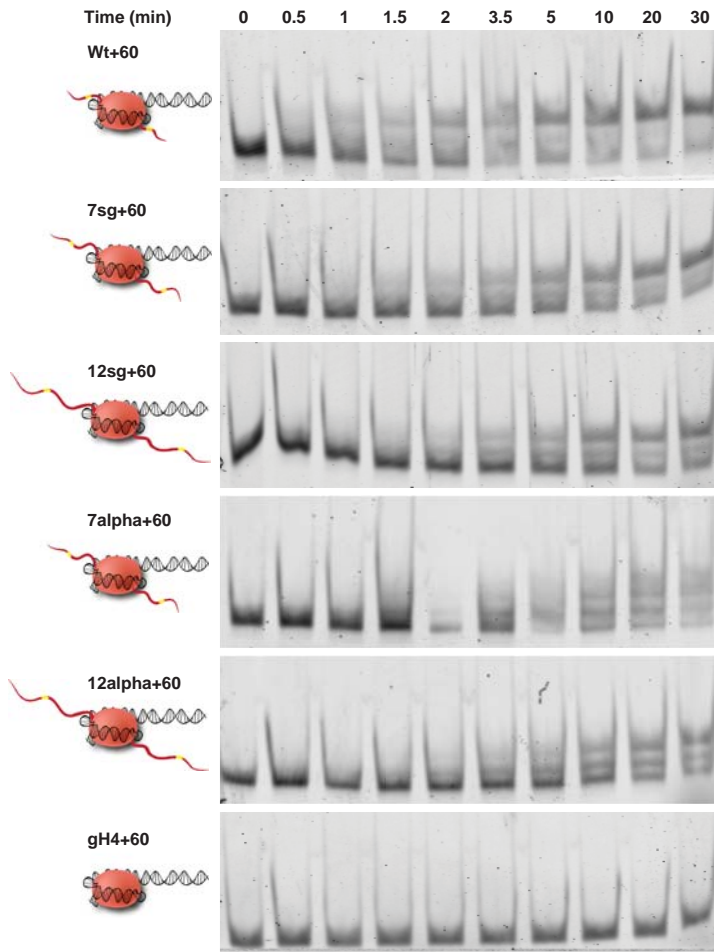
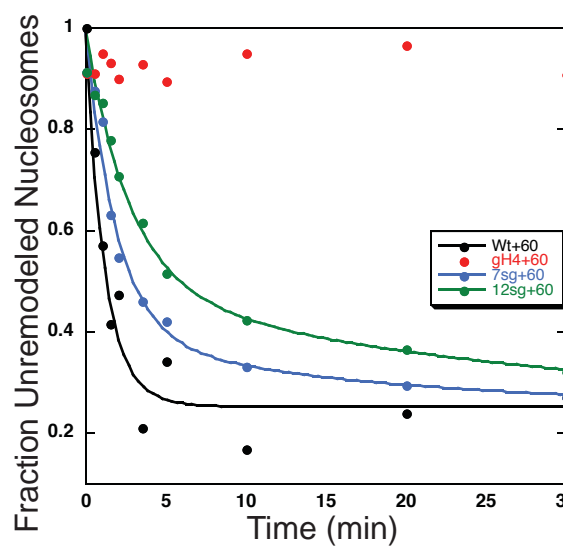


FIGURE 11

a.



b.



c.

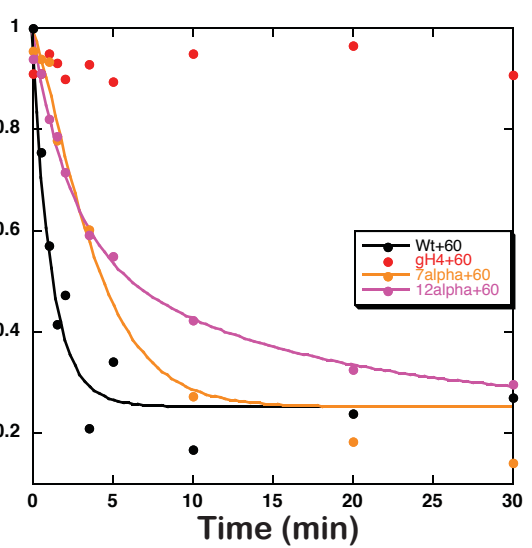
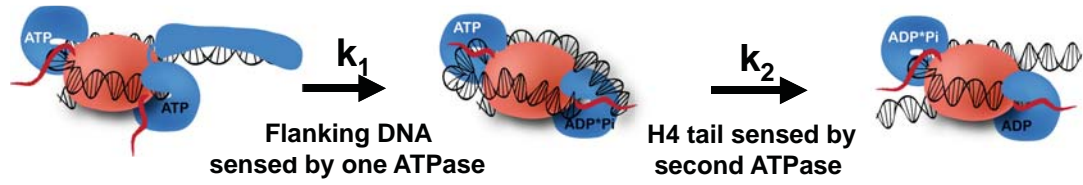


FIGURE 12

a.



b.

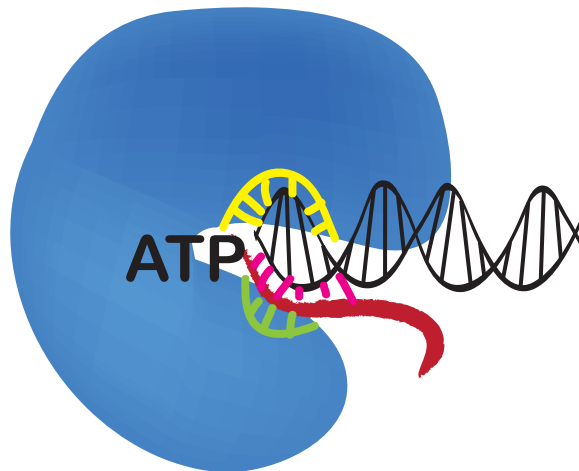


Table 1

	Relative to Wt		Relative to Δ DNA Δ H4T	
	ATPase	Remodeling	ATPase	Remodeling
wt	1	1	148.7037	5.5
Δflanking DNA	40.55556	3.86610879	3.666667	1.422619048
ΔH4 tail	32.51012	4.91489362	4.574074	1.119047619
ΔDNAΔH4T	148.7037	5.5	1	1

CHAPTER 4

Methods

Protein purification. Human SNF2h and the ACF complex were assembled and purified from SF9 cells as previously described¹.

Nucleosome Assembly. Nucleosomes were assembled as previously described on DNA containing the 147 bp 601 positioning sequence¹⁻³. DNA constructs with 20, 40, 60, or 78bp of DNA flanking the nucleosome were generated by PCR as previously described (Fig S1a). For fluorescence intensity-based binding studies, nucleosomes were labeled with a single Cy3 dye on the short DNA end by PCR using end-labeled primers (IDT). For measurement of nucleosome remodeling kinetics by FRET, histone H2A of the octamer was labeled with Cy5. A unique cysteine was engineered at residue 120 using QuikChange mutagenesis (Stratagene), and labeled with Cy5-maleimide under denaturing conditions as previously described before octamer assembly. Octamers with H2A-120C-Cy5 were then assembled into nucleosomes using Cy3 end labeled DNA with 20 or 78 bp of flanking DNA on one side. For negative stain EM experiments, nucleosomes were assembled as previously described with 60 bp of flanking DNA on one end, but in the absence of NP-40. For EPR studies, a unique cysteine was engineered into histone H4 at residue 15. Nucleosomes were assembled under reducing conditions with 0.5mM DTT. After nucleosome assembly, nucleosomes were transferred into DTT free labeling buffer (10mM KCl, 20mM MOPS, pH 7.0) by successive rounds of concentration and dilution using the centrifugal filter units, Microcon YM-100 (Millipore). Five-fold excess of Maleimide Spin Probe (N-(1-oxyl-2,2,6,6-tetramethyl-4-piperidiny) maleimide) to cysteines was immediately added after

buffer exchange and nucleosomes were left at room temperature overnight for labeling. Free spin probe was removed from the H4-A15C-MSL labeled nucleosomes by successive rounds of buffer exchange using centrifugal filter units.

EPR Spectroscopy. EPR measurements were performed with a Bruker EMX EPR spectrometer from Bruker Instruments (Billerica, MA). First derivative, X-band spectra were recorded in a high-sensitivity microwave cavity using 50-s, 100-Gauss wide magnetic field sweeps. For clarity only 80-Gauss are shown in Figure 1. The instrument settings were as follows: microwave power, 25 mW; time constant, 164 ms; frequency, 9.83 GHz; modulation, 1 Gauss at a frequency of 100 kHz. Each spectrum used in the data analysis is an average of 50-150 sweeps from an individual experimental preparation. For temperature dependence experiments, a stream of dry, temperature-controlled air was passed through the sample cavity, and the temperature of the sample was monitored by a thermistor in the chamber. The setup achieves temperature control within $<2^{\circ}\text{C}$ precision.

For EPR experiments in Chapter 2, Figure 1 using maleimide spin-labeled H4 tail nucleosomes, the following conditions were used: 4 μM nucleosomes (8 μM spin probes, as the nucleosome has two H4 tails) were measured in the presence of 8 μM SNF2h at room temperature in reaction buffer (12mM HEPES

pH 7.9, 4mM Tris pH 7.5, 60mM KCl, 0.5-1mM free MgCl₂, 0.32mM EDTA, 12% glycerol, 0.4mM DTT, 0.4mM BenzHCl, 0.4 mg/ml Flag Peptide) and various nucleotides and nucleotide analogues. For spectra in the presence of ADP, 2mM ADP-Mg²⁺ was used. For spectra in the presence of ADP•BeF_x, 0.5mM ADP, 0.5mM BeCl₂ and 2.5mM NaF, along with 0.5mM MgCl₂ was used.

For EPR experiments in Chapter 3, Figure 6 using 2'3'SLATP, the following conditions were used: 11.3 to 12uM nucleosomes as indicated in the legend, 30uM SNF2h, and reaction buffer (12mM HEPES pH 7.9, 4mM Tris pH 7.5, 60mM KCl, 0.5-1mM free MgCl₂, 0.32mM EDTA, 12% glycerol, 0.4mM DTT, 0.4mM BenzHCl, 0.4 mg/ml Flag Peptide) and 15uM of 2'3'SLATP in the presence of 0.5mM MgCl₂. For spectra in the presence of BeF_x, 0.5mM BeCl₂ and 2.5mM NaF were added after hydrolysis of 2'3'SLATP by SNF2h and nucleosomes. For experiments in Chapter 3, Figures 5 and 7 using 2'3'SLADP, the following conditions were used: 8uM nucleosomes, 16uM SNF2h and reaction buffer (12mM HEPES pH 7.9, 4mM Tris pH 7.5, 60mM KCl, 0.5-1mM free MgCl₂, 0.32mM EDTA, 15% glycerol, 0.4mM DTT, 0.4mM BenzHCl, 0.4 mg/ml Flag Peptide) and 10uM of 2'3' SLADP in the presence of 0.5mM MgCl₂. For spectra in the presence of BeF_x, 0.5mM BeCl₂ and 2.5mM NaF were added.

Deconvolution of spectra. The fraction of immobilized probe was calculated by deconvolution of spectra into mobile and immobilized components. Spectra were then fit using these two components as described in supplementary figure 1⁴.

For the temperature dependence experiments, at each temperature, the fraction

mobile and immobile probe was obtained by non-linear least squares fit of the spectrum to a sum of mobile and immobile representative spectra. EPR spectra of spin labeled nucleosomes without SNF2h only have a mobile component and were used as the mobile representative spectra. The immobilized component spectrum was obtained by subtracting the mobile representative spectrum from nucleosome + SNF2h spectra which represent a mixture of mobile and immobile probe. A separate basis set was derived at each temperature to correct for the low temperature broadening of the spectra.

Hydroxyl Radical Footprinting. ACF and nucleosomes with 60 bp of flanking DNA were dialyzed separately into reaction buffer (12mM HEPES pH 7.9, 4mM Tris pH 7.5, 60mM KCl, 3mM free MgCl₂, 0.32mM EDTA, 1mM DTT and 1mM BenzHCl) to remove glycerol. Nucleosomes were end-labeled with ³²P on the 5' end of the shorter flanking DNA side. 20nM nucleosomes were incubated with 100nM ACF, and enzyme activity was verified by gel shift (data not shown). For reactions containing ADP•BeF_x, 2mM ADP, 2mM BeCl₂ and 10mM NaF, along with 2mM MgCl₂ was used. Digestion with hydroxyl radicals was carried out as described previously, with a few modifications⁵. 0.5 ul each of the following solutions were placed on the inner wall of the reaction tube: (i) 20mM ferrous ammonium sulfate and 40 mM EDTA, ⁶ 100mM sodium ascorbate, and (iii) 30% H₂O₂. The reaction was initiated by spinning down the solutions, incubated for 1 min at room temperature, and stopped by the addition of 5 ul of 100mM thiourea and 0.5 ul 0.5M EDTA. Reactions were then ethanol precipitated using 5 ug of

blue dextran per sample as a carrier. The DNA was resuspended in loading buffer (90% formamide, 10% Bromophenol Blue- Xylene Cyanol loading solution (Sigma)), heated at 90C for 5 min and loaded on an 8% sequencing gel containing 7M urea. Using SAFA software, gels were corrected for distortions and the band intensities were measured⁷. Gel-loading efficiencies were normalized by aligning band intensities in the 30-45 bp region. Base pair assignments were determined using standards from the 601 sequence, generated using the Thermo Sequenase Dye Primer Manual Cycle Sequencing Kit (United States Biochemical Corporation). Depiction of the nucleosome with flanking DNA was generated by fusing the crystal structure of the nucleosome (PDB 1KX5) with a segment of 12bp B-form DNA (PDB 1BNA) in Coot and then visualized using Chimera⁸⁻¹⁰.

Fluorescence Binding Assay. Nucleosomes end labeled on the shorter DNA side of the nucleosome with Cy3 and either 40 or 78 bp of flanking DNA were incubated for 20 minutes at room temperature with varying amounts of SNF2h in reaction buffer (12mM HEPES pH 7.9, 4mM Tris pH 7.5, 60mM KCl, 3mM MgCl₂, 0.32mM EDTA, 12% glycerol, 0.02% Nonidet P40, 0.4mM DTT, 0.4mM BenzHCl, 0.4 mg/ml Flag Peptide) along with 0.1mg/mL BSA and nucleotide analogues concentrations as above. Fluorescence intensity of the cy3 probe was measured either using an Analyst HT plate reader (Molecular Devices) or an ISS K2 fluorometer. In the Analyst HT, the following filter set was used: 520-10 bandpass filter, 561 dichroic, and 580 bandpass. In the fluorometer, samples

were excited at 515nm and emission measured at 565nm. Longpass filters of 495nm and 530nm were used for excitation and emission monochromators respectively. The fluorescence intensity (z) as a function of SNF2h concentration (X) was fit to the following equation:

$$z = [a(K_{1/2}^n)+b(X^n)]/[(X^n)+(K_{1/2}^n)] \quad \text{Eqn (1)}$$

where a is the fluorescence intensity of unbound Cy3-labeled nucleosomes, b is the fluorescence intensity of fully bound Cy3-labeled nucleosomes, n is the Hill Coefficient, and $K_{1/2}$ is the concentration of SNF2h at which half the nucleosomes are bound. The average values for n and $K_{1/2}$ from three independent data sets are reported in the table in Figure 2e. In Figure 2b and 2e, for ease of visualization and comparison of different nucleotide analog states in the same plot, representative curves are shown, normalized from 0 to 1. Data was normalized as follows:

$$y = (z-a)/(b-a) \quad \text{Eqn (2)}$$

where y is the normalized fluorescent intensity, z is the raw fluorescent intensity value at a given concentration of SNF2h, a is the fluorescent intensity of unbound Cy3-labeled nucleosomes determined from the fit in Eqn (1), and b is the fluorescent intensity of fully bound Cy3-labeled nucleosomes determined from the fit in Eqn (1). The normalized fluorescent intensity (y) was then fit to Hill Equation:

$$y = (X^n)/[(X^n)+(K_{1/2}^n)] \quad \text{Eqn (3)}$$

where X is the concentration of SNF2h, n is the Hill Coefficient, and $K_{1/2}$ is the concentration of SNF2h at which half the nucleosomes are bound.

FRET-based experiments. Nucleosome remodeling rates were measured as described previously.¹ For the SNF2h remodeling experiments in Chapter 2, Figure 2, 5nM of FRET-labeled nucleosomes with 78bp of flanking DNA were incubated with varying concentrations of enzyme, 0.1mg/ml BSA, and reaction buffer (12mM HEPES pH 7.9, 4mM Tris pH 7.5, 60mM KCl, 3mM MgCl₂, 0.32mM EDTA, 0.02% (v/v) NP-40, 0.4mM DTT, 0.4mM BenzHCl, 12% glycerol, 0.4 mg/ml Flag Peptide) for 10 minutes at 30°C before initiation by adding ATP/MgCl₂ (2mM). The rate constants were obtained from an exponential fit as described previously¹. ACF experiments for Chapter 2, Figure 2 were conducted in an identical manner as the SNF2h experiments except that FRET-labeled nucleosomes with 20bp of flanking DNA were used instead of 78bp because ACF kinetics are too rapid to measure by manual mixing with longer flanking DNA lengths under saturating ATP concentrations. The observed rate constants (k_{obs}) were fit to the following equation:

$$k_{\text{obs}} = (k_{\text{max}}X^n)/[(X^n)+(K'_{1/2}^n)]$$

where k_{\max} is the maximal rate constant for remodeling, X is the concentration of SNF2h, n is the Hill Coefficient, and $K'_{1/2}$ is the concentration of enzyme at which $k_{\text{obs}} = (1/2)k_{\max}$.

ACF experiments in Chapter 3, Figure 2, were conducted in an identical manner as the SNF2h experiments except that four FRET-labeled nucleosome constructs were assembled, as described in Figure 2a: Wt nucleosomes with 20 or 80bp of flanking DNA or 80bp of flanking DNA, and H4 tailless (gH4) nucleosomes with 20 or 80bp of flanking DNA.

Electron microscopy and image processing. 10nM nucleosomes with 60bp of flanking DNA were incubated with 100 to 200nM freshly purified SNF2h for 10 minutes at 30°C in reaction buffer with low glycerol (12mM HEPES pH 7.9, 4mM Tris pH 7.5, 60mM KCl, 3mM MgCl₂, 0.32mM EDTA, 1-3% glycerol, 0.4mM DTT, 0.4mM BenzHCl, 0.4 mg/ml Flag Peptide) and 2mM ADP•BeF_x•Mg generated from 2mM ADP, 2mM BeCl₂ and 10mM NaF, 2mM MgCl₂). Images of SNF2h by itself were also obtained in the above conditions. 2.5uL reaction mixture was adsorbed to a glow-discharged copper grid coated with carbon film for 30 seconds followed by conventional negative stain with 0.75% uranyl formate¹¹. Images were collected using a Tecnai T12 microscope (FEI company, Hillsboro, OR) with a LaB₆ filament and operated at 120 kV accelerating voltage. All images were recorded at a magnification of 52,000X with an UltraScan 4096 x 4096 pixel CCD camera (Gatan Inc, USA). Images of tilt pairs were recorded with a defocus of -1.5um using an automated procedure as previously described¹².

All images were 2x2 pixel binned to the final pixel size of 4.04Å before any further processing. A total of 10,059 pairs of particles were selected interactive from 101 tilt pair images using the display program WEB associated with the SPIDER software package and windowed into 90 x 90 pixels images¹³. All subsequent image processing was performed using the SPIDER software package. Particles windowed from untilted images were subject to standard iterative multi-reference alignment and classification (K-mean, specifying 50 classes). All class averages were divided into 5 distinct views (shown in Figure 3a and b), and classes of the same view were merged together. Images of nucleosome with two SNF2h bound (shown in Figure 3a, top) were used for calculating 3D reconstruction by random conical tilt (RCT) technique¹⁴. Images of side views (Figure 3a, middle and bottom) were included during the angular refinement of the initial 3D reconstruction calculated from top view only. Adding side view images reduces the flattening and missing cone effects of random conical tilt 3D reconstruction. A total of 8,440 particles, including ten percent of the particle from untilted images of the same classes, were included in the final 3D reconstruction. We did not enforce any symmetry in the 3D reconstruction or during the refinement. The resolution of final 3D reconstruction was estimated to be ~ 27Å, based on Fourier Shell Correlation (FSC) = 0.5 criteria. 3D reconstruction of the nucleosome with a single SNF2h bound was calculated following the same procedure. 3D reconstructions were visualized by UCSF Chimera, atomic structure of the nucleosome (PDB 1KX5) was placed manually

into the 3D volume⁸. The handedness of the final 3D reconstruction was determined unambiguously by the calibrated RCT procedure. The handedness obtained by this procedure has been validated by all subsequent 3D reconstructions that have been generated using the same procedure. Once the handedness was determined, the nucleosomal “disc” could only be placed in one way into the 3D volume. In this placement we inferred the location of the nucleosome dyad from the “V” shaped protein density observed in the top view (see top panel in Fig. 3a) as this shape correlates with the protein density in the crystal structure. We hypothesize that due to selective positive staining of the DNA, the density corresponding to DNA is weaker than that corresponding to protein.

ATPase Reactions. ATP hydrolysis reactions were conducted as described previously

¹⁵. Briefly, nucleosomes, SNF2h, and ATP at the concentrations indicated in the figure legends were combined to a final volume of 30uL at 30°C in reaction buffer (12mM HEPES pH 7.9, 4mM Tris pH 7.5, 60mM KCl, 3mM MgCl₂, 0.32mM EDTA, 0.02% (v/v) NP-40, 0.4mM DTT, 0.4mM BenzHCl, 12% glycerol, 0.4 mg/ml Flag Peptide) and time points were collected and quenched manually as described previously¹⁵. For STO ATP reactions, only the γ -³²P-labeled ATP tracer was used at the indicated concentrations.

Gel mobility upshift experiments. These experiments were performed as described previously¹. Nucleosomes and either SNF2h or ACF at the

concentrations indicated in the figure legends were combined at room temperature for Chapter 3 Figure 5, and at 30°C for Chapter 3 Figure 11, in reaction buffer (12mM HEPES pH 7.9, 4mM Tris pH 7.5, 60mM KCl, 3mM MgCl₂, 0.32mM EDTA, 0.02% (v/v) NP-40, 0.4mM DTT, 0.4mM BenzHCl, 12% glycerol, 0.4 mg/ml Flag Peptide) and time points were collected and quenched manually as described previously. Nucleosome gels in Chapter 3, Figure 5 were stained with Ethidium Bromide, and gels in Chapter 3, Figure 11 were imaged directly in the Cy3 channel on a Typhoon Variable Mode Imager.

- 1 Yang, J. G., Madrid, T. S., Sevastopoulos, E. & Narlikar, G. J. The chromatin-remodeling enzyme ACF is an ATP-dependent DNA length sensor that regulates nucleosome spacing. *Nat Struct Mol Biol* 13, 1078-1083, doi:nsmb1170 [pii] 10.1038/nsmb1170 (2006).
- 2 Luger, K., Mäder, A. W., Richmond, R. K., Sargent, D. F. & Richmond, T. J. Crystal structure of the nucleosome core particle at 2.8 Å resolution. *Nature* 389, 251-260, doi:10.1038/38444 (1997).
- 3 Lowary, P. T. & Widom, J. New DNA sequence rules for high affinity binding to histone octamer and sequence-directed nucleosome positioning. *J Mol Biol* 276, 19-42, doi:S0022-2836(97)91494-7 [pii] 10.1006/jmbi.1997.1494 (1998).

- 4 Naber, N., Purcell, T. J., Pate, E. & Cooke, R. Dynamics of the nucleotide pocket of myosin measured by spin-labeled nucleotides. *Biophys J* 92, 172-184, doi:S0006-3495(07)70814-7 [pii] 10.1529/biophysj.106.090035 (2007).
- 5 Schwanbeck, R., Xiao, H. & Wu, C. Spatial contacts and nucleosome step movements induced by the NURF chromatin remodeling complex. *J Biol Chem* 279, 39933-39941, doi:M406060200 [pii] 10.1074/jbc.M406060200 (2004).
- 6 Shogren-Knaak, M. et al. Histone H4-K16 acetylation controls chromatin structure and protein interactions. *Science* 311, 844-847, doi:311/5762/844 [pii] 10.1126/science.1124000 (2006).
- 7 Das, R., Laederach, A., Pearlman, S., Herschlag, D. & Altman, R. SAFA: semi-automated footprinting analysis software for high-throughput quantification of nucleic acid footprinting experiments. *RNA* 11, 344-354 (2005).
- 8 Pettersen, E. et al. UCSF Chimera--a visualization system for exploratory research and analysis. *J Comput Chem* 25, 1605-1612 (2004).
- 9 Emsley, P. & Cowtan, K. Coot: model-building tools for molecular graphics. *Acta Crystallogr D Biol Crystallogr* 60, 2126-2132 (2004).
- 10 Drew, H. et al. Structure of a B-DNA dodecamer: conformation and dynamics. *Proc Natl Acad Sci U S A* 78, 2179-2183 (1981).
- 11 Ohi, M., Li, Y., Cheng, Y. & Walz, T. Negative Staining and Image Classification - Powerful Tools in Modern Electron Microscopy. *Biol Proced Online* 6, 23-34, doi:10.1251/bpo70 (2004).
- 12 Zheng, S. Q., Kollman, J. M., Braunfeld, M. B., Sedat, J. W. & Agard, D. A. Automated acquisition of electron microscopic random conical tilt sets. *J Struct Biol* 157, 148-155, doi:S1047-8477(06)00333-9 [pii] 10.1016/j.jsb.2006.10.026 (2007).
- 13 Frank, J. et al. SPIDER and WEB: processing and visualization of images in 3D electron microscopy and related fields. *J Struct Biol* 116, 190-199, doi:S1047-8477(96)90030-1 [pii] 10.1006/jsbi.1996.0030 (1996).
- 14 Radermacher, M. et al. Cryo-electron microscopy and three-dimensional reconstruction of the calcium release channel/ryanodine receptor from skeletal muscle. *J Cell Biol* 127, 411-423 (1994).
- 15 Narlikar, G. J., Phelan, M. L. & Kingston, R. E. Generation and interconversion of multiple distinct nucleosomal states as a mechanism for catalyzing chromatin fluidity. *Mol Cell* 8, 1219-1230, doi:S1097-2765(01)00412-9 [pii] (2001).

Publishing Agreement

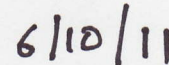
It is the policy of the University to encourage the distribution of all theses, dissertations, and manuscripts. Copies of all UCSF theses, dissertations, and manuscripts will be routed to the library via the Graduate Division. The library will make all theses, dissertations, and manuscripts accessible to the public and will preserve these to the best of their abilities, in perpetuity.

Please sign the following statement:

I hereby grant permission to the Graduate Division of the University of California, San Francisco to release copies of my thesis, dissertation, or manuscript to the Campus Library to provide access and preservation, in whole or in part, in perpetuity.

A handwritten signature in black ink, appearing to be 'H. Shi', written over a horizontal line.

Author Signature

A handwritten date '6/10/11' in black ink, written above a horizontal line.

Date